MANAGE DEMAND UNCERTAINTY WITH COST-FOR-DEVIATION RETAIL PRICING

By

JIANMIN ZHU

A dissertation submitted to the

Graduate School-New Brunswick

Rutgers, The State University of New Jersey

In partial fulfillment of the requirements

For the degree of

Doctor of Philosophy

Graduate Program in Industrial and Systems Engineering

Written under the direction of

Professor Mohsen A. Jafari

And approved by

_____

_____

_____

_____

_____

New Brunswick, New Jersey

October, 2014

ABSTRACT OF THE DISSERTATION

Manage Demand Uncertainty with Cost-For-Deviation Retail Pricing

by JIANMIN ZHU

Dissertation Director:

Mohsen A. Jafari

The current types of rate structures for the electricity retailing create a disconnection between retail and wholesale markets. The rate structures expose utility providers to the full risks of wholesale markets, while prohibiting the response of end-use customers to market dynamics. This disconnection is considered to be the primary cause of unusual volatility in electricity markets. In this dissertation, the author proposes a Cost-for-Deviation (CfD) retail pricing scheme, which is designed to minimize the demand uncertainty of individual customers. A series of experiments demonstrate that CfD pricing is able to reduce the demand uncertainty by 10%, as measured by the root mean squared deviation of the demand. Consequently, the community's cost of hedging the quantity risk in the real-time market is reduced by 38%. This dissertation also demonstrates the formulation and solution techniques for the day-ahead planning and real-time tracking optimizations that each customer faces under CfD. An efficient and robust approach, called Optimal Strategy Pool (OSP), is introduced to solve simulation-based on-line planning problems; and dynamic programming is adopted in neural network model-based predictive control. Both centralized and distributed mechanisms are studied for customers to

reduce CfD charges via collaborative demand management. Overall, CfD pricing effectively reduces the demand uncertainty by promoting a predictable consumption behavior.

ACKNOWLEDGMENTS

The author wishes to express sincere appreciation to Professor Jafari and Doctor Yan Lu for their assistance in the preparation of this dissertation.

TABLE OF CONTENTS

LIST OF TABLES

LIST OF FIGURES

ABBREVIATIONS

ANN	Artificial Neural Network
BAS	Building Automation System
CES	Community Energy Storage
CfD	Cost-for-Deviation retail pricing scheme
CHP	Combined Heat and Power
CPP	Critical Peak Pricing
DAP	(1) The electricity Day-Ahead wholesale Price (2) Day-Ahead retail Pricing
DG	Distributed Generator
DP	Dynamic Programming optimization
DR	Demand Response
ES	Exhaustive Search
EV	Electric Vehicle
FERC	the Federal Energy Regulatory Commission
GA	Genetic algorithm
GPS	General Pattern Search
HVAC	Heating, Ventilation and Air Conditioning
IBP	Incentive-Based (demand response) Programs
IEA	the International Energy Agency
ISO	Independent System Operator
LC	Load controller
LCOE	Levelized Cost Of Electricity
LMP	Locational Marginal Price
MGCC	MicroGrid Central Controller
NARX	Non-linear Auto-Regressive network with eXternal inputs
NERC	the North American Electric Reliability Corporation
OSP	Optimal Strategy Pool
PBP	Price-Based (demand response) Programs
PBS	Pattern-Based Selection
PCC	Point of Common Coupling

PDE	Partial Derivative Equations
PSO	Particle Swarm Optimization
PV	PhotoVoltaic panel
RMSD	Root Mean Squared Deviation
RTO	Regional Transmission Organization
RTP	(1) Real-Time retail Pricing (2) The electricity Real-Time wholesale Price
SVM	Support Vector Machine
TOU	Time-Of-Use retail pricing scheme
USDOE	the US Department of Energy
USEIA	the US Energy Information Administration

Chapter 1 Introduction

1.1 Objective

This dissertation proposes a new Cost-for-Deviation (CfD) retail pricing which charges the demand deviation of individual customers. Under this pricing scheme, the customers are encouraged to plan their demand carefully, and track the planned demand schedule as closely as possible in real-time. The two-phase control – the day-ahead planning and the real-time tracking – is expected to reduce the demand deviation of individual customers, and then minimize the overall demand uncertainty. In order to demonstrate the design and effectiveness of CfD, the author starts with the modeling and control optimization of a single building, under both conventional time-varying price and the new CfD price. Then, the scope extends to the demand side management within community microgrid, under CfD. A series of experiments demonstrate that (1) individual buildings are capable of the optimal control under time-varying price, but some special algorithm may be needed if simulation is involved in the on-line decision making; (2) CfD encourages the day-ahead planning and the real-time tracking, which are able to reduce the customer's demand deviation; (3) CfD reduces the community demand uncertainty and ultimately lowers the community cost; and (4) CfD promotes a predictable consumption behavior and collaborative demand management among customers.

1.2 Motivation

The electricity markets in many countries, including the US, consist of a wholesale market and a retail market. The wholesale markets are further split into a day-ahead market and a real-time market. The supply side and the demand side settle most of the electricity transactions in the

day-ahead markets and deal with the generation and consumption deviations in the real-time markets. The real-time electricity price is inherently more volatile than the day-ahead price. It is also likely that the real-time price is higher than the day-ahead price.

Utility providers function as brokers who participate in both wholesale and retail markets. In wholesale markets, utility providers act as buyers and electricity generators are sellers. And in retail markets, utility providers are sellers, who sell electricity to end-use customers. If actual demand is different to that submitted into day-ahead markets, utility providers will have to settle the deviation in real-time markets – by either purchasing the additional electricity or selling the excessive electricity. The cost of utility providers includes the costs in both day-ahead and real-time markets together with the risk hedging cost. If utility providers are assumed to be not-for-profit, their cost will eventually be shared by all the customers. Obviously, it is in utility providers' interest, and then in customers' interest, to have a predictable demand when submitting demand bids, because predictable demand means less demand uncertainty, and more reliance on day-ahead markets rather than risky real-time markets.

However, with the flat rate tariff, which is commonly implemented in the retail markets of the US, utility providers sell electricity at a fixed price. Customers are not incentivized to keep a predictable consumption manner. Utility providers, on the other hand, are exposed to the full risks in wholesale markets, including the price risk (due to the difference between predicted and actual price) and the quantity risk (due to the difference between predicted and actual demand). In order to hedge against those risks, utility providers have to raise the retail price, resulting in an unfair situation, where those customers with predictable demand share the elevated cost that is caused by the uncertain consumption behavior.

The proposed CfD rate structure is designed to address this problem. This rate structure first provides an hourly retail price schedule for the next operating day, and then requires the customers to submit their individual demand schedules. The customers are to follow their own demand schedules as closely as possible during the operating day, because the deviation of actual demand from the schedule will incur CfD charges. The demand side management under CfD, therefore, includes a planning stage and a tracking stage, resembling the day-ahead and real-time operations of electricity wholesale markets.

Compared to the flat rate and other time-varying pricing schemes, CfD is expected to have two major advantages. First, the day-ahead announcement of hourly rate schedule can be seen as a hybrid of the Time-of-Use (TOU) and the Real-time Pricing (RTP). The hourly rate carries the information about hourly dynamics of the market (although it is based on a forecast, rather than a realization), and the day-ahead announcement allows customers to plan consumption in advance, in order to fully utilize their demand response capacity. Second, CfD adds a novel, but crucial concept into the demand side management, which is the demand uncertainty. By charging on the demand deviation, CfD drives customers to maintain a predictable consumption behavior. The community as a whole will have less quantity risk in the wholesale market. As a consequence, a lower cost can be expected. The design of CfD pricing is well in line with the concept of "transactive energy", which proposes to use economic incentives to promote active participation of the demand side in wholesale and retail markets [1].

1.3 Contributions

In this dissertation, the author makes the following contributions:

- Introduces the concept of "demand uncertainty reduction" as an additional goal of the demand side management, which traditionally only includes energy saving and peak demand reduction;

- Proposes and demonstrates the use of an economic approach (i.e. the CfD retail pricing) in reducing the demand uncertainty;

- Formulates the day-ahead planning and the real-time tracking optimizations for the controls of a building under CfD;

- Explores a number of mechanisms by which collaborative demand management can be performed under CfD;

- Provides a solution technique for individual buildings to make on-line decisions under time-varying pricing.

1.4 Background and Literature Review

According to the International Energy Agency (IEA), the global energy consumption increased by 86% from 1973 to 2010, and the total carbon emission increased by 94% during the same period [2]. Among all primary energy sources, the fossil fuel (i.e., oil, coal and natural gas) accounts for over 80% in total [2]. This trend has raised increasing concern worldwide about the sustainability of the energy supply, and further about the possible, yet disastrous change of the world climate. The United States consumes 97.7 quadrillion BTU energy annually (2010) [3], which is about 27% of the entire world [2]. Buildings, both residential and commercial, account for 41% of total US energy consumption, more than industrial (31%) and transportation sectors

(28%) [3]. Over 75% of electric energy are consumed by building users [3]. This percentage is expected to increase, as a recent prediction shows that the commercial and residential energy uses will continue to grow, while the industrial and transportation consumption will most likely maintain their current levels [4]. Among different end uses, heating, ventilation and air conditioning (i.e. the HVAC system) and water heating together claim about 72% of the residential building energy and 36% in the commercial consumptions [5]. The implication is obvious: a more energy efficient and more environment friendly lifestyle, especially when it is related to the activities within building environment, would not only be in America's national interest, but also a critical goal for the entire world to pursue.

Researchers are actively investigating new technologies from various perspectives. Some are seeking new sources of energy. Some are trying to achieve higher efficiency in energy conversion, transition and storage. And others are applying intelligent planning, optimization and controls to both generation and consumption to minimize energy waste. In the past decades, we have seen many new techniques emerge, such as photovoltaic panels, wind turbine, Lithium-ion battery, building automation system (BAS) and smart grid technologies. The penetration of the renewable energy has reached 8% in 2011 and is projected to 11% by 2040 [4]. Although, to this point, some techniques may still be in the prototyping stage, many have reached, or are approaching, commercialization in different markets. The economic impact of the technology advancement is that the overall energy efficiency in the developed countries such as the US, has been nearly doubled from 1980 to 2011, according to the energy use per dollar of gross domestic product [4].

The energy system related studies can be roughly categorized into three domains: "building modeling and control optimization", "power grid" and "electricity markets". General overviews of these domains will be given in this section.

1.4.1 Building Modeling and Control Optimization

1.4.1.1. Simulation and Data-Driven Modeling

Prediction models are important for model-based control of building energy systems. Because the building energy system is a non-linear complex system with many subsystems and components interact with each other, it is extremely difficult to model using detailed physical modeling. Instead, the black-box and the gray-box approaches seem more suitable.

A typical gray-box approach is to first assume the structure of the system model based on laws of fundamental thermodynamics, and then estimate the system specific parameters with measured data, or using expert knowledge. A number of simulation software packages have integrated gray-box models for different components and subsystems. From those component/subsystem models, simulation platforms develop partial differential equation (PDE) systems at the whole building level. The equation systems are often solved to obtain the transient-state solutions (e.g. in TRNSYS [6]) or the quasi-steady-state solutions (e.g. in EnergyPlus [7]). Many researchers have adopted simulation techniques in the studies of building energy system controls. Morris *et. al.* built a test facility simulation model with TRNSYS, and used that simulation to examine the performance of temperature reset in reducing the cooling cost. They concluded that up to 51% of the total cooling load can be shifted to off-peak hours with the optimal temperature control [8]. Elliott coupled the computational fluid dynamic calculation with general purpose mechanical system simulation platform, ADAMS [9]. Mathews

and Botha constructed an HVAC system model on QUICKcontrol simulation platform [10]. They used that model to study the energy impact of component fault and degradation, as well as the performance of HVAC optimal operation strategies. Djunaedy *et. al.* connected a computational fluid dynamics module with a building simulation model, in order to get accurate result about the thermodynamic behavior of indoor air [11]. Xu and Zagreus [12], Xu and Yin [13] and Yin *et. al.* [14] used EnergyPlus simulation models to identify the optimal "precooling" strategy that can achieve most peak load reduction and least occupant thermal comfort loss. Trcka and Wetter *et. al.* from the Laurence Berkeley National Laboratory (LBNL) developed the Building Control Virtual Test Bed (BCVTB) which is able to couple a number of simulation software packages (such as EnergyPlus, Modelica, Radiance, MATLAB, etc.) as well as real BAS system or HVAC hardware [15-19]. Sagerschnig *et. al.* used BCVTB to link an EnergyPlus model of a large office building with MATLAB computing environment for simulation-based optimization [20]. Zhu *et. al.* used MLE+, which is a MATLAB program package derived from BCVTB [21], to couple EnergyPlus simulation evaluation with MATLAB global optimization algorithm [22]. Zhu *et. al.* linked building energy simulation with asset degradation and failure simulation in the study of building asset maintenance optimization [23]. Pang *et. al.* coupled an EnergyPlus model with real BAS (through BACnet protocol) for proof-of-concept demonstration of simulation-based predictive supervisory control [24]. Eisenhower *et. al.* used an analytical meta-model to extract the influential factors in a series of EnergyPlus models, and used the meta-model for control optimization [25].

In some other studies, where black-box modeling was used, the measured data were subject to statistical analysis and fitting to various statistical models or machine learning models. Compared to the simulation-based approaches, the data-driven model-based approaches demand less

engineering effort for model development and calibration. The optimization based on the black-box model is usually more computationally tractable than the simulation-based optimization. Popular data-driven modeling approaches include time-series model [26], Fourier series model [27], regression model [28], artificial neural network (ANN) [29-41], support vector machine (SVM) [42, 43] and fuzzy logic model [33, 38, 44-46]. MacArther *et. al.* fit the metered building energy consumption to a regression model to predict the building consumption profile [26]. Kreider *et. al.* enhanced the expert control system by ANN model for efficient and semi-automatic supervisory control [37]. Dhar *et. al.* used a Fourier series model to predict the heating and cooling load in a commercial building with outdoor air temperature [27]. Kajl *et. al.* combined ANN with fuzzy rule selection to evaluate building energy consumption [33]. Kalogirou and Bojic trained ANN models with simulated data, and used the network models to predict the energy consumption of a passive solar building [35]. Alcala *et. al.* applied genetic rule weighting and selection mechanism to construct a fuzzy logic controller for HVAC supervisory control [44]. Dong *et. al.* [42], Li *et. al.* [43] and Solomon *et. al.* [47] used SVMs to forecast building energy consumption with weather conditions. Yalcintas and Akkurt successfully used ANN to predict the chiller consumption in tropical climate [48]. Yang *et. al.* used adaptive ANN for on-line building demand prediction [41]. Their ANN is able to adapt itself to unexpected system changes through on-line accumulative training or sliding window training. Neto and Fiorelli compared an EnergyPlus simulation and an ANN model for the same building, and the conclusion was that both models are good for energy consumption forecast [39]. Zhou *et. al.* used a regression model to predict solar radiation, outdoor temperature and relative humidity, and the predicted weather was used in a gray model for building energy prediction [49]. Li *et. al.* used a hybrid genetic algorithm-adaptive network-based fuzzy inference system to forecast building energy

consumption [38]. Ferrieira *et. al.* used ANN based predictive control to optimize the indoor thermal comfort and energy saving [32].

1.4.1.2. Optimization Techniques

After a prediction model is developed, the model-based control problems will be formulated and solved by optimization algorithms. As stated above, the building energy system is a non-linear complex system whose analytical, physical model is difficult to obtain. Therefore, control optimization can only be performed with simulation models or black-box models. Wetter studied a wide spectrum of optimization algorithms in his doctorate dissertation [50], and later he compared the performance of optimization algorithms for EnergyPlus simulation-based optimization [51]. One of the important conclusions in his studies was that, due to the quasi-steady-state assumption and adaptive integration algorithm programmed in EnergyPlus engine, EnergyPlus simulation model is a discontinuous numerical approximation to the modeled system with respect to the design and control parameters, and the discontinuity can be substantial. The same issue exists in other quasi-steady-state simulation platforms. As a result, those optimization algorithms that require the system behavior to be continuous or smooth will not have good performance in these simulation-based optimizations. For example, in Wetter's study [51], when detailed simulation model was used, general pattern search (GPS), simplex algorithm and gradient based approaches all failed far from the optimal solutions. Instead, the evolutionary algorithms, such as genetic algorithm (GA) and particle swarm optimization (PSO), produced much better results.

In black-box model-based optimization, however, the selection of optimization algorithm becomes case dependent. For pure fuzzy logic model-based controllers, the optimization can only be done by brutal force search within entire rule spaces. Linear models are rare, and

therefore, linear optimization is usually seen in simple local control optimization problems. Non-linear models and non-linear optimizations are dominant in the HVAC model-based controls. Wang and Ma reviewed the non-linear local and global optimization algorithms in supervisory control application [52]. The strength and weakness of the optimization techniques are compared in [52].

Olafsson and Gopinath studied a new algorithm for simulation-based optimization with a finite but large number of decision variables [53]. In their algorithm, a "ranking-and-selection" approach was applied to significantly improve the performance of traditional adaptive random search. Chow *et. al.* used GA in their study of chiller control optimization [31]. Alcala *et. al.* applied GA on fuzzy logic rule base to select the optimal controls for HVAC systems [44]. Fong *et. al.* solved a simulation-based optimization problem for HVAC system control by GA [54]. Huh and Brandemuehl used complex search method to optimize the air-conditioning system operation parameters [55]. Yao and Chen studied decomposition-coordination algorithm in the HVAC control optimization [56]. The result showed that this algorithm and direct search algorithm found the same optimal solution, but decomposition-coordination algorithm works more efficiently in ultrahigh-dimensional optimization problems.

In Chapter 2, the author proposes a novel algorithm to solve the on-line optimization problem of the simulation-based controls for HVAC systems. In Chapter 3 and 4, existing and validated EnergyPlus simulation models are used to replace real buildings in data generation and testing. A class of ANN models, namely the non-linear auto-regressive network with external inputs (NARX), are used to develop system prediction models. To solve the control optimization problems, the dynamic programming technique is applied. The NARX prediction models, optimization formulation and solutions will be discussed in Chapter 3.

1.4.2 Power Grid and Electricity Market

Electricity is a form of secondary energy source. It is generated from a variety of primary energy sources (natural gas, coal, nuclear material, solar radiation, etc.) by power generation facility, transmitted and distributed by circuit network to the customers. Unlike other commodities, the delivery of electricity requires practically no time. With few exceptions, electricity is very difficult to store in bulk quantities. Therefore, the electricity supply and demand has to match exactly, in all locations and at all times. The supply/demand condition is reflected by the frequency on specific nodes. Under normal conditions, the frequency is maintained within a very narrow range around a certain level, indicating the balance between supply and demand. Imbalance of supply and demand will result in a frequency higher or lower than the defined level, which can potentially cause severe equipment damage.

However, meeting this requirement is challenging. First, the electricity generation needs considerable time to ramp up or down, which varies depending on the generation technology and plant operation condition. Second, a large portion of the demand is inelastic, meaning it is not sensitive to price changes, and difficult to predict. Third, there are physical constraints, security constraints and transmission loss in the transmission and distribution networks. Most importantly, uncertainty is ubiquitous in almost all elements of the energy system, for example, volatile fuel price, unstable wind and solar intensity, random outages of the equipment and unexpected peak demand due to human activity.

In this section, the demand and generation dispatching on the power grid will be discussed, followed by the background of electricity market operations.

1.4.2.1. Demand

Electricity demand is often characterized by base load and peak load. The base load is the demand that is stable in quantity throughout a period of time. For example, kitchen refrigeration and hot water generation constitute the base load of the vast majority of residential units. The peak load is the demand that appears during the peak consumption period of a day or a year, such as HVAC load in commercial buildings. The other loads are demand with less deterministic schedule and magnitude, such as home appliances. The aggregated load profile normally presents cyclic patterns. The daily and weekly cycles are obviously related to human activities; and the yearly cycle is usually a result of HVAC response to the seasonal change of the climate.

In general, electricity demand is not sensitive to short term price change (price inelasticity). The primary reason is that most customers, especially those residential and small commercial customers, do not receive dynamic price signals, as the flat rate and TOU rate dominate the retail markets. Another reason is that the major portion of individual demand is a necessity for their life or businesses. Only HVAC, lighting and some plug loads make the smaller portion, which may be used in response to price changes. However, in a longer term, demand can be much more responsive to price signals, including financial incentives provided by governments. The increasing installations of renewable on-site generation (wind turbines and photovoltaics), energy efficient lighting and expansion of the electric vehicle (EV) market are the most recent examples.

Because of its price inelasticity, demand forecasting becomes an important first step in the grid operation. Instead of individual building load prediction reviewed in Section 1.4.1, demand forecasting is conducted at an aggregated level. For example, a utility provider acts as buyer in the wholesale market. It procures electricity based on the predicted demand of all its customers. Therefore, the overall demand can be seen as a random non-stationary process composed of

tens of thousands of individual components. Individual components, i.e., individual customer demand, can be categorized into a number of groups, such as residential, commercial, industrial, as well as public or municipal uses. Each customer group can be further divided according to various demographic and economic factors – sizes, building types, business types, etc. Other than this, weather is the most important predictor that affects the hour-to-hour electricity demand. Almost all demand forecasting models involve weather factors either directly or indirectly (e.g. via time cycles). Similarly, social factors also contribute in certain cyclic (e.g., weekly pattern) or incidental (e.g., sport event) behaviors. A demand forecasting model is such a mathematical model that takes the historical data as well as forecasts of the aforementioned predictors and predicts the aggregated demand. A short-term forecast model usually predicts hourly or sub-hourly demands for a period of hours to days. A long-term forecast model predicts daily or monthly demand for a period of weeks to months, or, sometimes of years.

A large number of modelling techniques for demand forecasting have been reported. Several reviews are provided by Matthewman and Nicholson (1968) [57], Abu El-Magd and Sinha (1982) [58], Gross and Galiana (1987) [59], Moghram and Rahman (1989) [60] and Alfares and Nazeeruddin (2002) [61]. According to Alfares and Nazeeruddin, demand forecasting models can be grouped into nine categories: multiple regression, exponential smoothing, iterative reweighted least-squares, adaptive load forecasting, stochastic time-series, time-series models based on GA, fuzzy logic, ANN, and knowledge-based expert systems.

Forecasting the aggregated demand has been the only way of obtaining overall demand profile, which is required to enter the electricity wholesale market. Forecasting on the level of individual customers has been considered neither feasible nor necessary. The primary reason is that advanced forecasting requires investment in computation instrument and data access, which is

considered costly for individual customers, especially small households. Also, a model aggregating individual demand forecasts tends to have larger error than one predicting overall demand. The disadvantage of predicting aggregated demand is also obvious. Human behavior is the second major source of uncertainty (after weather) in demand forecasting and it varies substantially among customers. Aggregated techniques are unable to account for such uncertainty. When the utility provider uses this demand forecast to bid in the electricity market, it faces the quantity risk. The additional costs incurred by the quantity risk is shared by all the customers, by means of raising unit price. This is considered unfair, because it fails to distinguish the customers with predictable usage profile from the ones with irregular (hence uncertain) profile. Recent technical advancements in smart metering, internet-of-things, cloud data storage and computation have largely reduced the cost of home energy management systems. Especially with the provision of growing EV charging needs in residential and commercial communities, demand forecasting and management capability for individual customers will become a necessity.

Traditionally, the goals of the demand side management only include energy efficiency and peak load reduction. Various demand response (DR) programs and retailing tariffs are proposed/implemented to pursue these two goals, which will be detailed later in the "Retail Market" section (Section 1.4.2.3.C). Another important characteristic of the demand is its uncertainty. Demand uncertainty has been recognized in all studies about demand forecasting and many studies about stochastic optimizations for load scheduling. For example, in the studies of Samadi *et. al.* [62, 63], Conejo *et. al.* [64], Li *et. al.* [65] and Kim and Poor [66], the authors considered the uncertainty in residential demand when solving real-time load scheduling problems under time-varying prices. In the electricity wholesale market operations, demand

uncertainty is also considered as a major risk for both generation side and demand side. Ferrero and Shahidehpour studied the electricity procurement strategy considering the uncertainties in both demand and wholesale price [67]. Wang *et. al.* proposed oligopoly models describing strategic behavior in electricity markets with supply and demand uncertainties [68]. The uncertainty of demand is also considered when grid operators solve the unit commitment and real-time dispatch problems. Wu *et. al.* considered demand uncertainty when solving a stochastic model for the long-term security-constrained unit commitment problem [69]. However, in all those studies, the demand uncertainty is only considered as a set of statistical estimates, which are given and uncontrollable. There have been no studies, to the knowledge, that treat uncertainty as a controllable feature of the demand or set uncertainty reduction as a goal of demand side management.

In this dissertation, the author proposes to apply an economic measure to minimize demand uncertainty. Given that demand uncertainty is a source of risk in the wholesale market, uncertainty reduction is expected to reduce demand side risks and consequently reduce the customers' cost.

1.4.2.2. Transmission

Electric power transmission refers to the bulk transfer of electricity from generation facilities to substations near the end users. It is distinct from the local wires that transfer electricity from substations to individual customers, which are usually referred to as "power distribution". Electricity transmission is done through transmission networks, or "the grid". Most of transmission lines are high-voltage three phase alternating current lines. High voltage is necessary to reduce the energy losses in long distance transmission. As mentioned earlier, the supply and demand of electricity on the grid must be balanced all the time. This is a challenging task, as

many uncertain factors exist in both supply and demand ends, as well as the transmission grid itself. In North America (the US and part of Canada), most transmission lines are operated by Regional Transmission Organizations (RTOs) or Independent System Operators (ISOs). RTOs and ISOs only have subtle technical differences. This dissertation refers to them all as ISOs. There are 7 ISOs in North America: California ISO (CAISO), New York ISO (NYISO), Electric Reliability Council of Texas (ERCOT), Midwest Independent Transmission System Operator (MISO), ISO New England (ISO-NE), PJM Interconnection (PJM) and Southwest Power Pool (SPP). Most of ISOs are nonprofit organizations run under Federal Energy Regulatory Commission (FERC) and North American Electric Reliability Corporation (NERC). The main responsibility of ISOs includes: (1) coordinate the generation and transmission across the regional grid, and maintain supply and demand of electricity balanced; (2) operate the marketplaces for the trading of bulk electricity and some financial products; and (3) initiate long-term investment in generation and transmission infrastructure.

All dispatchable capacities within an ISO's jurisdiction form a power pool. To balance the supply and demand, ISOs dispatch the least costly capacity of the pool to meet the energy demand, while keeping the entire grid operating within the physical and reliability limits. The dispatch process has two stages: (1) day-ahead unit commitment, or day-ahead planning stage; and (2) economic dispatch, or real-time dispatching stage.

A. Day-ahead Unit Commitment

In unit commitment stage, ISOs determine what combination of generation units should be committed at each hour of the planning horizon (typically, 24 hours of the next day), based on the forecast of the hourly demand. This planning is often done on the day before the operation day, because some generators require up to several hours lead time before they can be brought

into service. Other physical constraints are also considered such as response time to the signal of changing output level, minimum and maximum output, minimum uptime and downtime, maintenance schedule, etc. The most important question is, given all of the above constraints, what unit combination incurs the least cost. The cost hereby includes fuel cost, non-fuel operation and administration cost. The overall per Megawatt-hour cost of each generation unit varies each hour, depending on many factors including, but not limited to, fuel prices and weather condition. Given the demand forecast, cost function of all units, and all constraints, the unit commitment problem that the ISO is trying to solve is a complex optimization problem with both integer and continuous variables [70-73]. A generic formulation given by [73] is as follows:

Decision variable: P_{it}

Minimize:
$$OC = \sum_{i=1}^{N}\sum_{t=1}^{T} FC_{it}(P_{it}) + MC_{it}(P_{it}) + ST_{it} + SD_{it} \quad \text{Eq. 1}$$

Subject to:
$$FC_{it}(P_{it}) = a_i P_{it}^2 + b_i P_{it} + c_i \quad \text{Eq. 2}$$

$$MC_{it}(P_{it}) = IM_{it} P_{it} + BM_{it} \quad \text{Eq. 3}$$

$$ST_{it} = TS_{it} + [1 - \exp(D_{it} / AS_i)]BS_{it} + MS_{it} \quad \text{Eq. 4}$$

$$SD_{it} = K_i P_{it} \quad \text{Eq. 5}$$

$$\nabla P_{it} \le \nabla P_{it,\max} \quad \text{Eq. 6}$$

$$\sum_{i=1}^{N} P_{it} = \hat{D}_t + loss_t \qquad \text{Eq. 7}$$

Generator output limit constraint

Reactive power limit constraint

Voltage limit constraint

Phase angle limit constraint

Transmission thermal limit constraint

"Must up/down", "Spinning Reserves" and "Crew Limit" constraints

where,

P_{it} denotes the power output of plant i (i=1, 2, 3, …, N) at time t (t=1, 2, 3, …, T);

In Eq. 1, the overall operational cost (OC) is formulated as the summation of fuel cost (FC, maintenance cost (MC), startup cost (ST) and shutdown cost (SD);

In Eq. 2, fuel cost (FC) is formulated as a quadratic function of power output;

In Eq. 3, maintenance cost (MC) is a linear function of power output;

In Eq. 4, startup cost (ST) includes fixed cost of turbine start (TS), variable cost for boiler start (BS, assuming exponential cool down process) and fixed maintenance cost for a start (MS);

In Eq. 5, shutdown cost (SD) is proportional to power output;

Eq. 6 defines the ramp limit;

Eq. 7 defines the load balance with offset term (*loss*);

Since the 1980s, there has been a trend of restructuring and deregulation of energy markets. In restructured or deregulated markets, generation units offer their bids to supply the demand. A bid is consisted of a cost function and some operational constraints of the unit. The final market clearing price is set by the maximum cost of the committed generation units, i.e. the locational marginal price (LMP). All committed units are required by contract to supply the specified quantity of electricity at the specified time, and will be paid at LMP rate. In this case, the previous objective that minimizes operational cost does not guarantee lowest prices. Instead, a new objective is adopted which is to maximize the profit (i.e., the revenue minus the operational cost) [74], as shown below [75]:

Decision variable: P_{it}

Minimize: $$J = \sum_{i=1}^{N}\sum_{t=1}^{T}(P_{it}C_t) - OC \quad \text{Eq. 8}$$

Subject to: $$\sum_{i=1}^{N} P_{it} \le \hat{D}_t \quad \text{Eq. 9}$$

Eq. 1~Eq. 6

Generator output limit constraint

Reactive power limit constraint

Voltage limit constraint

Phase angle limit constraint

Transmission thermal limit constraint

"Must up/down", "Spinning Reserves" and "Crew limit" constraints

where,

in Eq. 8, the profit (J) is defined as the total revenue minus operational cost (OC). And the revenue is calculated as the power output (P) multiplied by forecasted LMP (C);

in Eq. 9, a softer demand constraint replaces the previous load balance constraint (Eq. 7), as has been explained in [74].

Many modifications are made to the above generic formulations in different studies. For example, the formulations of fuel cost, maintenance cost, startup cost and shutdown cost (Eq. 2~Eq. 5) can be replaced by different models. Besides generation units, the scheduling of other types of power injection can also be considered, such as imports from other utilities and purchases from distributed generation [76].

A wide spectrum of numerical optimization techniques has been adopted to solve the unit commitment problem, including Exhaustive Search, Priority Listing, Dynamic Programming,

Integer Linear Programming, Branch-and-Bound, Lagrangian Relaxation, Interior Point Optimization, Taboo Search, Simulated Annealing, Expert System, Fuzzy System, ANN, GA, Evolutionary Programming, Ant Colony Search and various hybrid models. Comprehensive review can be found in [73].

B. Real-time Dispatch

Similar to unit commitment, the objective of real-time dispatch is to achieve the most efficient (minimum cost or maximum profit) scheduling of generation and to meet the demand. But real-time dispatch is required to respond in (near) real-time. Due to many uncertainties, the actual demand and generator operating conditions may be different from the forecast in day-ahead unit commitment. The grid operator has to adjust the generation dispatch accordingly. The adjustment is done by automatic generation control. The idea is the dispatchable generators with the lowest marginal cost should be used first. And the marginal cost to serve the last Megawatt demand sets the real-time market price. Figure 1 illustrated a typical power pool of an ISO. All generation units are sorted by marginal generation cost and represented by dots in the chart of marginal cost versus cumulative generation. This type of curves is usually referred to as "generation stack" or "supply stack".

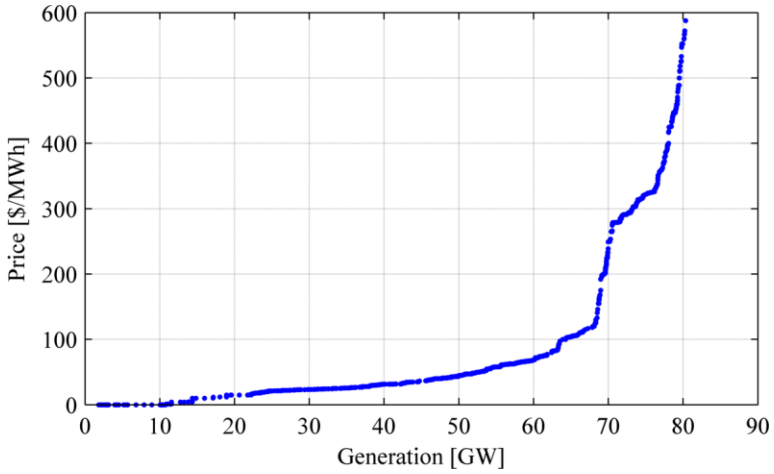

Figure 1 Typical generation stack of an ISO

Since the last dispatched unit defines the price, price spikes may occur when no more low cost generation is available for dispatch. Therefore, it is beneficial to maintain a set of relatively low cost generation units (called "operating reserves") whose output level can be quickly adjusted ("spinning reserves") or can be brought up online in short notice ("non-spinning reserves"). Some ISOs have DR programs called "Direct Demand Curtailment" that allows the operator to control certain demand directly.

Similar to real-time dispatch, some scholars have proposed "environmental dispatch" which adds environmental cost minimization as another objective of the optimization [77-79].

1.4.2.3. Market Operation

The solution to the day-ahead unit commitment and real-time dispatch problems relies on the realization of the cost function of each generation unit. There are two approaches by which the generation cost can be determined. In traditionally regulated markets, the utility companies are usually naturally formed monopolies that have vertical market power, which means the companies own generation plants, transmission lines, distribution networks and access to

customers. Such markets are noncompeting but their operation has to comply with regulations. The generation costs in these markets are calculated by the utility companies. This is called "cost-based rate", which may include the capital cost, fuel cost, maintenance cost, tax and administrative expenses. The grids in Southeast, Southwest, Inter-Mountain West and Northwest regions operate in this manner.

Grids in other regions are using market-based approach. The ISOs organize regional markets that are open to generators, utility providers (also known as load serving entities, or LSEs) and transmission customers. The generation cost is resolved in competing auctions among generation units. Corresponding to the day-ahead unit commitment and the real-time dispatch problems, regional markets also have day-ahead and real-time components, together with several more sophisticated markets where various hedging arrangements can be traded, such as swing contracts, virtual bidding, financial transmission rights, call options and put options. The price calculation in both day-ahead and real-time markets is based on the concept of LMP [80], which is defined as the marginal price at a specific location and a specific time. The resulting LMPs have incorporated: (1) energy generation cost with optimal dispatch, (2) locational congestion cost, and (3) transmission loss marginal cost.

A. Day-ahead Wholesale Market

The day-ahead market is a forward market in which hourly clearing LMPs are determined for each hour of the next operating day based on submitted generation offers, demand bids, increment offers, decrement bids and bilateral transaction schedules. A typical sequence of day-ahead market operation is as follows:

- The utility providers submit hourly demand schedules for which they commit to purchase the electricity at day-ahead LMPs. They may also submit decrement demand bids which define the demand quantity with various LMP ranges;
- The generators submit unit availability schedules, self-scheduled generation and supply offers. The supply offers are increment generation levels conditioned with LMPs. Certain system parameters are also required in offer submission, including the minimum and maximum output level, minimum and maximum uptime/downtime, lead time, etc.;
- The transmission customers may submit bilateral transaction schedules;
- The grid operator solves the day-ahead unit commitment problem and determines the generation dispatch schedule for each generation unit, quantity schedule for each utility to purchase, together with the corresponding day-ahead LMP schedule. The resulted schedules consist of financially binding commitments of the generators and the utility providers.
- Day-ahead accounting settlements for these contracts are performed: the generators are obligated to inject electricity of the quantity specified in the day-ahead schedule, and get paid based on the generation bus day-ahead LMPs; the utility providers are obligated to withdraw the electricity as determined by the day-ahead schedule, and pay based on the load bus day-ahead LMPs.

Such design of day-ahead market ensures all market participants have the opportunity to schedule generation, consumption and transmission activities in advance, and largely mitigate the price risk in real-time operation. The supply offer competition, together with unit commitment optimization, lead to the most efficient grid operation, while the involvement of

generator physical operating limitation, transmission capabilities and reserve requirements ensures robust operation of the system.

B. Real-time Wholesale Market

The real-time market is also called balancing market. After the day-ahead market has been cleared, those generation resources that are selected by day-ahead unit commitment will carry their supply offers into the real-time market. Generators that are available, but not selected or have extra capacities, are able to submit modified offers to the real-time market. During each hour of the operating day, at a specific time interval (e.g., 5 minutes as in PJM market), real-time LMPs are calculated for all generation and load buses. Real-time LMP calculation considers a series of input data that reflect the actual real-time operating conditions. Such input data include the latest supply offers, dispatchable external transactions, current and past grid conditions and updated constraints for generation and transmission. The grid operator will solve a real-time dispatch problem to determine what additional generation resources or external transactions should be involved to meet the projected system demand in the next time interval (e.g. 5 minutes). The real-time LMPs are set by the most costly generation/transaction needed by the optimal dispatch to meet the last unit of demand.

Real-time market financial transactions are settled at real-time LMPs. Real-time accounting settlement is separated from the day-ahead market settlement. Utility providers will pay for the demand that exceeds their day-ahead scheduled quantities, or will receive payment for the deviation if demand is lower than the day-ahead scheduled quantities, based on real-time LMPs of corresponding load buses [80]. Generators will get paid for the electricity that is more than the day-ahead scheduled quantities, or will pay for the deviation if generation is lower than the day-ahead scheduled quantities, based on real-time LMPs of corresponding generation buses

[80]. Transmission customers pay congestion charges for bilateral transaction quantity difference from day-ahead schedules, based on the real-time LMPs [80].

The real-time market provides strong financial signals to generators and drives electricity generation to adjust according to the actual demand and grid conditions. In well designed and operated markets, the real-time LMPs are converging towards day-ahead LMPs [80]. Greater price convergence between day-ahead and real-time markets suggests higher efficiency in grid operation.

C. Retail Market

Electricity retailing deals with the distribution of electricity from substations to end-use customers. Historically, most retail markets are dominated by naturally formed monopolies. Customers in those markets do not have alternative choices for electricity supply. In recent years, competition in electricity supply has been introduced in many countries, such as Norway, the United Kingdom, Australia, New Zealand and the entire European Union. In the US, by 2010, 17 states and the District of Columbia have adopted electric retail choice programs that allow customers to buy electricity from competitive retail suppliers. Introduction of competition in electricity retails was considered beneficial for market health, technology and service innovations and lower generation cost [81, 82]. However, the experiences of retail competitions tell a different story. In most European countries, the customer switching rates are very low – below 10% in many counties, like Italy, Denmark, France, Germany, Netherlands and Belgium. And 85 to 95% of electricity is provided by incumbent companies, rather than new entrants [83]. In the US, electric retail choice programs are most welcome by large commercial and industrial customers, however, the participation rates in residential customers are low in almost all of those states [84]. A 2005 report from US FERC attributes the low participation to absence of

incentives for suppliers to enter the retail market [85]. On one hand, most states require utilities to sell electricity at regulated retail prices, therefore, market competition has a limited role in setting the price. On the other hand, the electricity wholesale price has been increasing during the test period, but the regulated retail price failed to follow this trend. Defeuilley argues from the perspective of customers that the cost for switching suppliers is potentially high [83]. This cost includes transaction cost (contracting and negotiation), search cost (looking for a better supplier) and learning cost (becoming familiar with the new service). Defeuilley also adds that electricity retailing itself does not generate significant revenue, and homogeneity of the good results in limited innovation in value-added services, which makes it difficult to offer any differentiation. Therefore, the *status quo* is that most electricity retail markets are non-competing and subject to regulation. Most studies are focusing on improving the market efficiency and reliability by introducing better design of rate structure or demand side management into regulated retail markets.

Flat rates are most commonly implemented in the retail markets. The utilities sell electricity to the customers at a fixed price defined by service agreements. This price typically represents the average cost of generating and delivering electricity, and it is not updated frequently. Fixed retail price leads to disconnection between retail and wholesale markets, which has been considered by most scholars as the primary cause of unusual price spikes in wholesale markets [86]. With fixed price, the customers are not exposed to the dynamics of the wholesale market. When there is an imbalance between supply and demand (e.g., unit outages and transmission congestion), the customers are unable to adjust their demand accordingly. Costly generation units have to be brought online, sending spot price roaring. This explains the price spikes of June 1998 (a $7,500/MWH bid) and July 1999 (a $10,000/MWH bid) in the wholesale market of the Midwest.

From December 2000 to January 2001, the electricity spot price in the CAISO market reached $1,400/MWH and triggered 2001 California Electricity Crisis. Although many coincidental events have been blamed to cause this crisis, such as drought, delayed construction of new plants and market manipulations, the fixed retail price became the top of the tier. This crisis drove Pacific Gas and Electric and Southern California Edison into bankruptcy because they purchased electricity at extremely high spot prices and sold at low fixed rates. In fact, using fixed prices, the utility companies have to absorb full risks in wholesale markets, including price risk, quantity risk, as well as regulation risk [87]. It is commonly agreed since the crisis that demand side participation is necessary to maintain system stability. How to reform the power industry towards more and better demand response (DR) has become a hot topic.

DR, as defined by FERC, is "*changes in electric usage by end-use customers from their normal consumption patterns in response to changes in the price of electricity over time, or to incentive payments designed to induce lower electricity use at times of high wholesale market prices or when system reliability is jeopardized.*"[88] In response to the stress on the grid, the electricity customers have basically three types of choices. They can reduce the demand (i.e. load shedding) by turning off some electrical equipment. Or, they can reschedule energy uses from peak periods to off-peak period (i.e. load shifting). Some customers may choose to bring on on-site generators to reduce the net power draw from the grid [89].

DR programs have been established by almost all ISOs in the US. Generally, these programs can be classified into incentive-based programs (IBPs) and price-based programs (PBPs) [89, 90]. IBPs pay participating customers to reduce their loads upon requests by grid operators. The classical IBPs reduce the customer loads through direct load control or using interruptible loads. Direct load control allows the grid operator to remotely shutdown participating customers' equipment on a short notice, while interruptible load programs ask customers to reduce net

demand to a predefined level. In these two types of IBPs, the participating customers usually receive payment upfront in the form of bill credit or reduced rate. Market-based IBPs also exist, such as emergency DR program, demand bidding, capacity market and ancillary services market [89, 90]. Emergency DR pays customers incentives for measured load reduction during grid emergencies. Demand bidding lets customers who are capable of load reduction participate as negative demands in electricity wholesale markets. Capacity market allows customers to submit load reduction capacity as supply offer in the wholesale market. In the ancillary services market, customers can bid load curtailment in the spot market as operating reserves.

Some PBPs, on the other hand, incur demand charge on the maximal demand during a billing cycle in addition to the usage charge. The demand charge rate is given and fixed. This demand charge structure drives customers to reduce peak load and avoid demand spikes. More PBPs now use time-varying price to convey the information of supply/demand relation in the wholesale market. The three basic dynamic pricing structures are critical peak pricing (CPP), TOU and RTP. With CPP, the utility is permitted to declare peak periods on short notice, a few times in a year. During the peak periods, electricity price is very high due to observed high demand. The total number of peak period declarations is limited by agreement. The price during peak periods can be fixed (CPP-F) or variable (CPP-V). In TOU pricing, the peak periods, off-peak periods and normal periods within a day or during a year are defined by agreements, corresponding price for each period is also defined. With RTP, the retail price updates in real-time (actually every 5 to 60 minutes) following the dynamics of the wholesale spot price. The performance of time-varying pricing is studied in a number of simulation and implementation experiments.

Caves, *et. al.* reported that exposure of a small portion of retail loads to real-time market can provide significant price relief and stability [86]. They also recognize the diversified price elasticity of customer demand. Customers with higher elasticity may benefit from dynamic prices, while those with less flexibility can choose to stay with fixed price.

Faruqui and George analyzed the result of California's Statewide Pricing Pilot experiment, and claim that dynamic rates (CPP and TOU) are able to reduce the peak demand of residential and small to medium commercial and industrial customers, but the effect varies depending on many factors [91].

In another experiment carried out by NYISO, price-responsive load programs were established to offer customers limited and highly structured participation in the wholesale market. The result showed that the participation of customers in wholesale markets helps the system prevent forced outages when demand is high [92].

Kirschen showed that customer price elasticity is a critical indicator of the demand responsiveness towards market dynamics [93]. Increasing short-run elasticity may improve the operation of markets. However, the author also acknowledged that enhancing customer elasticity is not an easy task.

Borenstein studied the long-term efficiency gain from TOU and RTP using simulation [94]. He reported that even with relatively low price elasticity, the long-term efficiency gain from RTP is still significant. TOU can only capture a very small share of the efficiency gains from RTP.

Allcott conducted simulation studies which exposes customers to PJM wholesale markets [95]. The author discovered that the customer demand tends to be price sensitive, and the net response to peak price would be conservation of energy rather than delayed consumption.

The real-time price elasticity of customers has been estimated using data collected from different countries or regions, for example, Gulf Cooperation Council countries [96], the US [97], Cyprus [98], Taiwan [99], Israel [100], Netherlands [101, 102], Sweden [103] and India [104]. Although it is reasonable that customers with different cultural backgrounds may have diverse elasticity, all results show that the customer elasticity is generally low. Lijesen argues that low elasticity is due to lack of awareness of real-time prices [102]. The implication of this argument is, in order to achieve the full benefit of dynamic pricing, technical investment in load and price monitoring will be necessary.

Moreover, the price responsiveness also varies by end uses. End uses like refrigerator are not elastic at all. Other end uses may have distinct elasticity to TOU and RTP. For example, customers are likely to accept delayed use of microwaves; therefore, such loads have a higher elasticity to both TOU and RTP. As a contrast, building HVAC systems have restrictions that prevent complete shutdown. So planning in advance will be needed to minimize energy cost while meeting all operational requirements. As a result, HVAC loads can be elastic to TOU, but not so much to RTP. Recognizing the variation of elasticity among end uses suggests that it is possible to achieve the maximum elasticity by applying hybrid rate structure of TOU and RTP, such as day-ahead retail pricing (DAP).

Mohsenian-Rad and Leon-Garcia studied the optimal control of residential load under RTP combined with inclining block rates. They concluded that the capability of price prediction is

necessary to achieve optimal load control under RTP. Even a rudimentary weighted average price prediction can help in load scheduling and minimize the energy cost [105].

Goldman *et. al.* studied the DR strategies for customers in government, education, public works, commercial, healthcare and manufacturing. They found that public works customers have the lowest substitution elasticity while manufacturing customers are most responsive to the price. Reasonably, DR strategies differ among the studied customer groups too [106].

As mentioned before in the "Demand" section (Section 1.4.2.1), all the existing DR tariffs are designed to send proper signals to the customers so that the customers are able to respond to the supply/demand condition on the grid. The demand side management under those tariffs are targeting to energy saving and/or peak load reduction. Although, the importance of demand uncertainty has been well recognized in load scheduling, market strategy and grid operations, the current demand side management practices do not include uncertainty reduction into its objective. No rate structure has been proposed to promote such controls. In this dissertation, the author proposes a new retail rate structure, called CfD, which incurs charge on the deviation between the customer's actual demand and the day-ahead plan. By charging on the demand deviation, CfD is expected to force the customers to keep a predictable consumption manner, and thus reduce the demand uncertainty that is caused by human behavior. Given that quantity risk is a major risk that the utility providers (or the community microgrids) are faced in the wholesale markets, CfD is expected to lower that risk, and, in the end, reduce the energy cost.

1.4.3 Microgrid

The concept of microgrid emerged when the potential of distributed generators (DGs) became recognized [107, 108]. In order to better utilize DGs, Lasseter *et. al.* proposed a system approach

that views a cluster of distributed generators, storage and associated loads as a subsystem, which can operate either in connection with utility grids or as an isolated smaller network [107, 108]. According to USDOE Microgrid Exchange Group, a microgrid is defined as "*a group of interconnected loads and distributed energy resources within clearly defined electrical boundaries that acts as a single controllable entity with respect to the grid. A microgrid can connect and disconnect from the grid to enable it to operate in both grid-connected or island-mode*". As illustrated by Figure 2, a typical architecture of a community microgrid consists of residential loads (individual households), non-residential building loads (e.g., restaurants, stores), public facility loads (e.g., street lights), DGs (e.g., PV panels, wind turbine, gas turbines, etc.), community energy storage (CES), connecting lines (including circuits, feeders, breakers and fuses), controllers (microgrid central controller, DG controllers and load controllers) and communication instruments. The microgrid is connected at low voltage, and interfaces with the utility grid through point of common coupling (PCC).

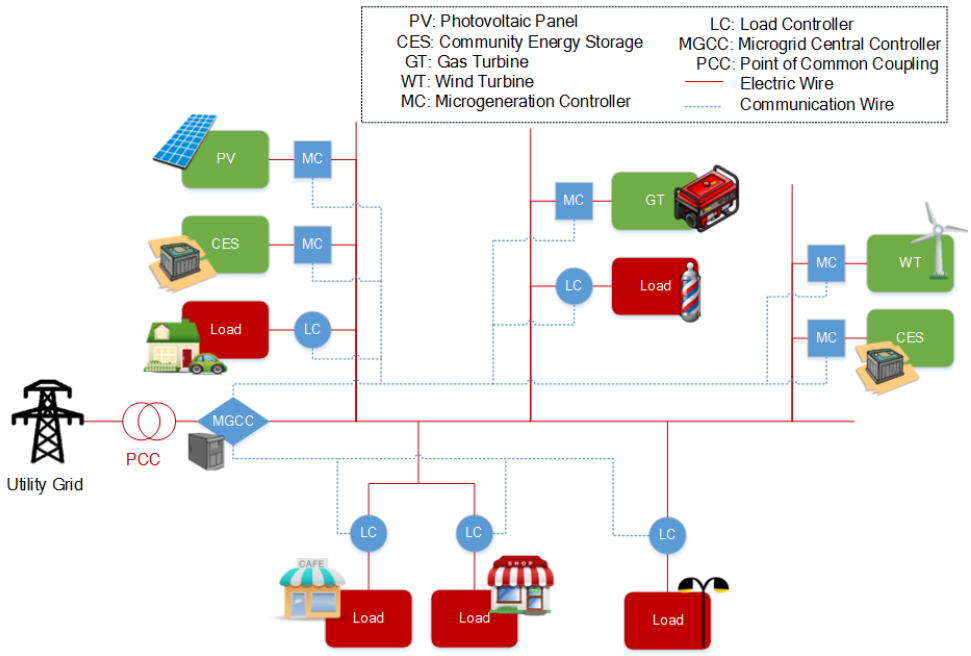

Figure 2 Typical architecture of a community microgrid

Compared to the traditional utility grid, a microgrid has a lot of benefits. First of all, it enhances the reliability and security of the grid operation. Traditional utility grids are vulnerable to component outages, transmission congestion and sabotage. When the grid is experiencing stress, for example, in a heat wave, outage of one node can easily get propagated to other nodes, causing a massive blackout. In such circumstances, part of the grid being able to isolate itself and operate without interruption will be attractive, especially for mission-critical operations. A few successful examples were reported after Hurricane Sandy striking the Mid-Atlantic region in 2012. During the hurricane, the local grid failed, and the microgrid at Federal Drug Administration research facility in Maryland switched into island mode, relying entirely on natural gas turbines for two and half days without interruption [109]. Princeton University campus in New Jersey isolated its grid from the utility grid, and sustained for three days with about 11 Megawatts total on-site generation. Second, as DGs co-localize with loads, the transmission loss will be minimal, the power quality can be improved, and heat exhaust produced by power generation can be reused locally by combined heat and power (CHP) equipment, which significantly increases the overall energy efficiency. Third, the use of renewable energy substantially reduces the fuel cost and carbon emission in power generation. Fourth, microgrid promotes distributed load control and generation control, as well as cooperation between customers, driving the innovations in optimal energy management of the microgrid. Intelligent controls are particularly important in the context of dynamic pricing. And last but not least, a microgrid can be seen from the grid operator's point of view as one entity. More cost reduction can be expected if microgrid actively participates in the operation of the utility grid and electricity markets. When microgrid is in connection with the utility grid, and microgrid load is low, microgrid may act as a net generation unit and submit a supply offer into the wholesale market. Also, with advanced load controls,

microgrid will be able to submit demand bids. Cost reduction comes from sales of both energy and ancillary services.

Considering these benefits, microgrids are particularly suitable for commercial/industrial campuses, military bases, remote "off-grid" campuses and residential communities. However, microgrid also poses several challenges, including islanding protocols, standards, communication protocols, privacy concerns and instrumental cost. Moreover, several technical problems are also challenging: (1) reliable and seamless transition between grid-tied and island modes is technically difficult; (2) voltage and frequency control becomes difficult when complex generation and load situation is encountered; (3) bulk energy storage is still relatively expensive; (4) energy management of intermittent generation by renewables (PV panels and wind turbines) is still an actively studied topic; (5) with increased possession of electric vehicles (EVs), EV charging poses tremendous stress to the microgrid infrastructure; and (6) strategy and techniques for microgrid's participation in the energy market.

In microgrids, distributed control coupled with networked communication has enabled collaborative energy management. The collaboration is often accomplished by bidding and in a hierarchical manner. For example, a common practice to solve competing EV charging demand problem is as follows: each EV charging controller maintains its own utility function together with a list of operational constraints. All charging controllers submit their utility functions and constraints to a higher level coordinator who aggregates all the demand bids, solves an optimization problem maximizing the overall utility within all constraints, and then dispatches the charging [110]. Similar solutions have been adopted in load scheduling control within a building [111], DG generation [112] and storage charging/discharging [113], among other microgrid applications.

In this dissertation, the microgrid operation under CfD creates opportunity for the customers to collaborate in tracking their demand schedules. Such collaboration can be accomplished in various ways, including a centralized tracking control and a distributed tracking control. The centralized tracking control is conducted by the higher level coordinator, or the MGCC in this case, similar to the hierarchical system mentioned above. And the distributed tracking only involves two customers, one of which plays as the buyer and the other is the seller. The transaction is determined in a proposal-approval fashion between the two parties. Details will be discussed in Chapter 4.

A selection of microgrid literatures are reviewed in the following.

Heydt studied the impact of EV charging to the power grid in 1983 [114]. The author pointed out that, on-peak or near-peak recharging is an important factor to consider in EV deployment. He suggested load management that shifts on-peak charging to off-peak period.

Lasseter described the earliest architecture design of microgrid and a conceptual design for load management and protection [107, 108]. He also proposed a basic approach of voltage and frequency regulation through droop.

Dimeas and Hatziargyriou proposed an agent-based control scheme for the microgrid operation [110]. This is a decentralized approach where entities are represented by agents at three levels: utility grid/market operator, microgrid central controller (MGCC) and local controller (load controller or generator controller). Each agent has its own input, output and decision criteria. Higher level of agent coordinates the microgrid operation by conducting market-like auctions and negotiations. This system was tested by both simulation and laboratory environment.

Katiraei *et. al.* studied the autonomous operation of microgrid during and subsequent to islanding [115, 116]. The authors used a generation unit that is interfaced via a power electronic converter, which has independent real and reactive power control to maintain angle stability and voltage quality within the microgrid. The author concluded that the presence of an electronically-interfaced generation unit can ensure stability of the microgrid.

Guttromson *et. al.* studied the detailed load modeling for residential units, including the explicit models for HVAC and non-HVAC appliances [117]. The models considered such exogenous factors as weather, grid voltage and frequency, fuel prices, etc. The models are implemented in a packed simulation environment named Power Distribution System Simulation.

Chassin *et. al.* from USDOE's Pacific Northwest National Laboratory developed GridLAB-D, an open-source power system modeling and simulation environment [118-121]. This platform incorporates generation modeling, power flow modeling, end-use modeling, dynamic pricing and demand response, and market operation. It is also capable of integrating with other existing simulation tools.

Galus and Andersson did simulation studies on demand management of grid with large amount of EV charging [122]. In their model, each charging EV is represented by an independent agent that solves its own optimization decision problem. All EVs are connected to an energy hub that has multiple energy sources. An EV manager agent is managing the charging activities of all EV agents, by implementing a non-linear pricing scheme and optimization. The optimal dispatch maximizes the total utility of the EV agents connected.

Shi *et. al.* simulate prototype microgrid operations for urban area and rural area of China [123]. The simulation was conducted on the platform of MATLAB/Simulink. The model simulates

both steady and dynamic characteristics of the three phase microgrid prototype. Various operation modes and possible disturbances have been taken into account during the simulation.

Badawy *et. al.* reviewed two approaches of agent-based demand side management: a price-based control (indirect control) and direct load control [124]. The price-based control relies on a hierarchical system that passes market signals (price) through coordinator agent, local controller agents and device controller agents. At each control level, the coordination is done through auctions and negotiations. Non-market-based control is conducted by a higher level controller maximizing the overall utility, while the utility function of each lower customer is generated by the lower controller agent. The author concluded that both approaches are able to achieve the goal, but both have strengths and weaknesses.

Huang and Liu applied a self-learning, neural network-based mechanism to manage residential energy use [125]. Special emphasis was put on home battery use in connection with the microgrid. The proposed management scheme is able to improve the performance as it learns from the real-time operation and environment. Simulation studies demonstrated the financial benefit gained from this management scheme.

Li *et. al.* investigated the optimal demand response of households towards dynamic pricing [65]. Each household solves an optimization problem that maximizes its individual net benefit subject to consumption and power flow constraints. The utility company solves another optimization problem to determine the optimal price to maximize social benefit. The authors proposed a distributed algorithm for both utility and households to jointly determine the optimal price and demand schedule.

Tanaka and Maeda proposed a simulation-based design method for microgrids with energy storage [126]. This designing method consists of a time-marching simulation with an energy storage management algorithm and the evaluation method for the microgrid. The method was implemented to optimize the design of the resort community.

Vuppala *et. al.* brought up the argument of fairness in microgrid demand response [127]. With fairness in consideration, the authors proposed a simplified pricing model which, according to the simulation experiments, is fair and is able to flatten the demand curve.

Zhu *et. al.* studied demand management problem in community microgrid, with home EV charging and community energy storage in the system [128]. The authors showed that EV charging significantly influences the microgrid peak load, while the combination of a number of demand management strategies could effectively alleviate the peak load by as much as 8%.

Widergren *et. al.* presented their preliminary findings in a residential DR control demonstration project [129]. In this project, an RTP retail tariff was implemented to a community microgrid. The microgrid demand management is accomplished by distributed load scheduling of individual customers, and real-time bidding transactions of supply and demand.

1.5 Summary

The main objective of this dissertation is to propose and demonstrate the new CfD retail pricing. This new pricing is designed to minimize the demand uncertainty of individual customers. It introduces the concept of uncertainty reduction into demand side management. Under CfD, the customers are going to share the quantity risk in the electricity wholesale market, while the price risk is left to the utility providers. Such risk sharing is considered to be fair and efficient. This

chapter reviews the background about building energy system modeling and control optimization, power grid operation, electricity market and microgrid. Literature reviews are provided in those fields.

The rest of this dissertation is organized as follows: in Chapter 2, a simulation-based optimization technique is demonstrated for HVAC demand response. Chapter 3 studies the day-ahead planning and real-time tracking control optimizations in a single building, under CfD. Chapter 4 examines CfD within a microgrid environment. Its effectiveness of reducing overall cost and promoting collaborative demand management will be investigated.

Chapter 2 Simulation-Based Optimization for HVAC Demand Response

Abstract

Model-based control optimization is crucial for buildings to reduce cost under time-varying price-based DR. Detailed simulation is a powerful gray-box modeling tool but suffers from intensive computation requirement, and therefore, is challenging to use for on-line planning applications. In this chapter, the author presents a novel two-stage approach, named Optimal Strategy Pool (OSP). This approach moves time-consuming simulation evaluations to off-line as much as possible. It creates a compact set of candidate solutions (i.e., the optimal strategy pool), based on clustering guided, off-line evaluations, and hence minimizes the requirement for on-line simulation evaluations. The case studies with both small and large solution spaces all demonstrate that OSP is superior to traditional genetic algorithm and other heuristic methods, in terms of greater efficiency and robustness, for on-line planning optimization.

2.1 Introduction

Simulation is a gray-box modeling approach in the building energy domain. With simulations, the system operation and control processes can be described with considerable details and also with high accuracy. For this reason, simulation tools have received increasing attention in recent years, for the purpose of design verification as well as code compliance. However, using simulation models in model predictive control (MPC) faces significant obstacles. First of all, running simulation models is usually very time consuming. Secondly, in simulation-based optimization, there exists no system model in analytical form, so any algorithm that requires computation of Hessian matrix or gradient cannot apply directly. Wetter and Wright [51]

compared different optimization algorithms for the performances in simulation-based optimization. They concluded that, simulation evaluation introduces significant discontinuity (2% as reported) to the objective function. Because of this discontinuity, those algorithms requiring objective function to be smooth, such as GPS and gradient-based approaches, all failed far from the optimum. Instead, heuristic search methods such as PSO and GA obtained better optimal solutions with a relatively small number of simulation evaluations. Even with such algorithms as PSO and GA, it still takes a long time to find a suboptimal solution for a moderate size simulation-based control optimization problem. This is why simulation is rarely seen in any on-line applications, as on-line decision making requires problems to be solved in a relatively short time.

This chapter addresses the problem of simulation being too time-consuming for simulation-based on-line control optimization. The rest of this chapter is organized as follows: In Section 2.2, the control optimization problem for HVAC demand response is formulated; Section 2.3 explains different optimization techniques studied in this work, including a novel approach named Optimal Strategy Pool (OSP); Section 2.4 presents a case study that implements OSP optimization in on-line strategy selection; and some arguments are made in Section 2.5.

2.2 Problem Formulation

A simulation-based on-line optimization problem for HVAC DR control is studied in this chapter. The subject building is assumed to be a large commercial building equipped with advanced BAS. The building owner has signed into a DR program with the utility, which allows the utility to declare CPP a few times in a year, for the expected peak period in the next day. The

electricity price during the peak period will be significantly higher than usual. Figure 3 shows a simplified CPP price schedule used in this study.

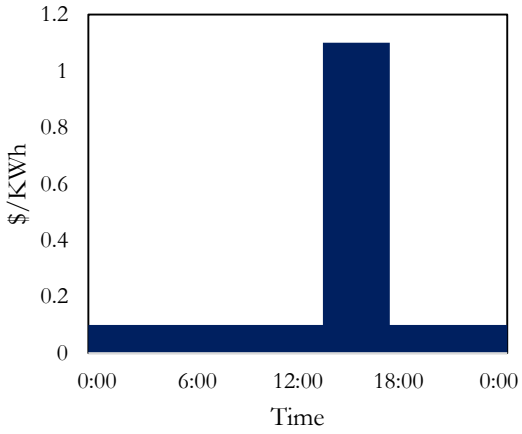

Figure 3 Simple CPP rate schedule

Under this price schedule, the building operator is motivated to plan in advance to lower the energy usage during the peak period, in order to minimize the energy cost. Another objective of the control optimization is to minimize the thermal comfort loss, as measured by Fanger's Predicted Percent of Dissatisfied (PPD) [130]. One way of consolidating multiple objectives into one objective function is by weighted sum (Eq. 10).

$$F = w_c \bar{c} + w_u \bar{u} \qquad \text{Eq. 10}$$

where,

c denotes the energy cost;

u denotes the thermal comfort loss;

$\bar{c}$ and $\bar{u}$ are energy cost and thermal comfort loss after min-max normalization, respectively;

w_c and w_u are the weight coefficients of energy cost and thermal comfort loss, respectively. Choosing the weights is up to the building owner's decision.

2.2.1 Subject Building and Simulation Model

In this chapter, a large education facility in Berkeley, California, is used as the subject (Figure 4). The subject building has 7 floors and total of 141,000 square feet conditioned area, hosting research labs, offices, auditoriums, etc. There are 135 zones, 6 Air Handling Units (AHUs), 110 Variable Air Volume (VAV) terminals, 1 electrical chiller, 1 absorption chiller, 2 cooling towers and other HVAC components. All HVAC systems are operating with 24×7 schedules.

A detailed simulation model is developed by Yin *et. al.* for the subject building on DOE's whole building energy simulation engine, EnergyPlus. All the HVAC components and chilled water and hot water plants are modeled. The internal gains, equipment operations and controls are also included. The occupancy schedules are based on field survey; office rooms are occupied from 8:00 to 21:00 each day. The lighting and plug loads are calibrated using the data from dedicated sub-meters on each floor. The HVAC component performance curves are derived from trending data, which is recorded by the existing BAS. Model calibration is done on both whole building and component levels. If the simulation time step is set at 15 minutes, the difference between simulated and measured monthly energy is within 10%. The hourly energy has less than 20% error [131].

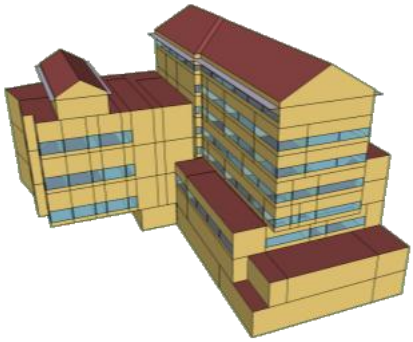

Figure 4 Simulation model of the subject building

2.2.2 DR Strategies of HVAC system

In commercial buildings, HVAC equipment, lighting and other appliances can be used for DR. Most lighting and appliance loads can be turned off immediately upon requests, so they have the instantaneous load reduction capability. As a contrast, HVAC system requires sophisticate controls and planning in order to contribute in the peak load reduction. The reason is two fold. First, the HVAC system is responsible for maintaining a comfortable and healthy indoor environment, complete shutdown of the HVAC system or certain components is prohibited. Instead, sophisticate controls are necessary to reduce the peak load, while keeping the indoor environment within acceptable ranges. Second, the HVAC energy consumption is influenced by control inputs and many other factors, such as weather and occupancy. The building thermal system is a non-linear complex system with considerable time delay. Therefore, planning will be necessary to take all these factors into peak load reduction optimization.

The DR strategies of HVAC systems have been studied extensively using analytic, simulation and field approaches [8, 13, 132-134]. Advanced controls of thermostat setpoints and HVAC equipment operations have been developed to reduce the building peak load. For example, Xu and Yin [13] tested the potential of "pre-cooling" thermostat setpoint strategy in reducing the

peak HVAC load in large commercial buildings in California hot climate zone. The authors observed 20-30% peak load reduction being achieved on hot days, with night pre-cooling and raising the cooling setpoint in the critical time period. Field survey results showed that the thermal comfort had not been compromised during the test. Yin, *et. al.* [134] presented their studies on optimization of pre-cooling strategies using calibrated simulation model. They developed a Demand Response Quick Assessment Tool (DRQAT), which was built based on EnergyPlus. Optimal DR strategies were identified by simulations, and were implemented in a test building. The measured consumption agreed with the simulation result, and the power consumption during the peak period was reduced by 15%-30%.

In general, a control strategy can be represented by a vector of controllable variables. In this chapter, pre-cooling and exponential set-up strategy is applied [12, 13], namely the global temperature setpoint adjustment (GTA). Plus, supply air temperature setpoint (SAT), and supply fan pressure setting (SFP) are considered in DR control. The strategy designs are detailed as follows.

GTA: The cooling setpoints of all zones are subject to change throughout the peak event day. As depicted in Figure 5, between 0:00 and T_1, the cooling setpoint is set at the baseline value; between T_1 and T_2, the cooling setpoint is set at a lower value for pre-cooling; between T_2 and T_3, the cooling setpoint is set up exponentially; and between T_3 and 24:00, the cooling setpoint is set back to the baseline level. All zones are assumed to follow the same GTA strategy. To reduce the size of solution space, only the three time points (i.e., T_1, T_2 and T_3) are considered as decision variables. The setpoint values at T_1, T_2 and T_3 are fixed (they are 72 ºF, 70 ºF and 78 ºF, respectively, in the case study). Furthermore, discretization and boundary constraints

apply to the time points (in the case study, time points can only be integer hours within the following ranges: $5 \le T_1 \le 9$, $T_1 < T_2 \le 14$, and $17 \le T_3 \le 19$).

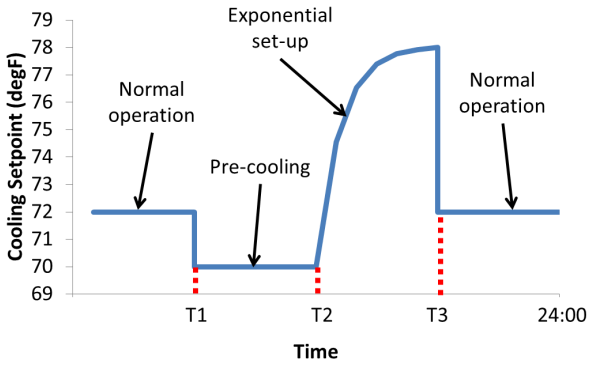

Figure 5 Thermostat setpoint schedule of GTA strategy

SAT: Two AHUs in the building are subject to DR control optimization. They use the same SAT setpoint, whose baseline value is 56 ºF; and they share the same supply air duct. SAT setpoint values between 51 and 60 ºF are explored, with an interval of 1 ºF. It is assumed that SAT setpoint only changes at the beginning of the peak event day and maintains constant throughout the entire day, in order to simplify the problem.

SFP: The two supply fans (SF-2A and SF-2B) in the building are variable air volume fans. The operation speed is controlled by a proportional-integral-derivative controller (PID controller) to maintain the fan pressure at a fixed setpoint, which is currently 1350 Pa. SFP setpoint values between 1150 Pa and 1350 Pa are explored, with an interval of 50 Pa. Similarly, to reduce the complexity of the problem, it is assumed that SFP setpoint only changes at the beginning of the peak event day and maintains constant during the entire day.

To this point, a DR strategy vector has five decision variables, which are GTA(T_1), GTA(T_2), GTA(T_3), SAT and SFP. The total number of strategies is 5250, according to the above discretization.

2.3 Optimization Techniques

2.3.1 Exhaustive Search (ES)

The first step is to establish the "ground-truth", i.e. the optimal DR strategy for each representative profile, which we consider as the true optimum. It is accomplished by exhaustively evaluating all 5250 candidates in the search space. This step is extremely time-consuming; therefore, ES is only performed off-line, and not considered as an option for on-line optimization. However, by doing so, a benchmark can be established for comparing the accuracy and efficiency of different optimization algorithms.

2.3.2 Pattern Based Selection (PBS)

To apply PBS in on-line decision making, a look-up table is created to map each weather pattern to one DR strategy. The lookup table is created by first identifying patterns in the daily weather, and then for each pattern, identifying the optimal strategy for the representative weather profile (though off-line ES). While in on-line optimization, the weather pattern of the next day is first determined based on the weather forecast. Then, according to the lookup table, a strategy is selected and implemented for the next day control. The PBS optimization assumes that the weather pattern identification carries enough insight about the association between weather patterns and optimal DR strategy. Such assumption is subject to test in this chapter.

Since, in Berkeley, California, the peak events are usually announced for hot summer days, typically in August, local weather conditions of August are subject to study in this chapter. In the work by Liao, *et. al.* [135], 19 patterns are identified from the historical weather records of the months of August between 2002 and 2010. For each August day, the hourly dry bulb temperature and its simulated baseline peak load form a 25-dimensional sample point. Using principal component analysis (PCA), the 25-dimensional sample points are projected to 3-dimensional space, and about 85% of sample variance remains. Then K-means algorithm is applied to partition the samples into clusters. Liao *et. al.* found at least 19 clusters are required to ensure the variance in each cluster is lower than a pre-determined threshold. The Euclidean mean of each cluster is considered as the representative profile for a weather pattern. The representative profiles of all 19 August weather patterns are depicted in Figure 6. The sample frequencies of all weather patterns are plotted in Figure 7. This chapter uses this pattern identification result for PBS and OSP optimizations (which will be detailed later). Pattern 2, 4 and 19 are selected as the typical hot, mild and cool August weather pattern, respectively, for result presentation. The technical detail of weather pattern identification is out of the scope of this dissertation.

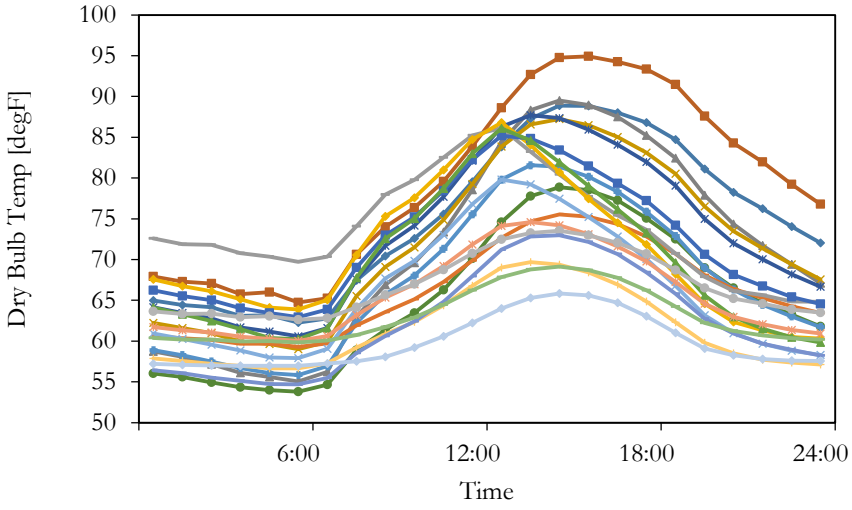

Figure 6 Representative profiles of 19 daily weather patterns

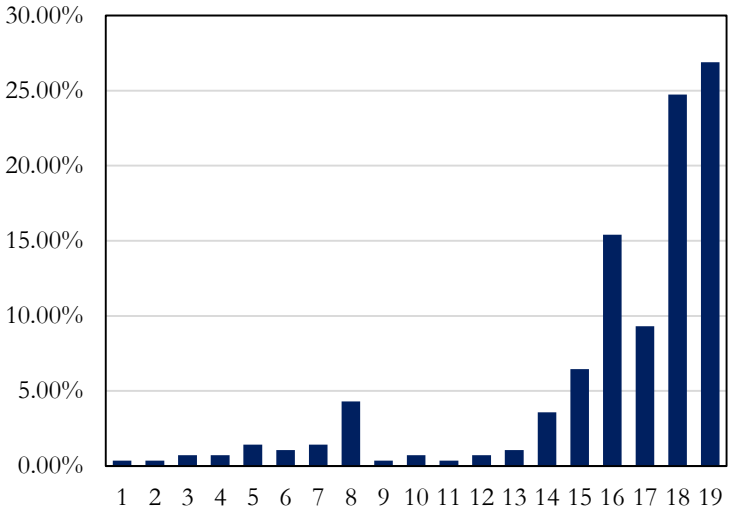

Figure 7 Sample frequency of weather patterns

2.3.3 Genetic Algorithm (GA)

GA can be dated to 1950s when biologist Barricelli [136] and quantitative geneticist Fraser [137] simulated the evolution process of natural species using computer programs. Later,

Bremermann [138] and Bledsoe [139] and many others started to apply this concept to solve optimization problems. GA finds applications in many fields successfully, including building energy area. Chow, *et. al.* [31] applied GA in absorption chiller control. Nassif, *et. al.* [140] used GA in the HVAC component models of building Energy Management and Control System, so the component models are able to adapt themselves to changing dynamics by self-tuning. More studies employ GA in parameter estimation in system identification. For example, Xu and Wang [141] apply GA in frequency domain regression and obtained optimal simplified thermal models of a building envelope. Azadeh, *et. al.* [30] use GA to identify the best structure of artificial neural network to predict electrical energy consumption. And Huang and Lam [142] optimizes HVAC controller parameters by GA.

There are two requirements in GA. One is a genetic representation of solutions – either binary, which is widely used, or other encodings. The other requirement is a fitness function that evaluates the relative preference of each solution. In this chapter, the candidate strategies are translated into binary strings, and Eq. 10 serves as fitness function.

GA initializes by randomly generating a collection of candidate solutions (individuals), called "population". In each generation, all individuals are evaluated by the fitness function. A portion of the population is selected through a fitness-based process, where solutions with better fitness values are more likely to be selected. The selected individuals generate the next generation of population by recombination and mutation. Recombination operation takes a fragment from each of the two parents, and forms the genomes of the child individuals. Mutation simply changes a small part of the genome with a certain probability so as to introduce variations to the population. As soon as a new population is generated, the algorithm repeats the cycle of

evaluation, selection and reproduction, until the stopping criteria is met – either the population remains homogeneous for several generations, or the maximal number of generations is reached.

In this chapter, GA optimization is implemented in MATLAB with the Global Optimization Toolbox. The configuration of GA is listed in Table 1. The discussion about tuning the GA parameters is beyond the scope of this dissertation.

Table 1 GA configuration

Population size	50
Creation function	Uniform
Scaling function	Rank
Selection function	Stochastic Uniform
Elite count	2
Crossover fraction	0.8
Crossover function	Scattered
Mutation function	Uniform with rate=0.3
Maximum generation	20
Function tolerance	1.00E-06

2.3.4 Optimal Strategy Pool (OSP)

In this dissertation, a new optimization scheme is tested, namely the Optimal Strategy Pool. The scheme includes two stages: Stage I is off-line stage and Stage II is on-line decision making.

Stage I: ES is performed off-line first. So F in Eq. 10 is obtained, for representative profile of Pattern i (i =1, 2, 3, …, 19), and for candidate strategy j (j =1, 2, 3, …, 5250). Instead of choosing only one optimal strategy, a few top strategies are chosen to form a strategy pool of Pattern i, denoted by J_i. The selection follows Eq. 11.

$$F_{ij} \le \alpha F_i^* \qquad \text{Eq. 11}$$

where F_i^* denotes the best fitness value among all strategies, for the representative profile of pattern i, and α is the pre-determined threshold, and $\alpha = 1.1$ is used in this study. Let N_i be the number of strategies in J_i. The selected strategies are sorted by ascending fitness values. Let j^k be the k-th strategy in J_i ($k = 1, 2, 3, \ldots, N_i$). Each of the selected strategies will be assigned with "likelihood" score, L. The likelihood scores are determined by Eq. 12 and Eq. 13.

$$\sum_{k=1}^{N_i} L_{ij^k} = 1 \qquad \text{Eq. 12}$$

$$\frac{L_{ij^{k+1}}}{L_{ij^k}} = \beta, \ (k = 1, 2, 3, \ldots, N_i - 1) \qquad \text{Eq. 13}$$

where β is a pre-determined ratio, and $\beta = 0.5$ is used in this study.

To aggregate strategy pools for all patterns, i.e. to generate the optimal strategy pool (OSP), the overall likelihood score of strategy j for all weather patterns is calculated by Eq. 14:

$$L_j = \sum_{i=1}^{I} p_i L_{ij} \qquad \text{Eq. 14}$$

where I is the total number of weather patterns, and p_i is the probability that the weather of planning day is of Pattern i. p_i can be estimated by the sample frequency of each pattern, as presented in Figure 7. If a strategy is only selected by strategy pools of one or two patterns and with low likelihood in each pool, such strategy will have a low overall likelihood, and can be removed from the OSP. Since, the resulting OSP will contain a smaller number of candidate

strategies, ES within the pool can provide the best solution for a given profile of forecasted weather. And this search can be conducted on-line.

2.4 Experiment Results

2.4.1 Exhaustive Search (ES)

Off-line ES is extremely time-consuming, as it takes about 2 minutes to evaluate a strategy for one weather profile by simulation (on a personal PC laptop). So it takes about 7.3 days (5250 evaluations) to finish ES for one weather profile. True optimal strategies identified by ES are presented in Table 2, and the comparison between the baseline and optimal consumption profiles are plotted in Figure 8.

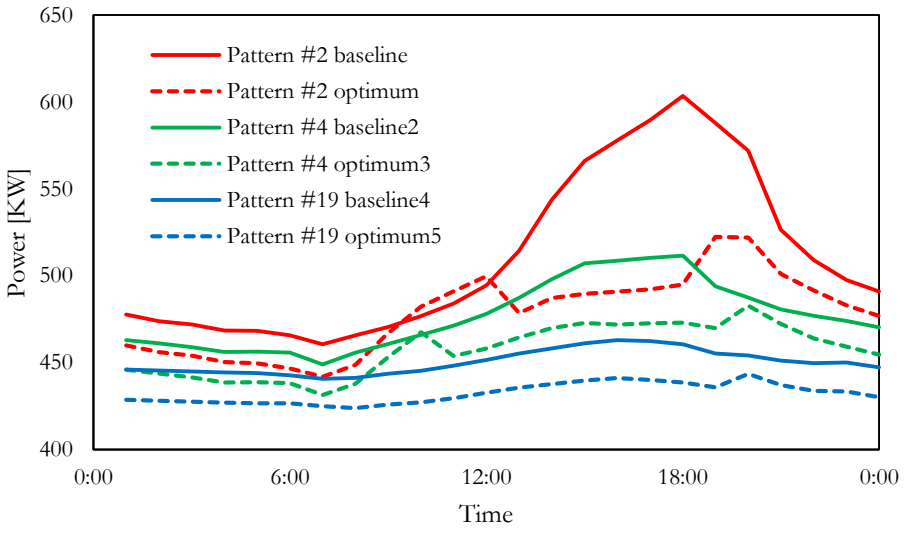

Figure 8 HVAC demand schedules with optimal DR strategies

Table 2 Optimization by ES

Weather Pattern	Optimal DR Strategy						Baseline Peak Load (KW)	Optimal Peak Load (KW)	Peak Load Reduction (KW)
	ID*	GTA (T_1)*	GTA (T_2)*	GTA (T_3)*	SAT*	SFP*			

1	4817	9	10	18	60	1150	531	480	51
2	4823	9	12	18	60	1150	603	495	109
3	4818	9	10	19	60	1150	520	476	43
4	4818	9	10	19	60	1150	512	473	38
5	4818	9	10	19	60	1150	512	474	38
6	4755	6	7	19	60	1150	482	457	24
7	4818	9	10	19	60	1150	487	462	25
8	4800	8	9	19	60	1150	478	454	25
9	4818	9	10	19	60	1150	502	469	32
10	4818	9	10	19	60	1150	497	469	29
11	4818	9	10	19	60	1150	500	469	31
12	4818	9	10	19	60	1150	495	468	27
13	4818	9	10	19	60	1150	481	458	23
14	4818	9	10	19	60	1150	475	452	24
15	4818	9	10	19	60	1150	476	452	24
16	4755	6	7	19	60	1150	467	444	23
17	4755	6	7	19	60	1150	472	449	23
18	4755	6	7	19	60	1150	468	445	23
19	4755	6	7	19	60	1150	463	441	22

ES optimization shows that the optimal DR strategies are able to reduce the peak load by as much as 18% - about 109 kW - on a typical hot day (Pattern 2), 38 kW on a typical mild day (Pattern 4) and 22 kW on a typical cool day (Pattern 19).

2.4.2 Genetic Algorithm (GA)

For the representative profile of each weather pattern, GA is tested with 20 trials. Table 3 shows the optimal strategy for the representative profile of Pattern 2 obtained in all 20 trials. In 19 out of 20 GA trials, except Trial #5, the true optimal DR strategy can be obtained ([9, 12, 18, 60, 1150] as identified by ES). This is a 95 % probability of obtaining the optimum. The average number of simulation evaluations is 372. Similar results can be obtained for all 19 weather patterns (Table 4). Generally, with GA, obtaining the optimum is not guaranteed, but the probability of obtaining a top 3 DR strategy is high (p(3) in Table 4). Meanwhile, the number of simulation evaluations is reduced from 5250 to about 372, in average.

Table 3 GA result for representative profile of weather Pattern 2

Trial #	GTA(T_1)*	GTA(T_2)*	GTA(T_3)*	SAT*	SFP*	# of evaluations
1	9	12	18	60	1150	357
2	9	12	18	60	1150	470

3	9	12	18	60	1150	319
4	9	12	18	60	1150	400
5	8	9	18	60	1150	310
6	9	12	18	60	1150	361
7	9	12	18	60	1150	342
8	9	12	18	60	1150	390
9	9	12	18	60	1150	322
10	9	12	18	60	1150	334
11	9	12	18	60	1150	432
12	9	12	18	60	1150	386
13	9	12	18	60	1150	360
14	9	12	18	60	1150	366
15	9	12	18	60	1150	369
16	9	12	18	60	1150	378
17	9	12	18	60	1150	422
18	9	12	18	60	1150	395
19	9	12	18	60	1150	376
20	9	12	18	60	1150	347
ES (Ground Truth)	9	12	18	60	1150	5250

Table 4 GA success rates and efficiency

Weather Pattern	**p(1)[1]**	**p(2)[2]**	**p(3)[3]**	**Ave. # of evaluations**
1	95%	95%	95%	346
2	95%	95%	95%	372
3	50%	50%	95%	365
4	35%	35%	100%	359
5	75%	75%	75%	379
6	95%	95%	100%	337
7	30%	70%	85%	365
8	35%	100%	100%	356
9	95%	95%	95%	392
10	60%	60%	95%	388
11	80%	80%	80%	381
12	40%	85%	85%	378
13	20%	70%	90%	354
14	10%	50%	70%	352
15	30%	75%	100%	359
16	90%	100%	100%	327
17	100%	100%	100%	337
18	90%	100%	100%	315
19	85%	100%	100%	337

2.4.3 Optimal Strategy Pool (OSP)

2.4.3.1. OSP Construction

[1] probability of obtaining the optimum

[2] probability of obtaining the optimum or the 2nd best

[3] probability of obtaining the optimum, the 2nd or the 3rd best

From the ES result for the representative profiles of all 19 weather patterns, a strategy pool is established for each pattern. The strategy pools for Pattern 2, 4 and 19 are presented in Table 5. Notice that 7 strategies are selected for Pattern 2, and 2 strategies for Pattern 4 and Pattern 19, respectively. Strategy 4817 has been selected for both Pattern 2 and 4. The OSP is constructed by aggregating all strategy pools, Table 6. Notice that only 13 strategies are included in the OSP, so 13 simulation evaluations will be required for Stage II on-line decision making.

Table 5 Optimal and near-optimal DR strategies

Weather Pattern 2			Weather Pattern 4			Weather Pattern 19		
DR Strategy	**F**	**Likelihood Score**	**DR Strategy**	**F**	**Likelihood Score**	**DR Strategy**	**F**	**Likelihood Score**
4823	0.4242	0.5039	4818	0.3391	0.6667	4755	0.2926	0.6667
4820	0.4246	0.2520	4817	0.3399	0.3333	4728	0.2938	0.3333
4826	0.4247	0.1260						
4817	0.4248	0.0630						
4829	0.4279	0.0315						
4827	0.4284	0.0157						
4824	0.4284	0.0079						

Table 6 Optimal strategy pool

DR strategy ID	Overall likelihood score	GTA (T_1)*	GTA (T_2)*	GTA (T_3)*	SAT*	SFP*
4818	8.2381	9	10	19	60	1150
4755	4.2000	6	7	19	60	1150
4817	2.3963	9	10	18	60	1150
4800	1.8857	8	9	19	60	1150
4728	0.6667	5	6	19	60	1150
4779	0.6095	7	8	19	60	1150
4823	0.5039	9	12	18	60	1150
4820	0.2520	9	11	18	60	1150
4826	0.1260	9	13	18	60	1150
4754	0.0667	6	7	18	60	1150
4829	0.0315	9	14	18	60	1150
4827	0.0157	9	13	19	60	1150
4824	0.0079	9	12	19	60	1150

2.4.3.2. OSP Validation

To validate the OSP, 13 historical August days of Berkeley, California, are randomly sampled for testing. The result of OSP is compared with the ES optimization and other two on-line

optimization algorithms – PBS and GA. The optimal DR strategies obtained by each algorithm are shown in Table 7.

Table 7 Optimal DR strategies identified by different algorithms

Sample Day (Pattern)	Algorithm			
	ES	PBS	GA	OSP
1 (Pattern 19)	4728	4755	4728	4728
2 (Pattern 3)	4818	4818	4818	4818
3 (Pattern 9)	4818	4818	4818	4818
4 (Pattern 8)	4779	4800	4755	4779
5 (Pattern 14)	4818	4818	4779	4818
6 (Pattern 13)	4800	4818	4800	4800
7 (Pattern 16)	4755	4755	4755	4755
8 (Pattern 8)	4800	4800	4755	4800
9 (Pattern 18)	4755	4818	4755	4755
10 (Pattern 18)	4755	4755	4755	4755
11 (Pattern 17)	4755	4755	4755	4755
12 (Pattern 14)	4800	4818	4779	4800
13 (Pattern 16)	4755	4755	4755	4755

As discussed in Section 2.3.2, PBS seems to be a perfect on-line optimization algorithm, because it does not require any on-line simulation evaluations. However, according to our result, PBS algorithm identifies optimal strategies different than those identified by ES (the "ground-truth"), for Sample Day 1, 4, 6, 9 and 12, which means PBS fails for those sample days. The success rate of PBS is thus 8 out of 13 (62%). GA performs slightly better, as it fails for Sample Day 4, 5, 8 and 12, thus the GA success rate is 9 out of 13 (69%). As a contrast, OSP successfully identifies the optimal DR strategies for all sample days (100% success rate). Furthermore, OSP only requires 13 on-line simulation evaluations, which is 3.5% of evaluations needed by GA, and 0.2% of evaluations needed by ES. On a PC with 2.40 GHz CPU, ES takes 7.3 days, GA takes 12 hours, but OSP only takes less than 30 minutes to identify the optimal DR strategy for a given

weather profile. This result is good enough for simulation-based on-line optimization for HVAC DR control.

2.4.3.3. Larger Solution Space

The previous solution space contains 5250 DR strategies. Although the size of this solution space has been reduced intentionally, as only a few controllable points are involved, and only discrete values are considered for each point, simulation-based ES optimization still requires several days to reach an optimum. In real applications, an on-line DR controller is supposed to deal with more controllable points, and higher resolution would be expected. Thus, ES optimization is not feasible for on-line response. Its use for off-line optimization with pattern representative weather profiles will become less tractable. For this reason, the performance of the OSP optimization scheme needs to be tested with larger solution spaces.

Consider the case where condenser water supply temperature setpoint (CWST) and chilled water supply temperature setpoint (CHWST) are added to the decision variables. These are two control points in the water system, and they are related to the other two major consumers of energy in HVAC system – the chiller and the tower fans. The baseline values of these two setpoints are 78.4°F for CWST and 50°F for CHWST. When adding to the previous GTA, SAT and SFP, CWST has an integer value between 75 and 81 °F, and CHWST takes an integer value between 40 and 60 °F. With two more dimensions, the search space expands from 5250 solutions to over 700,000, making off-line ES optimization too expensive. Therefore, the "ground-truth" has to be established via a global optimization method other than ES, e.g. GA. The result is presented in Table 8. Notice that, in this study, the EnergyPlus model has been modified and the constraint is relaxed so that $GTA(T_1)$ can be equal to $GTA(T_2)$, so the optimal peak load is different to the

result of Table 2. The relaxing of the constraint is inspired from the previous result, which suggests that pre-cooling phase may not be necessary for cool days of Berkeley, California.

Table 8 GA optimization result on larger solution space

Weather pattern	GTA (T_1)*	GTA (T_2)*	GTA (T_3)*	SAT*	CWST*	CHW ST*	SFP*	F*	Peak Load	# of runs
1	8	8	18	60	81	41	1150	0.7174	700	893
2	9	13	18	60	78	40	1150	0.7852	742	708
3	9	10	19	60	81	40	1150	0.7437	704	805
4	9	9	19	60	80	41	1150	0.6896	684	1052
5	9	9	18	60	80	41	1150	0.6821	689	775
6	8	8	19	60	75	41	1150	0.6260	626	829
7	8	8	19	60	76	41	1150	0.6329	643	780
8	9	9	19	60	75	40	1150	0.5762	620	852
9	9	12	19	60	76	40	1150	0.6005	653	925
10	9	9	19	60	76	40	1150	0.6002	656	827
11	9	9	19	60	77	40	1150	0.6216	668	830
12	8	8	19	60	76	40	1150	0.6208	660	916
13	8	8	19	60	75	40	1150	0.6051	625	954
14	8	8	19	60	75	41	1150	0.5605	613	801
15	7	7	19	60	75	41	1150	0.5443	616	954
16	7	7	19	60	77	41	1200	0.5849	586	1323
17	7	7	19	60	75	40	1150	0.6111	606	769
18	7	7	19	60	75	41	1150	0.5314	583	824
19	7	7	19	60	75	40	1150	0.5767	573	840

GA optimization requires about 877 simulation evaluations on average to identify the optimal strategy. It takes approximately 10 hours (for the modified model, which is faster than the previous one). An OSP is created off-line based on this result. A total of about 3800 DR strategies have been evaluated by GA optimization. Among all those strategies, 97 are selected into OSP, as 97 spikes are identified from the strategy overall likelihood spectrum (Figure 9).

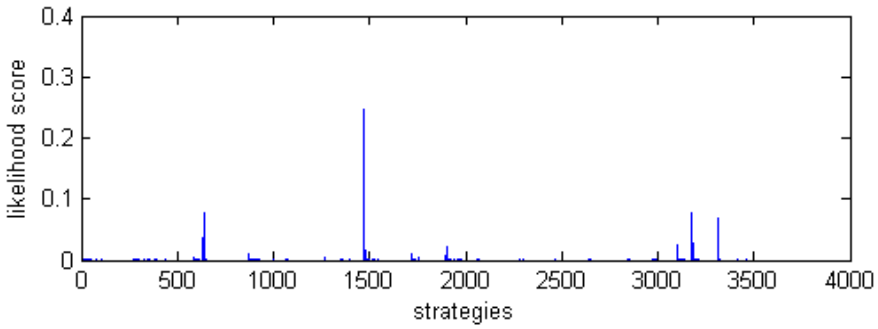

Figure 9 Strategy likelihood spectrum

To validate the OSP algorithm, PBS, GA and OSP algorithms apply to the same 13 sample days in Table 7. The new comparison is shown in Table 9.

Table 9 Comparison of PBS, GA and OSP on larger solution space

Sample Day		**Algorithm**		
		PBS	**GA**	**OSP**
1 (Pattern 19)	Opt. DR strategy	[7,7,19,60,75,40,1150]	[7,7,19,60,75,41,1150]	[7,7,19,60,75,40,1150]
	F*	0.5858	0.5858	0.5858
2 (Pattern 3)	Opt. DR strategy	[9,10,19,60,81,40,1150]	[9,9,19,60,80,40,1150]	[9,9,19,60,80,41,1150]
	F*	0.7008	0.6923	0.6923
3 (Pattern 9)	Opt. DR strategy	[9,12,19,60,76,40,1150]	[9,12,19,60,76,40,1150]	[9,12,19,60,76,40,1150]
	F*	0.6063	0.6063	0.6063
4 (Pattern 8)	Opt. DR strategy	[8,8,19,60,75,40,1150]	[8,8,19,60,75,40,1150]	[9,9,19,60,75,40,1150]
	F*	0.5899	0.5899	0.5886
5 (Pattern 14)	Opt. DR strategy	[8,8,19,60,75,40,1200]	[8,8,19,60,75,40,1150]	[9,9,19,60,75,40,1150]
	F*	0.5669	0.5639	0.5608
6 (Pattern 13)	Opt. DR strategy	[7,7,19,60,75,41,1150]	[8,9,19,60,75,40,1150]	[9,9,19,60,75,40,1150]
	F*	0.606	0.608	0.6016
7 (Pattern 16)	Opt. DR strategy	[6,6,19,60,75,41,1150]	[8,8,19,60,75,40,1150]	[7,7,19,60,75,40,1150]
	F*	0.5973	0.5961	0.5961
8 (Pattern 8)	Opt. DR strategy	[8,8,19,60,75,40,1150]	[7,7,19,60,75,40,1150]	[9,9,19,60,75,40,1150]
	F*	0.5956	0.5977	0.593
9 (Pattern 18)	Opt. DR strategy	[7,7,19,60,75,40,1150]	[7,7,19,60,75,40,1150]	[7,7,19,60,75,40,1150]
	F*	0.5385	0.5385	0.5385

10 (Pattern 18)	Opt. DR strategy	[7,7,19,60,75,40,1150]	[8,8,19,60,75,40,1150]	[8,8,19,60,75,41,1150]
	F*	0.5296	0.5295	0.5295
11 (Pattern 17)	Opt. DR strategy	[7,7,19,60,75,41,1150]	[6,6,19,60,75,41,1150]	[9,9,19,60,75,40,1150]
	F*	0.5798	0.5816	0.5792
12 (Pattern 14)	Opt. DR strategy	[8,8,19,60,75,40,1200]	[8,8,19,60,75,40,1150]	[9,9,19,60,75,40,1150]
	F*	0.557	0.5541	0.552
13 (Pattern 16)	Opt. DR strategy	[6,6,19,60,75,41,1150]	[7,7,19,60,75,40,1150]	[7,7,19,60,75,40,1150]
	F*	0.5683	0.5674	0.5674

In this study, OSP requires 97 simulation evaluations, 89% less than GA (877 evaluations, on average). The strategies identified by OSP are the same or even better ones than the ones identified by GA and PBS, in terms of the smaller objective values. Thus we are able to claim that the two-stage optimization scheme with OSP is more advantageous than GA and PBS for on-line simulation-based HVAC DR control optimization.

2.5 Discussion

Whole-building detailed energy simulation is a gray-box modeling technique, which blends in both equation systems from physical modeling (the white-box model) and parameter approximation from empirical studies and statistics (the black-box model). The simulation models are mainly used for design verification, energy audit, local control optimization and code compliances. There also exist studies that attempt to apply simulations in supervisory control optimization [14, 22, 25, 143]. However, simulation-based approach has several drawbacks which render it very challenging for control optimization applications.

First, it takes an enormous engineering effort to develop and calibrate a detailed model. A model for whole-building control optimization requires sufficient accuracy – not only on whole-building and annual simulation level, but also on subsystem level (air handlers, chilled water loop and condenser loop), component level (chiller, fans and pumps), and sometimes zone level, with hourly or sub-hourly time resolution. In order to reach that accuracy level, large amount of

trending data will be required for calibration, existing control logics need to be studied and implemented in the simulation, and field surveys and audits have to be conducted to generate good internal gain profiles. In any cases, none of these would be a trivial task. For example, in the study by Zhu, *et. al.* [22], it took the authors 12 months to calibrate the model, and 70% of the time was spent in developing fan and chiller performance curves and implementing cooling tower control logics.

Secondly, even after careful modeling and calibration, the model accuracy may be still questionable. The fact is that most information about a building and its system's behavior is hardly certain. The actual weather condition (recorded or forecasted) includes more factors than only dry bulb temperature, relative humidity and a hand-full others that are considered in the simulation, and it has more frequent dynamics than 15-minute or 60-minute average that is often used. Infiltration rate, plug-in uses, occupancy levels and occupant body heat gain are very hard to measure. The actual performance of major equipment often deviates significantly from the technical documentations, due to variations in installation and maintenances. Plus, noisy sensors, faulty systems and false implementations of control logics, can all contribute to the uncertainty of the HVAC system. According to an in-person discussion with Dr. Jin Wen from Drexel University, substantial differences are observed from the energy consumption of two HVAC systems which are intentionally built to be identical. The implication is that if a system can behave differently from its design, a simulation-model that tries to approximate this system may also deviate. Therefore, in the actual modeling practices, a 10~20% error would be generally acceptable for whole-building hourly consumption, and even larger error can be expected for more detailed levels and finer time resolutions.

And last, but most importantly, simulation is a computation-intensive process, and simulation-based optimization often involves extensive simulation evaluations. Therefore, heavy computation burden is nearly inevitable. This is especially true if traditional search algorithms are employed [22, 51]. In this chapter, a new two-stage optimization scheme, OSP, is proposed in order to move simulation evaluations to off-line as much as possible. The comparison between OSP and PBS suggests that on-line simulation evaluation is still needed in order to identify the optimal DR strategy with enough confidence. In this study, OSP requires about 30 to 40 minutes to identify an optimal control strategy, which is acceptable for day-ahead planning, but definitely unacceptable for faster response.

The key of this OSP optimization scheme is that a knowledge base, which is represented by the "optimal strategy pool", can be created based on off-line computation. This optimal strategy pool is supposed to contain a smaller number of candidate strategies, and therefore, turns on-line simulation-based optimization feasible. The PBS strategy is heuristically qualified for this type of two-stage scheme, and is seemingly more favorable, as no on-line simulation would be needed. However, the experiment results (Table 7 and Table 9) suggest that the optimal strategy for the representative profile of a weather pattern is not necessarily the optimum for the individual profile that belongs to this pattern. This further means that the patterns obtained by the way described in [135] have weak inference power in the DR strategy selection. The success of OSP optimization suggests that the optimal strategy for an individual weather profile is among the top choices for the pattern's representative profile. Ideally, if all top choices for all representative profiles are selected to generate a "pool", such pool should be able to cover the optimal strategy of most individual profiles.

Chapter 3 Day-ahead Planning and Real-time Tracking Under Cost-for-Deviation Pricing

Abstract

A new retail tariff called Cost-for-Deviation (CfD) is proposed in this dissertation. CfD targets to reduce the demand uncertainty at individual customer level, and then mitigate the utility provider's quantity risk in the wholesale market. Under this new rate structure, individual buildings will perform day-ahead planning and real-time load tracking control optimizations in order to reduce the cost. This chapter provides the formulation of the two-stage control problems. An ANN model is used in the model-based optimizations in both stages. The experiments demonstrate that, under CfD, day-ahead planning and real-time tracking are effective in reducing the building demand deviation, especially in the case where some unexpected event might cause significant demand surge. It is also shown that accurate forecasts of weather and occupancy are helpful in demand uncertainty reduction. In the end, CfD encourages the predictable consumption behavior among individual customers. This is expected to reduce the quantity risk of the entire community in the wholesale market.

3.1 Introduction

Flat rate and static TOU price are typical in the current electricity retail markets of the US. With these rate structures, the wholesale market and the retail market are loosely connected [86]. The utility providers absorb the full risk of the market uncertainties, including the price risk [144] and the quantity risk [93]. On the other hand, even though the customers tend to be price sensitive, they do not actively respond to the dynamic supply/demand condition in the market due to absence of incentives. Consequently, the utility providers have to hedge against the risks

by raising retail price, and the customers have to accept the higher prices [145]. This process does not account for the diversity in individual consumption behavior.

In order to avoid the above "lose-lose" situation, stakeholders are seeking for a new rate structure, which connects supply ends and customer ends more tightly, and promotes efficient energy usage as well as fair sharing of the risk. In the past few years, various DR programs have been implemented in the regional markets of the US. The time-varying price-based DR is particularly popular, including, but not limited to, TOU, DAP and RTP. TOU pricing scheme divides daily consumption into peak and off-peak periods. Different prices apply to different periods. Weekday/weekend and summer/winter variations are also accounted for. The prices are often issued weeks or months ahead and remain unchanged for the entire period of the contract. Due to lack of timeliness and time granularity, TOU pricing conveys a limited amount of information about the hour-to-hour dynamics of the market. Therefore, it can only moderately shape the demand profile. As a contrast, RTP gives residential customers access to an hourly electricity price that is based on the wholesale market price. Although the long-term benefit of RTP has been widely recognized [94], it remains debatable whether full exposure to the wholesale market is, in the short term, beneficial to the customers. The reason is that it is quite challenging for individual customers to be sufficiently equipped to retrieve highly dynamic market information, and make quick and wise decisions, proactively. Failure in doing so will yield high volatility of the cost on the customer side. DAP can be considered as a hybrid of TOU and RTP. It announces hourly retail price schedule day-ahead based on the predicted spot market price. With DAP, customers are able to schedule demand in advance and fully utilize their demand elasticity to achieve maximum energy saving and/or demand reduction. Also,

hourly price schedule carries substantial information about market dynamics, although it is based on prediction rather than realization.

The primary goal of DR programs is to reduce the demand when the grid is experiencing peak load. According to US FERC's report [146], DR programs have achieved success in terms of lowering the peak demand on the grid. However, DR programs do not reduce the uncertainty of the market demand, even though demand uncertainty has been recognized by many researchers as an important factor in demand side management, market strategies and grid operations (see the review in Section 1.4.2.1). In those studies, demand uncertainty is represented by a set of statistical parameters that are given or subject to learning, but not controllable. It is only a condition that must be accounted for while making energy saving or cost reduction control decisions. Few, if any, of those studies set uncertainty reduction as one of the demand management targets, because currently no retail tariff has been designed to mitigate the quantity risk that faces the utilities in wholesale markets. The common practice to hedge quantity risk is by raising the retail price. This approach does not consider the variety in customer behavior, and hence creates an unfair situation where those customers who are not the major source of uncertainty have to share the elevated cost that is caused by the uncertainty in the other customers' consumption.

A new CfD rate structure is proposed in this chapter, aiming to promote fair sharing of the risk among utility and individual customers. CfD assumes that the customers have good understanding of their own behavior and, therefore, are able to predict their individual demand schedules with sufficient certainty. Then the customers are responsible for making the commitment of the demand schedule ahead of time (e.g. commit a 24-hour demand schedule one day in advance) and tracking such schedule in real-time. The difference between the planned

and actual demand schedules will incur CfD charge, whose rate is defined by contractual agreement. By aggregating demand schedules planned by all individual customers, the utility will be able to calculate its demand bid to the day-ahead wholesale market. Since the quantity risk is hedged by CfD charge, the utility can rely more on the day-ahead market, which has less risk, rather than on the risky real-time market. As a result, the overall cost of the utility may be reduced. With the assumption that the utility company is not-for-profit, lower cost is equivalent to smaller utility bills for all customers. The risk sharing is accomplished by transferring the quantity risk to the customers and leaving most of the price risk to the utility. Note that, this CfD pricing differentiates from the existing "contract for difference", which is a type of price hedging contracts between the retailers and the generators in the wholesale markets.

The details and performance of the CfD rate structure at microgrid or community level will be discussed in Chapter 4. In this chapter, the study focuses on individual building optimal control. Under CfD, the customers will face two problems: (1) given hourly retail price schedule and the forecasts of the weather and occupancy for the next day, how to identify the optimal demand schedule; this is a "Day-ahead Planning" optimization problem. Once obtained, the optimal demand schedule is submitted to the utility. (2) Given a planned demand schedule, how to minimize the CfD charge in real-time, i.e. how to control the actual demand in order not to deviate far from the planned schedule. Hence, a "Real-time Tracking" optimization must be solved at each hour, considering the latest realization of weather, occupancy and system response, as well as the updated forecasts for the near future.

This chapter gives an example of using ANN for the model-based predictive control in planning and load tracking. The ANN model is developed to approximate an office building that is simulated by an EnergyPlus model. Based on the nature of the ANN model and the problem

formulation, dynamic programming technique is used to solve both planning and tracking problems. The performance of CfD in terms of lowering the building's demand deviation is investigated, and additional experiments are designed to study the influences of such factors as weather forecast, occupancy forecast and CfD rate. It is shown that, under CfD, day-ahead planning and load tracking, together with timely update of the condition forecast, are able to reduce the building's demand deviation. It is worth pointing out that ANN is only one of many modeling approaches that could work for the predictive control under CfD. The presented problem formulations along with the solution technique are not the only way of addressing the problems.

The main purpose of this dissertation is to introduce the concept of uncertainty reduction in demand management, in addition to the conventional energy efficiency and peak demand reduction. The uncertainty management is implemented via an economical approach, which is the proposed CfD retail pricing.

The rest of this chapter is organized as follows: Section 3.2 details the formulations of the day-ahead planning and the real-time load tracking optimization problems. Section 3.3 describes the ANN model development. Section 3.4 presents the validation for the prediction model and control optimization. The results of a base case and a series of experiments are presented in Section 3.5. Section 3.6 discusses the results and gives concluding remarks.

3.2 Problem Formulation

3.2.1 Day-ahead Planning

In both "Day-ahead Planning" and "Real-time Tracking" optimizations, the decision variable is the control action (thermostat setpoint, in this study) at each hour of the next day. While making a day-ahead plan, the customer is provided with the hourly retail price schedule for the next day. The hourly forecast of the next day's weather can be obtained from internet weather services. The customer is assumed to be able to forecast the building's occupancy schedule. The planning objective will be to minimize the sum of total energy cost and thermal comfort violation penalty (Eq. 15). The energy cost is calculated by multiplying the hourly demand with the hourly price. The comfort violation penalty at each hour is proportional to the comfort range violation. At any time, if the room air is too cold, the thermal comfort violation is defined by how much (in degrees) the room temperature is lower than the lower bound of comfort range; or, if it is too hot, the violation equals to the temperature difference between the room air and the upper bound of comfort range (Eq. 16). The energy consumption and average room temperature are calculated from a prediction model (Eq. 17). Also boundary constraint applies to the control input (Eq. 18). The Day-ahead Planning optimization problem can be formulated as follows:

The <u>Day-ahead Planning</u> optimization (Phase I, deterministic):

Decision variable: x^I

Minimize: $$G^I = \sum_{t=1}^{H} \left(C_t P_t^I + p_1 u_t^I + p_2 l_t^I \right) \quad \text{Eq. 15}$$

Subject to: $$T^l - l_t^I \le T_t^I \le T^u + u_t^I \quad \text{Eq. 16}$$

$$\left[\begin{matrix} P_t^I \\ T_t^I \end{matrix} \right]_{t=1}^{H} = F\left(x_t^I \Big|_{t=1}^{H}, \hat{\omega}_t \Big|_{t=1}^{H} \right) \quad \text{Eq. 17}$$

$$x^l \le x_t^I \le x^u \qquad \text{Eq. 18}$$

where,

t: the time step;

H: the planning horizon (the next day);

C: the vector of the hourly price schedule (C_t is the element associated with time step t);

F: the function of the prediction model;

P^I: the vector of planned demand schedule (P_t^I is the element associated with time step t);

T^I: the vector of average room temperature (T_t^I is the element associated with time step t);

$\hat{\omega}$: the vector of weather and occupancy forecast ($\hat{\omega}_t$ is the element associated with time step t);

T^u and T^l: the upper and lower bound of thermal comfort range, respectively;

u^I and l^I: the vectors of violations of upper and lower bound of comfort range, respectively (u_t^I and l_t^I are the elements associated with time step t);

p_1 and p_2: the coefficients to convert comfort violation into dollar cost;

x^I: the vector of thermostat setpoint schedule (x_t^I is the element associated with time step t);

By solving this problem, the optimal solution, x^I, will be the control action schedule, and the corresponding demand schedule, P^I, will be submitted to the utility.

3.2.2 Real-time Tracking

During the next day, from 0:00 to 0:59, the planned control action for the first hour, i.e. x_1^I, will be executed. Starting from 1:00, the recourse optimization will be needed, because the observed occupancy and weather start to deviate from their forecasts. For the real-time tracking during the next day, the optimization is to minimize the expected CfD cost and penalties due to thermal comfort violation and change of action for the remainder of the day (Eq. 19). The CfD cost is defined to be proportional to the squared difference between planned demand and the actual one. The change of action penalty is proportional to the squared difference between the planned setpoint and the actual one.

The <u>Real-time Tracking</u> optimization (Phase II, At time step k):

Decision variable: $x_t^{II}\big|_{t=k}^{H}$

Minimize:
$$G_{t=k}^{II} = \sum_{t=k}^{H} [q_1 \left(P_t^I - P_t^{II}\right)^2 + q_2 \left(x_t^I - x_t^{II}\right)^2 + p_1 u_t^{II} + p_2 l_t^{II}] \qquad \text{Eq. 19}$$

Subject to:
$$\left[\begin{matrix} P_t^{II} \\ T_t^{II} \end{matrix}\right]\Bigg|_{t=k}^{H} = F\left(x_t^{II}\Big|_{t=k}^{H}, \hat{\omega}_t^k\Big|_{t=k}^{H} \right) \quad \text{Eq. 20}$$

$$T^l - l_t^{II} \le T_t^{II} \le T^u + u_t^{II} \quad \text{Eq. 21}$$

$$x^l \le x_t^{II} \le x^u \quad \text{Eq. 22}$$

where,

P^{II}: the vector of actual demand conditioned on the realization of weather and occupancy, ω (P_t^{II} is the element associated with time step t);

q_1: the Cost-for-Deviation (CfD) charge rate;

q_2: the penalty rate of the change of action (setpoint);

$x_t^{II}\Big|_{t=k}^{H}$: the vector of thermostat setpoint schedule determined at time step t for the remainder of the time horizon (x_t^{II} is the element associated with time step t);

The real-time tracking optimization is conducted at each hour since 1:00, because the weather and occupancy forecasts together with system responses are updated every hour for the remainder of the day. As a result, only the first element of the optimal solution (i.e. $x_{t=k}^{II}$) will be executed, at each hour.

The bill for the building (Z) is calculated as shown in Eq. 23.

$$Z = \sum_{t=1}^{H} \left[C_t P_t^{II} + q_1 \left(P_t^{I} - P_t^{II} \right)^2 \right] \quad \text{Eq. 23}$$

At the end, the performance of the day-ahead planning and real-time tracking, under CfD, will be evaluated by root mean squared deviation, or RMSD, of hourly demand (Eq. 24).

$$RMSD = \sqrt{\frac{1}{H} \sum_{t=1}^{H} \left(P_t^{I} - P_t \right)^2} \quad \text{Eq. 24}$$

where, P is the vector of actual demand (P_t is the element associated with time step t).

Eq. 17 and Eq. 20 in the above optimization problems involve a system prediction model. This model is crucial to model-based predictive control. Section 3.3 and 3.4 give an example of developing and validating such model.

3.3 Prediction Model

The implementation of CfD rate structure requires individual customers to be capable of predicting their demand based on occupancy and weather forecasts. This prediction model must be accurate, robust, and adaptive to the behavior change of customers. However, as in Chapter 2, the study of simulation-based control optimization shows that simulation evaluation could be a very time-consuming process. It can be impractical to involve many simulation evaluations in on-line optimization. Instead, a fast, yet accurate model is necessary for control optimization, especially for fast response and real-time predictive control. Several data-driven modeling approaches fit such needs, including time-series model [26], Fourier series model [27], regression model [28], ANN [29-41], support vector machine [42, 43] and fuzzy logic model [33, 38, 44-46]. Among these approaches, ANN is particularly popular.

ANN is a mathematical and simplified representation of biological neural networks. Depicted in Figure 10 is a typical Multilayer Perceptron (MLP) ANN proposed by Rumelhart, *et. al.* [147], in 1986. An MLP consists of at least three layers, namely "input layer", "hidden layer" and "output layer". On each layer, inputs from the neurons on the previous layer to neuron j of this layer (x_{1j}, x_{2j},…, x_{Mj}) are weighted (by timing w_{1j}, w_{2j},…, w_{Mj}) and summed by the cell body (Eq. 25), when the sum exceeds a certain threshold, the neuron is activated (y_1, y_2,…, y_N).The activation function can be written as Eq. 26.

$$h_j = \sum_i w_{ij} x_{ij} \qquad \text{Eq. 25}$$

$$y_i = f(h_j) = \begin{cases} 1 & if\ h_j > \theta \\ 0 & if\ h_j \le \theta \end{cases} \qquad \text{Eq. 26}$$

It was proven by Cybenko [148] that, with one or more hidden layers with sigmoid activation functions, MLP can approximate any continuous function, no matter the function is linear or not.

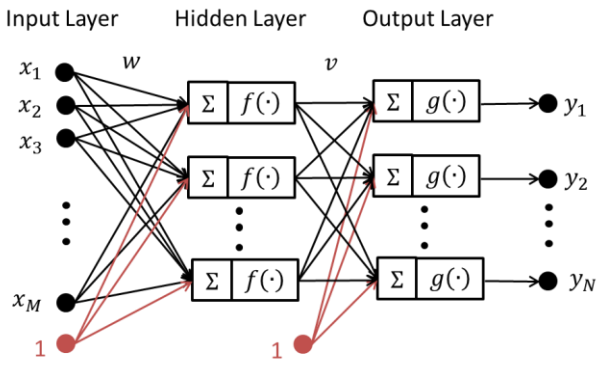

Figure 10 Multilayer Perceptron model

Given that the building thermal system is a non-linear system, whose current state is influenced by the states and control inputs back in time, a Non-linear Auto-Regressive with eXogenous inputs (NARX) network will be a suitable model for such a system. The mathematical expression of this model can be formalized as follows:

$$z(t) = F\begin{bmatrix} x(t), x(t-1), x(t-2), \ldots, x(t-d_x) \\ y(t), y(t-1), y(t-2), \ldots, x(t-d_y) \\ z(t-1), z(t-2), \ldots, z(t-d_z) \end{bmatrix} \quad \text{Eq. 27}$$

where z is the system state variable, x is the control inputs and y is the uncontrollable inputs from external of the system. d_x, d_y and d_z are the corresponding time delays. The NARX network architecture is depicted in Figure 11.

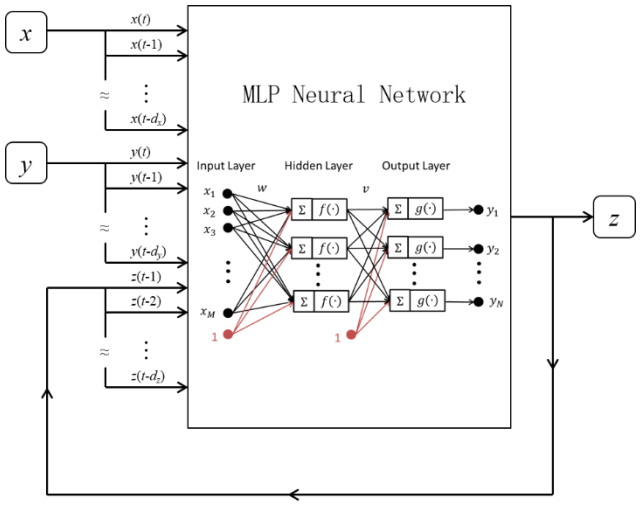

Figure 11 NARX network structure

Because the network model is most sensitive to the input range between -1 and 1, min-max normalization and de-normalization are conducted for data pre- and post-processing. The normalization procedure also ensures no particular factor will outweigh others due to large numerical values.

The activation function of the hidden nodes is sigmoid function shown in Figure 12*a*. The activation function of the output nodes is a linear output function shown in Figure 12*b*. The Levenberg-Marquardt back-propagation algorithm (LMA) [149] implemented by MathWorks MATLAB Neural Network Toolbox [150] is employed to train the NARX network.

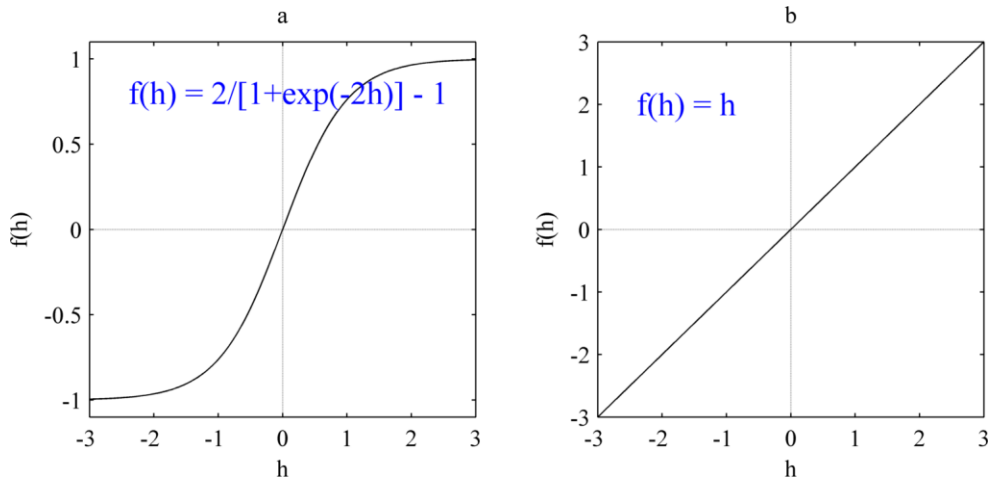

Figure 12 a. Sigmoid activation function of hidden nodes; b. Linear activation function of output nodes

Ideally, the prediction model should be trained using dataset collected from a real building, and the model-based predictive control should be tested on the same building. However, the author does not have a real building readily available for data collection and testing. As an alternative, the author uses an existing EnergyPlus simulation model of a "Reference Medium Office" building, which is developed and validated by the National Renewable Energy Laboratory of USDOE [151]. The basic information about the building is summarized in Table 10, and the geometry is illustrated in Figure 13.

Table 10 Summary of the demonstration building (Reference Medium Office)

Building Location	Chicago, IL
Building Function Type	Office

Floor area	8361 m^2 (90,00 ft^2)
Floor number	3
Number of conditioned zones	15
Window-to-wall ratio	0.50
HVAC system	Standard VAV system with minimum outside air, hot water reheat coils, central chilled water cooling coil. Central Plant is single hot water boiler, electric compression chiller with water cooled condenser.

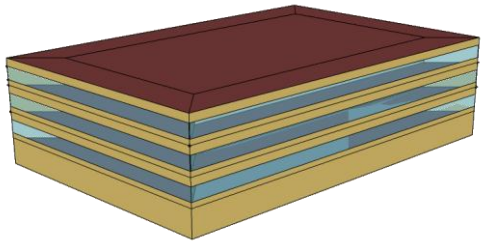

Figure 13 Reference medium office - building geometry

Replacing a real building with a simulation model provides two benefits. First, data collection from a real building can be very expensive. The variation in the dataset, regarding weather, internal loads and control inputs, might be insufficient for developing a prediction model. As a contrast, if an existing and validated simulation model is used as a data generator, data variation can be ensured by intentionally introducing variation into simulation input. Second, a simulation model can be a test bed for extensive experiments. Another yet to prove hypothesis is that a fairly calibrated simulation model could serve as an initial training dataset generator to develop a first prediction model. This prediction model can then be refined by on-line adaptive training using measured data (if available from the real building).

In this study, a dataset is generated by a simulation using the weather of the months of July in the years 2001-2012 along with random occupancy and thermostat setpoint. The dataset includes

time (day-of-week and hour-of-day), weather (dry bulb temperature, relative humidity and wind speed), occupancy level (normalized to 0~1, and lighting and plug-load levels are assumed to be the same as occupancy), thermostat setpoint as well as corresponding system responses (energy consumption and average room temperature). The inputs and responses of years 2001~2003 are used for training and those of 2004 are used for validation to avoid model over-fit. All permutations of network parameters are tested – the size of the first hidden layer is between 2 and 14, the size of the second hidden layer ranges between 0 and 6, and the delay is from 1 step to 4 steps. All trained networks are subject to both hourly and day-ahead prediction tests. The network that makes the best predictions in both tests is selected for planning and tracking optimization.

3.4 Validation

3.4.1 Prediction Model

The NARX model predictions are subject to both hourly and day-ahead prediction validation tests. In the hourly prediction test, the prediction model is called at each hour to make prediction for the next hour. In the day-ahead prediction test, prediction is made for the next 24 hours, by calling the model recursively and using the information available in the day-ahead. In both tests, model responses to randomly sampled weather, randomly generated occupancy and control inputs are compared to EnergyPlus simulation results. Statistical metrics are used to evaluate the prediction accuracy on building demand, including mean absolute percentage error (MAPE), root mean square error (RMSE), coefficient of variation (CV) and coefficient of determination (R^2) [36]. The formulas of these metrics are given as follows.

$$MAPE = \frac{1}{T}\sum_{t=1}^{T}\frac{|y_t - \hat{y}_t|}{y_t} \quad \text{Eq. 28}$$

$$RMSE = \sqrt{\frac{1}{T}\sum_{t=1}^{T}(y_t - \hat{y}_t)^2} \quad \text{Eq. 29}$$

$$CV = \frac{\sqrt{\frac{1}{T}\sum_{t=1}^{T}(y_t - \hat{y}_t)^2}}{\frac{1}{T}\sum_{t=1}^{T} y_t} \quad \text{Eq. 30}$$

$$R^2 = 1 - \frac{\sum_{t=1}^{T}(y_t - \hat{y}_t)^2}{\sum_{t=1}^{T}\left(y_t - \frac{\sum_{\tau=1}^{T} y_t}{T}\right)^2} \quad \text{Eq. 31}$$

where, y_t is the observed (EnergyPlus simulated) system response at time t, and $\hat{y}_t$ is the corresponding prediction by the NARX network.

Among all tested NARX configurations, the one with 5 first layer nodes, 4 second layer nodes and 2-step delay (denoted by NARX-H05H04D02) gives the best prediction results. Compared to similar studies in [36, 39, 41, 152-154], the number of layers and number of neurons may be different but around the same magnitude. Our model has 2 time step delays (2-hour lag), similar to 1~2 hour lags in other cases with similar building size.

The evaluation matrices of NARX-H05H04D02 network are summarized in Table 11 and Table 12. The interpretation of this result is as follows. This network gives very good load predictions in both tests. The load predictions in the hourly test are slightly more accurate than those in the day-ahead prediction test. In hourly predictions, the predicted load by this model has about 7.6

KW error (5.3%), in average. The prediction model explains 98% of the variation of the building demand. The error relative standard deviation is about 5.9%. This prediction accuracy is better than the results in [36, 38, 39], which are two studies using ANN models to approximate real building data. Our result is about the same level as reported by [36], which uses ANN models to fit EnergyPlus simulation data. Therefore, the NARX-H05H04D02 network load prediction is validated.

The room temperature predictions have 0.7 °C errors (2.5%), in average. The prediction model explains 90% of the variation of the room temperature. The error relative standard deviation is about 3.1%. The temperature prediction error is slightly higher than those in [152-154], where errors range between 0.1 °C and 0.6 °C. The results of those studies are based on the measured room temperature of single spaces without HVAC or with simple heater. As a result, those datasets have less variation. The simulated system in our study is a medium size multi-zone office building with complex HVAC system and controls. The room temperature subject to prediction is a weighted average across all conditioned zones. Plus the training and testing datasets are generated with random control signals. Therefore, a slightly less accurate temperature prediction model is considered acceptable in our case, because it is built for a much more complicated subject system.

Table 11 NARX-H05H04D02 network load prediction evaluation

Test	MAPE	RMSE	CV	R^2
Hourly	0.053	7.6	0.0587	0.9815
Day-ahead	0.058	8.5	0.0647	0.9702

Table 12 NARX-H05H04D02 network room temperature prediction evaluation

Test	MAPE	RMSE	CV	R^2
Hourly	0.025	0.7	0.0314	0.9032
Day-ahead	0.025	0.7	0.0305	0.8767

The time series plots of load and room temperature, comparing the NARX model prediction and EnergyPlus simulation are presented in Figure 14 and Figure 15.

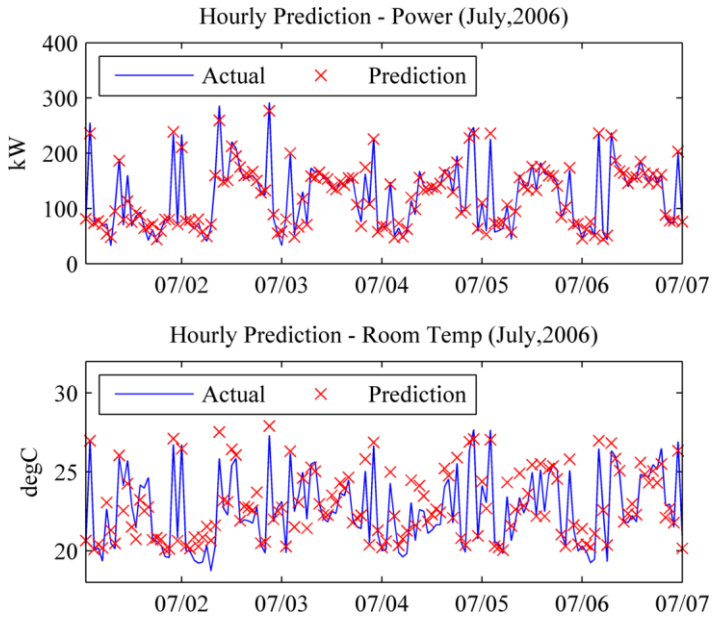

Figure 14 NARX-H05H04D02 network hourly prediction

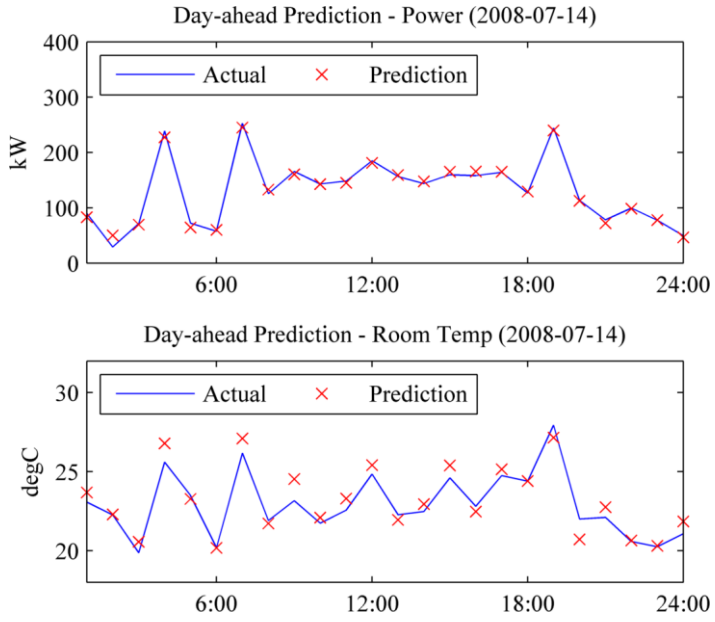

Figure 15 NARX-H05H04D02 network day-ahead prediction

3.4.2 Control Optimization

Under CfD pricing, individual buildings are charged for the demand deviation. Therefore, in real-time load tracking control, an optimization problem is solved at each time step to minimize the CfD charge for the remainder of the day. Also, included in the real-time optimization objective function are the penalties for thermal comfort violation and change of actions. It is reasonable to hypothesize that with a greater CfD rate, the optimal solution will lean towards more thermal violations and change of actions and less demand deviation. We validate the control optimization by testing this hypothesis.

Various CfD rates are tested, with other parameters as summarized in Table 13. The optimization algorithm used to solve the problem is detailed in the next section. The corresponding RMSDs and the customer's billed costs are shown in Figure 16 and Figure 17. It is clear that greater CfD rate will drive the customer harder in load tracking, and result in lower

RMSD. However, the improvement is relatively minor, when CfD rate is greater than 0.01 $/KW^2, because RMSD approaches to the error of load prediction by the NARX model (7.6 KW, see Section 3.4.1). Meanwhile, the combined consequence of slow reduction of demand deviation and increase of CfD rate is that CfD charge grows steadily and becomes a greater portion of the customer's bill, from 8% when CfD rate is 0.005 $/KW^2 to 42% when it is 0.03 $/KW^2. This result proves the previous hypothesis that the control optimization, especially the real-time tracking, works as expected.

The CfD rate of 0.01 $/KW^2 is used in all the following experiments in Chapter 3 and Chapter 4. With this CfD rate, the CfD charge makes about 27% of the customer's utility bill (Figure 17).

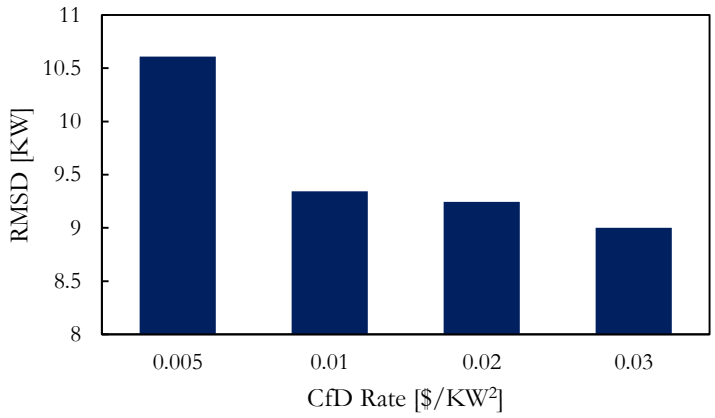

Figure 16 Impact of CfD rate to the demand deviation

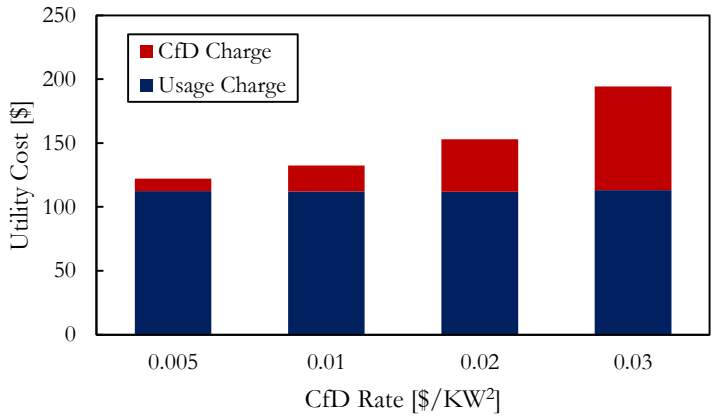

Figure 17 Impact of CfD rate to the customer's utility cost

3.5 Experiments

In this section, the performance of planning and load tracking optimizations under CfD is studied using designed experiments. The influence on the demand deviation by planning optimization, tracking optimization, weather forecast, occupancy forecast, unexpected event and forecast update are investigated.

3.5.1 The Base Case

Consider July 12th, 2013 for the base case. At 21:00 on the day-ahead, i.e. July 11th, 2013, the hourly weather forecast for the next day is pulled from *wunderground.com*. The dry bulb temperature forecast is plotted by the red curve in Figure 18*a*. And the occupancy forecast plotted by the red curve in Figure 18*b* is the average occupancy schedule of typical office buildings, as reported by [155]. During the operating day, at each hour, the latest hourly weather forecast for the next 24 hours is pulled from *wunderground.com*. Meanwhile, the occupancy forecast remains unchanged. The actual occupancy ratio is randomly generated according to the same profile and distribution as reported in [155].

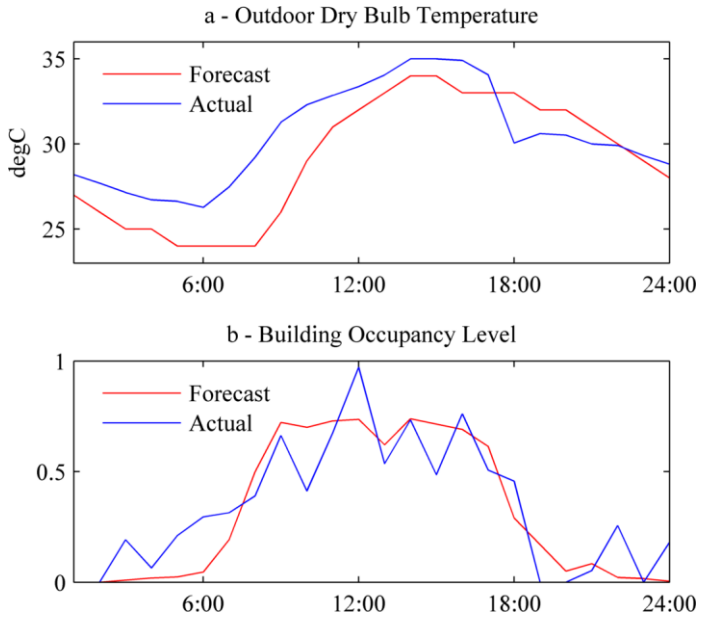

Figure 18 Actual conditions vs. forecasts

The hourly retail price schedule used in the base case study is illustrated in Figure 19. This schedule is announced day-ahead by the utility.

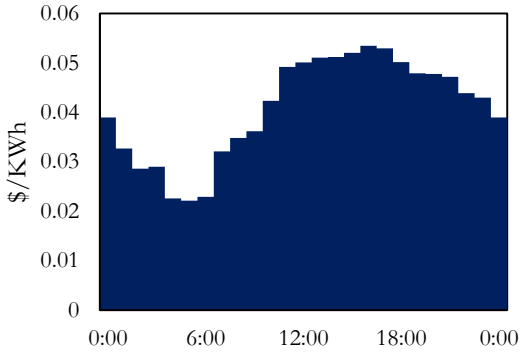

Figure 19 Hourly retail price (C) of the operating day

Other parameters involved in the day-ahead planning and real-time tracking optimizations are summarized in Table 13.

Table 13 Optimization parameters

Parameter	Value
p_1	100
p_2	100
q_1	0.01
q_2	0.5
T^l	21
T^u	25
x^l	18
x^u	27

Section 1.4.1.2 has reviewed the optimization techniques involved in other supervisory control studies. In this study, the prediction model (NARX network) is a non-linear approximation of the simulated building. Therefore, only non-linear optimization techniques are suitable. Dynamic Programming (DP) can be a good choice for the optimization, because the prediction model has the following characteristics:

(1) The prediction model is to be evaluated at discrete steps, and there are a finite number of steps;
(2) At each step, the system state in the next step is determined by the current decision, the current state, and the states several steps back;
(3) At each step, the decision is limited within a finite candidate set (discretized setpoint);
(4) The objective function is additive at each step.

Note that, characteristic (2) does not rigorously meet the recursive requirement for applying DP, because DP requires that the next state is a function of only the current state and current decision – previous states should not enter the formula [156]. In other words, due to the thermal inertial nature of the system, any decision made at current step will have influence to not only the

immediate next state but also states several steps in the future. However, a simple modification of the DP algorithm can solve this problem, as long as the number of future states affected by current decision is fixed and known (d_x in Eq. 27). In this case, the decision to make, at any step, is the setpoint for the current step plus the ones of $d_x - 1$ steps in the future, i.e., the solution space increases from 1-Dimensional to d_x-Dimensional. Correspondingly, the state space also increases from 1-Dimensional to d_x-Dimensional. Then the new formulation meets all requirements for DP.

DP guarantees to obtain the global optimal setpoint sequence, however, it can easily become intractable when the size of solution space increases (e.g., d_x is too large). Fortunately, the thermal system is usually considered as a second order system, third- or higher order models are rarely used to describe building thermal behavior. Thus, the dimension of the solution space is usually lower than or equal to 4. The resolution of indoor temperature control is at 0.5~1 °C – finer resolution does not have a significant advantage in terms of cost-benefit. Consequently, the solution space is within controllable range. If higher resolution control, together with higher order system, are considered and DP becomes inappropriate for this problem, other solvers can be employed, such as GA and PSO. The exploration of using those solvers other than DP is beyond the scope of this study.

By solving the planning stage problem, the planned demand schedule (red curve in Figure 20*a*) and corresponding thermostat setpoint schedule (red curve in Figure 20*b*) are determined. If the planned control is executed without tracking control, the actual consumption will be the one shown by the green curve in Figure 20*a*. If real-time tracking is conducted, the actual demand schedule will be as shown by the blue curve in Figure 20*a*.

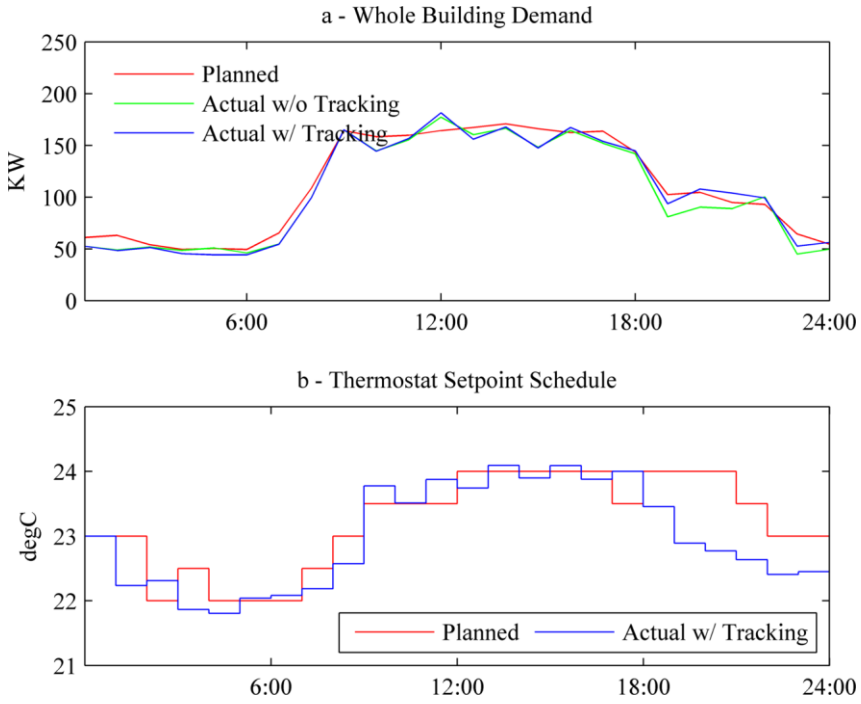

Figure 20 The base case results

As demonstrated, the real-time tracking optimization keeps the actual demand schedule close to the planned schedule. The RMSD is reduced by 1.1 KW (about 10%), as shown in Figure 21.

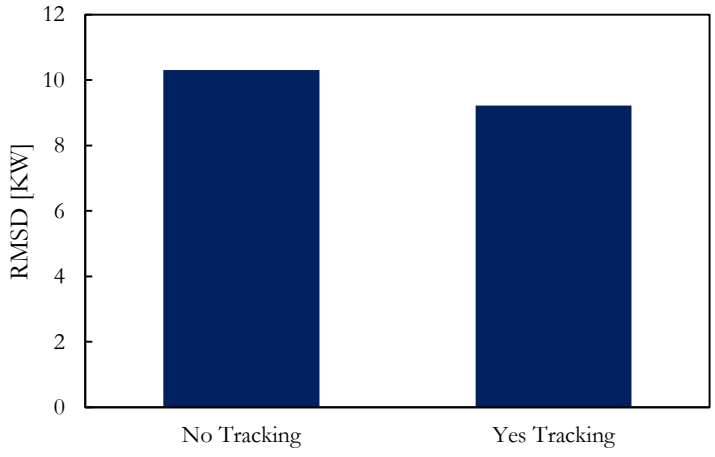

Figure 21 The base case demand deviation

3.5.2 Weather Forecast

In day-ahead planning, the optimal demand schedule is obtained based on the next day's hourly retail price, together with the weather and occupancy forecast available at the time of planning. The weather forecast could be a major source of uncertainty. Hypothetically, an accurate day-ahead weather forecast may help in limiting the demand deviation. To prove this hypothesis, three historical July days are selected as examples for typical weather forecasts with low, medium and high error, respectively (Figure 22). The result, as plotted in Figure 23, shows clearly that inaccurate weather forecast raises the building RMSD from 9.1 KW (low error) to 11.6 KW (high error). Also, the load tracking optimization is able to partially mitigate the demand deviation caused by weather forecast error. A medium error weather forecast is used in all other experiments in this chapter.

This result also suggests that the customers under CfD will be motivated to improve their weather forecast. A better weather forecast will help the customers lower demand deviation, and thus reduce the CfD charges.

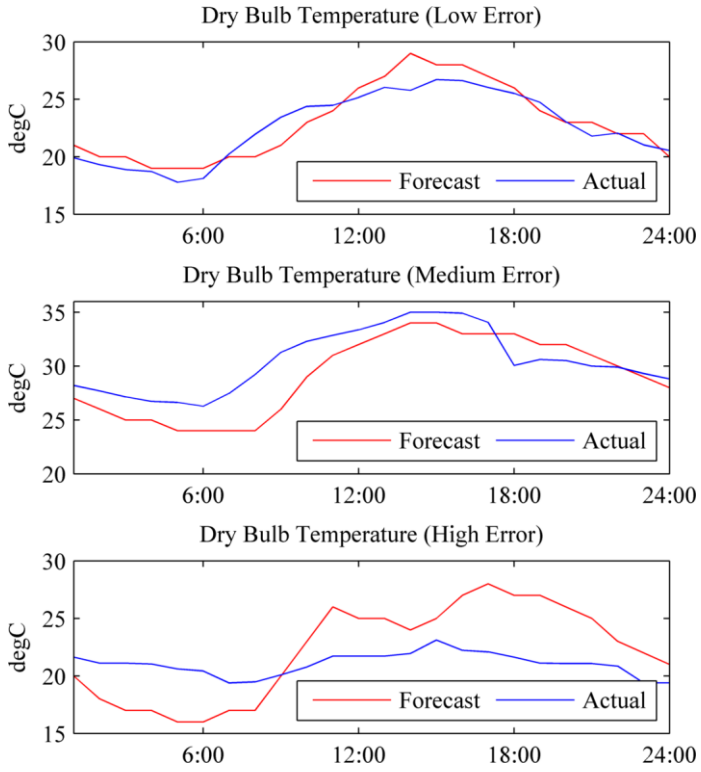

Figure 22 Weather forecasts with various levels of error

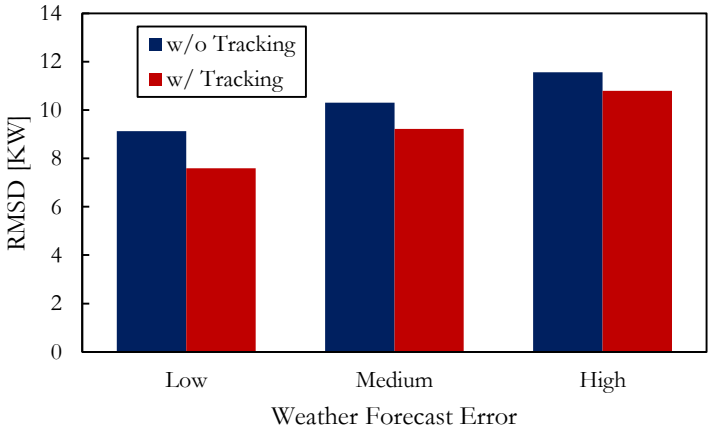

Figure 23 Impact of weather forecast error on demand deviation

3.5.3 Occupancy Forecast

The occupancy level is another major source of uncertainty in the day-ahead planning. CfD pricing holds individual customers responsible for forecasting their own occupancy schedules. An occupancy schedule is the aggregated level of non-HVAC consumption, including lighting and plug-in appliances. It is assumed without proof that the customers are capable of making such prediction, either by averaging over ordinary operation days in the past or based on activity schedules. In order to examine the impact of occupancy forecast error to demand deviation, three scenarios are subject to tests, where the occupancy forecasts are the same as the average occupancy reported in [155], but the actual occupancy profiles are randomly generated with low, medium and high deviations, respectively (Figure 24).

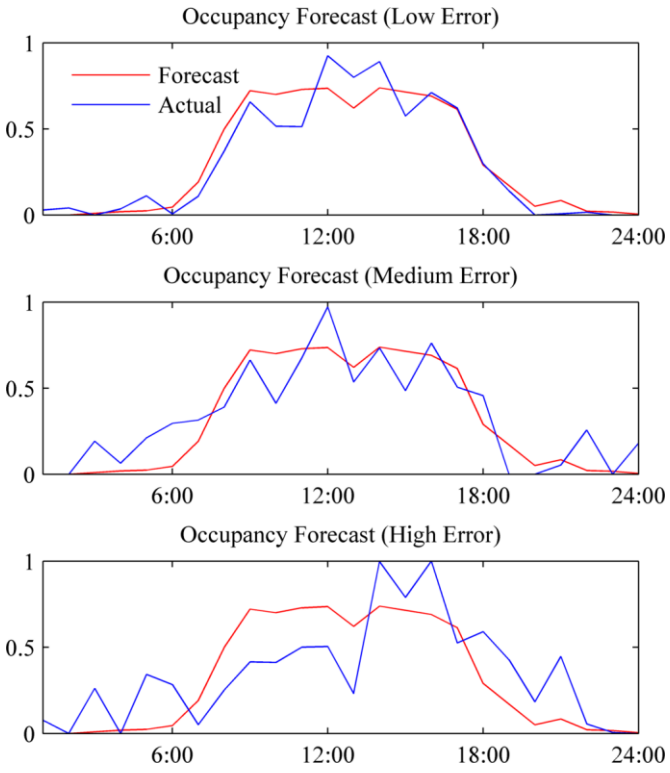

Figure 24 Occupancy forecasts with various levels of error

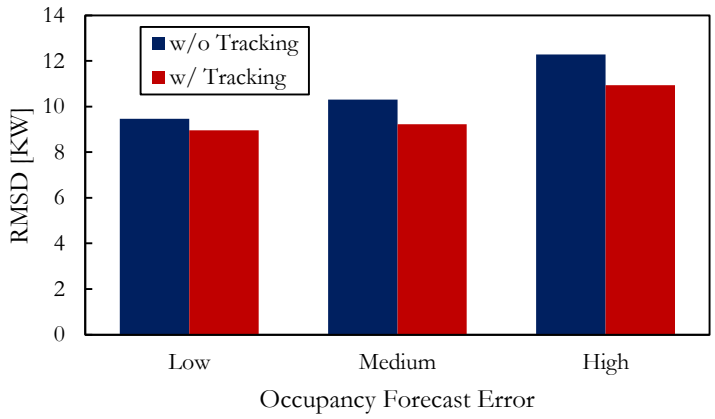

Figure 25 Impact of occupancy forecast error on demand deviation

According to the result shown in Figure 25, it is clear that the RMSD increases from 9.5 KW to 12.3 KW as the occupancy forecast error grows from low to high. This suggests that CfD retail pricing also drives the customers to better predict their demand level, or in other words, encourages a predictable consumption behavior. This is expected to reduce the overall uncertainty in the community demand, which will lead to savings of cost in the wholesale market. Such hypothesis is subject to test in Chapter 4. A medium error occupancy forecast is used in all other experiments in this chapter.

3.5.4 Unexpected Event and Forecast Update

Occupancy forecast error sometimes may be due to unexpected events. It is reasonable to believe that customers are able to update the occupancy forecast in real-time, if certain unexpected incident is about to happen. A major goal of CfD pricing is to reduce the demand fluctuation under those circumstances.

The following experiment is designed to examine the influence of unexpected increase of occupancy level. Consider the same setting as in the base case, except that the actual occupancy

level reaches maximum from 14:00 to 18:00, due to an event. Also assume that this event was not accounted for in the day-ahead plan. The actual occupancy and the forecast at the time of planning are illustrated in Figure 26*a*. The demand deviation of these two scenarios is plotted by the bar series of "No Event" and "Unexpected Event" in Figure 27. The result shows that the unexpected event raises the RMSD by 3.2 KW (about 31%) when load tracking is not conducted. Load tracking does not reduce the RMSD. Instead, it adds another 0.5 KW to the RMSD. This is because the occupancy forecast used in load tracking optimization is not updated with the event.

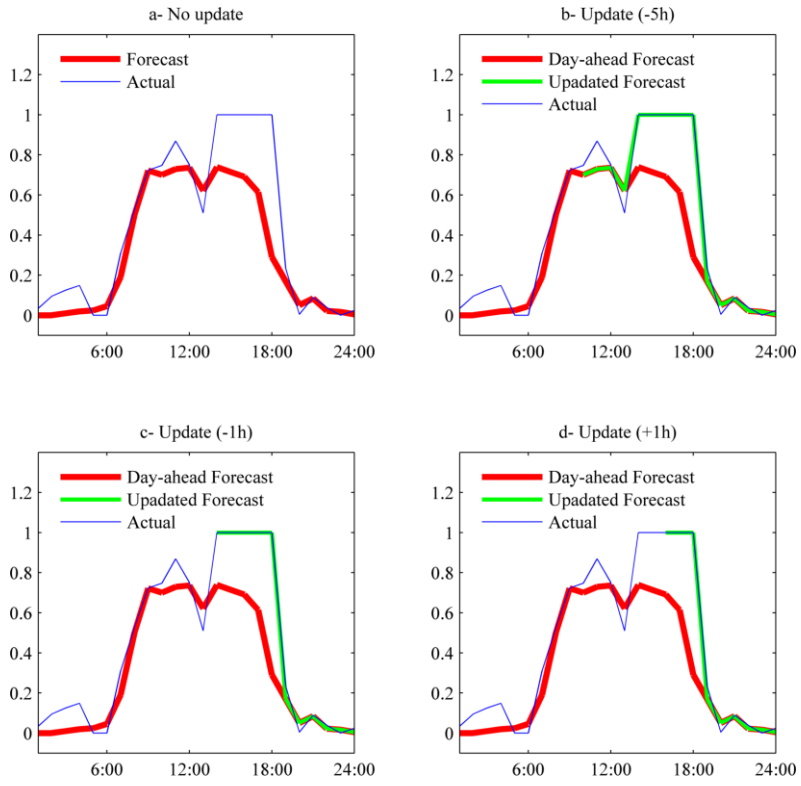

Figure 26 Occupancy level with unexpected event and forecast update

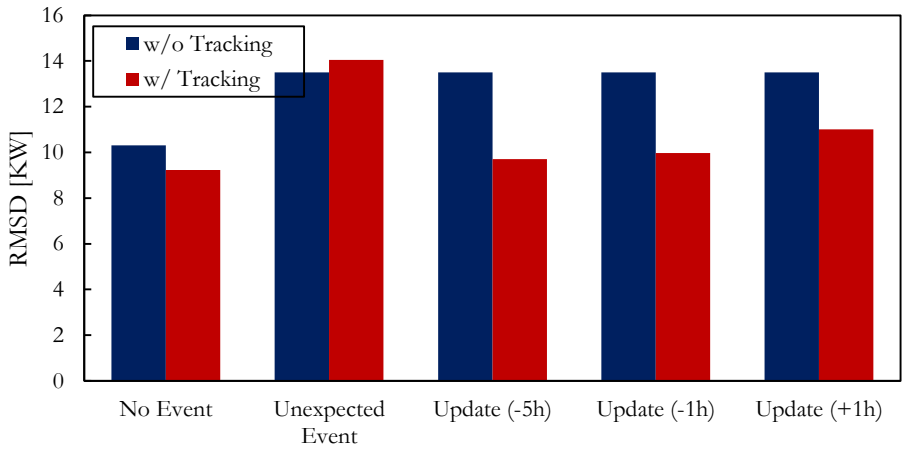

Figure 27 Impact of unexpected event and forecast update

A major question here is to determine if the demand deviation will be reduced by load tracking, if the occupancy forecast is updated with unexpected event several hours before. Three additional tests are conducted where the occupancy forecast is updated at 9:00 (5 hours in advance, denoted by "-5h", Figure 26*b*), 13:00 (1 hour in advance, denoted by "-1h", Figure 26*c*) and 15:00 (1 hours after the beginning, denoted by "+1h", Figure 26*d*), respectively. The bar graph in Figure 27 clearly shows that with forecast update, load tracking is able to reduce the RMSD by as much as 3.8 KW (about 28%). The most demand deviation reduction is achieved by an update 5 hours in advance. However, load tracking with forecast update only partially mitigates the deviation caused by the unexpected event, because the resulting deviation level is still slightly higher, compared to the case with tracking and without event.

The implication of this result is obvious, in order to have a lower CfD charge, the customers will be willing to avoid unexpected event and maintain a predictable consumption profile. In case an unexpected event happens, the customers will try to update the occupancy forecast as early as possible, during the real-time operation.

3.6 Discussion

Current retail rate structure completely exposes utility providers to the market risk caused by demand uncertainty. Raising the unit price seems to be the only countermeasure. However, higher prices mean more cost for all customers. The author intends to design a new rate structure which incentivizes individual customers to reduce demand deviation. The logic is that customer activities are a major source of demand uncertainty. It is reasonable to assume that individual customers are able to understand, and then forecast their own activities. Therefore, it is fair for them to bear the risk associated with their activities.

Under the proposed CfD pricing structure, the customers are responsible to pay for the usage charge plus the CfD charge related to the deviation between actual and planned demand. Individual customers will need models to predict their energy demand. Optimizations are conducted in both day-ahead planning and second day real-time tracking. Simulation experiments demonstrate that real-time load tracking is able to reduce the RMSD by 10%, in the base case. The accuracy of weather and occupancy forecasts significantly influence the demand deviation. As a result, CfD drives the customers to make as accurate forecasts as possible for planning and tracking. If an event happens which was not accounted for in the day-ahead plan, significant increase of demand deviation will be expected (as much as 31% RMSD increase). The load tracking control is able to partially mitigate the deviation rise (about 28% RMSD reduction) as long as the forecast is updated with the event. And the experiment shows that the earlier update may help reduce the demand deviation slightly. The CfD rate affects both demand deviation and the customer's cost. According to the experimental result, CfD rate increase from 0.005 $/KW^2 to 0.03 $/KW^2 will reduce the RMSD by 15%, but raises the customer's CfD charge by 7.3 times.

A deterministic formulation of the day-ahead planning is studied in this chapter. An attempt of using stochastic optimization, which considers the uncertainty of forecasts in day-ahead planning failed, as the stochastic formulation suffers from major dimensionality issues. How to incorporate CfD charge minimization into planning optimization remains to be solved in future studies.

This chapter studies the model-based predictive control for day-ahead planning and real-time load tracking, for a single building under CfD pricing. The experiment results prove that CfD pricing gives strong incentive to the customers to (1) make consumption plans, (2) maintain real-time demand close to the plan, (3) invest in the improvement of weather forecast and demand prediction models and (4) keep full awareness about their own activity schedules. In all, CfD pricing promotes the customers to maintain a predictable consumption profile. It is hypothesized that predictable consumption profiles of individual customers are able to bring down the community's cost in the wholesale market. This is subject to tests in Chapter 4.

Chapter 4 Reduce Community Demand Uncertainty by Cost-for-Deviation Pricing

Abstract

In the previous chapter, it has been demonstrated that individual customers will perform planning and load tracking optimizations in order to reduce cost under CfD. These control optimizations can reduce the demand deviation of individual customers. In this chapter, the details of CfD rate structure is provided. The author shows that the reduction of individual demand deviation will lower the community's cost for hedging the risk in the real-time wholesale market. This will, in the end, generate savings for all customers. Furthermore, CfD creates opportunity for buildings to manage demand collaboratively. A centralized collaboration and a distributed collaboration mechanisms are presented in this chapter. By conducting "demand transaction" between two customers, the participants are able to avoid high CfD charges.

4.1 Introduction

In Chapter 3, the demand deviation defined by Eq. 24 is used to measure the demand uncertainty at the individual building level. It has been demonstrated by experiments that CfD tariff drives individual customers to conduct day-ahead planning and real-time tracking in order to reduce demand deviation, and ultimately to lower CfD charges. Better demand prediction model, accurate weather forecast and occupancy forecast as well as event update are all encouraged by CfD. Therefore, CfD can be an effective economic approach to control demand uncertainty at individual customer level. Adding the CfD charge to the customers' utility bills can only be

justified if it leads to a reduction of the customers overall cost. This chapter examines the effectiveness of CfD at a community level.

In this chapter, a community microgrid with multiple buildings is considered. Under CfD pricing, individual buildings conduct day-ahead planning and real-time tracking controls independently, as is discussed in Chapter 3. At microgrid level, the utility provider or the MGCC calculates the demand bid to submit to the day-ahead wholesale market, by aggregates the day-ahead demand plans of individual customers. During the operating day, the utility provider will be charged at the day-ahead price and the real-time price for its procurement in the corresponding wholesale markets. On the other hand, the utility provider will get paid by individual customers for the electricity usage as well as CfD charges. Under the assumption that the utility provider is not-for-profit, the customers' overall payment will be equal to the community's cost in the wholesale markets, with a proper risk measure considered.

Risk hedging is involved in most, if not all, retail pricing models. The cost for hedging the market risks makes a significant portion of the community's electricity cost [157, 158]. Therefore, reducing the market risk contributes to the cost reduction. There are a number of measures to characterize risks of portfolio, such as variance, value-at-risk (VaR) and conditional value-at-risk (CVaR). Variance is usually employed by mean-variance model with the assumption of normal or log-normal distribution. So it can fail to characterize asymmetric risk distribution or distributions with fat tails. [159] Also, because it will lead to a non-convex formulation, it is challenging to incorporate mean-variance model into stochastic optimizations [160, 161]. VaR is a widely used risk measure. For a specific confidence level α and time horizon, VaR_α of a portfolio is defined as the threshold value such that the probability that the loss will not exceed this value is α [162]. VaR works well with normal or log-normal risk distribution, but it is not a

coherent risk measure because it may lack sub-additivity when applied to non-normal distributions [162]. CVaR is a modification of VaR, but it is a coherent risk measure [162, 163] because it satisfies the requirements of monotonicity, sub-additivity, homogeneity and translational invariance [164]. For a specific confidence level α and time horizon, $CVaR_\alpha$ of a portfolio is defined as the expected loss in the $(1-\alpha)\times 100\%$ worst cases [162, 163]. CVaR measure has been widely adopted in electricity retail price determination, as has been reported by [157, 158]. In this dissertation, CVaR is used to measure the risk associated with real-time market transaction.

At a community microgrid level, CfD also creates opportunity for individual buildings to collaborate in real-time load tracking in order to reduce CfD charges. In previous studies of microgrid, collaboration is seen between DGs and loads [112], between DGs and CES [113], among different loads within one building [111], or among competing EV chargers [110]. In those cases, collaboration is accomplished by a higher level controller who conducts optimization and allocates the resources – this is centralized decision making. The centralized load tracking collaboration that is to be demonstrated in this chapter follows the same idea. Additionally, this chapter explores a new distributed load tracking mechanism, where decisions are made by individual customers who are assumed to be independent and reasonable.

The rest of this chapter is organized as follows: Section 4.2 details the problems, including a description of the subject community model, the CfD tariff calculation, the calculation of the community cost function, and the formulation of collaborative load tracking optimizations. Section 4.3 describes the prediction model used in the experiments. Section 4.4 presents the validation for the building prediction model, the community model and the collaboration model.

The results of a base case and a series of experiments are presented in Section 4.5. Section 4.6 discusses the results and gives concluding remarks.

4.2 Problem Formulation

4.2.1 Community Microgrid

CfD is an electricity retail pricing scheme. It is supposed to be implemented in a retail market where one utility provider and multiple customers form a microgrid. Such microgrid can be a community or an industrial/commercial campus. Without loss of generality, a community microgrid is subject to study in this chapter.

A typical community microgrid consists of customer loads, DGs, CES, connecting lines, controllers (including MGCC and distributed generation and load controllers) and communication devices, as illustrated by Figure 2. A simplified community microgrid model is studied in this chapter, which only has two buildings and one MGCC (Figure 28). Each building has its own LC. LC is an intelligent device that monitors and controls the load it attaches to. There are many BASs available in the market for large commercial buildings. A number of home automation systems emerge for small residential buildings, in recent years, such as Synco from Siemens Building Technology. Existing products may be programmed with only simple decision making algorithms. Those with more sophisticated functionalities and stronger computation power can be expected in the near future [165]. The following four critical features of LCs are emphasized in this study:

- **Communication**. LCs are able to communicate with MGCC to get information such as price and weather forecast, and pass demand schedules to MGCC. LCs can also communicate to each other for collaborative demand management.
- **Monitoring**. LCs are connected to meters, sensors and device controllers in the buildings. The consumption levels, as well as operation status, of all energy consuming devices are continuously monitored.
- **User interface**. LCs have human-machine interface that allows users to input personal preferences and schedules.
- **Decision making**. Most importantly, the day-ahead planning and real-time load tracking optimization algorithms are programmed in LCs. LCs are able to decide the demand schedules to submit day-ahead, as well as control action sequences in real-time. During real-time, LCs may also determine whether to conduct demand transaction with other buildings, and, if yes, what the optimal transaction schedule would be.

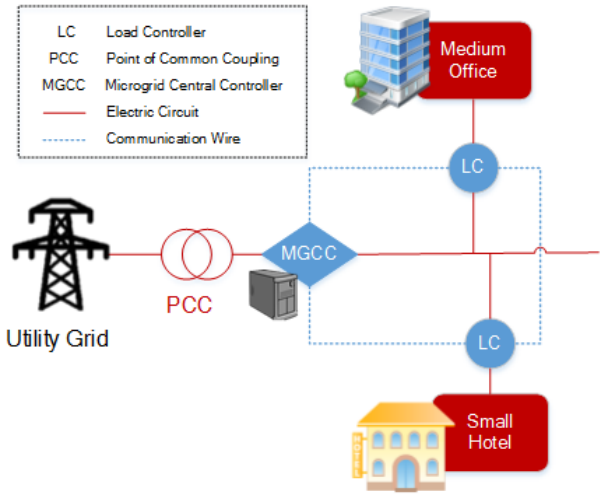

Figure 28 A simplified community microgrid

MGCC is an automatic central controller for microgrid operation and energy management. Generally, it coordinates load, DG production, CES charging and discharging, power quality across the microgrid and the transition between "grid-tied" and "island" modes. In most microgrid designs, MGCC also functions as the representative of the entire microgrid on the utility grid operation and activities in electricity markets. In this study, the MGCC's market role is emphasized. It can be seen as the representative of the utility provider, who is responsible for collecting demand schedules from all the customers, making forecasts for microgrid demand schedules, submitting demand bids in day-ahead wholesale market, and settling the demand deviation in real-time wholesale market.

4.2.2 Retail under CfD

Under CfD pricing, the bill that each customer pays for energy consumption during each hour is split into two parts. The first part is the energy cost, which is calculated by the customer's energy usage during the hour multiplying by the energy price of that hour. The hourly price is announced before customers submitting demand schedules day-ahead. The second part is the CfD charge, which is proportional to the squared deviation between planned and actual demand in that hour. The coefficient in CfD charge calculation is called CfD rate, and is assumed to be given here. The overall bill is obtained by summing up all hourly bills for a billing cycle (e.g. a day or a month). The operation of individual building under CfD has been studied in Chapter 3. In this chapter, the operation of multiple buildings within a community microgrid is subject to test.

Regarding the hourly price announced day-ahead, three assumptions are made for the utility provider:

Assumption 1: It is assumed that over a long period of time, the cost of purchasing electricity from wholesale market is fully shared by all customers, and that the income from sale is fully used by the utility provider to cover the cost. Proper risk hedging cost is considered as part of the utilities' cost. For those utility companies that are seeking for profit, the customers' total bill can be calculated by adding a certain level of profit to the cost - it will not change the conclusion on CfD's effectiveness.

Assumption 2: The utility provider only operates one microgrid. Therefore, it is assumed to be a price taker in both day-ahead and real-time markets. This assumption is valid because a microgrid is supposed to have a much smaller load and generation capacity compared to the load and capacity on the grid that is operated by an ISO.

Assumption 3: CfD requires an accurate hourly retail price to be given *prior to* customers submitting demand schedules. Therefore, it is assumed that the utility provider is able to accurately predict the day-ahead wholesale price. According to many studies, day-ahead wholesale price prediction can be very accurate [166-169]. With this assumption, the utility provider will face price risk in the wholesale market. However, price risk is inevitable to the utility provider, no matter what retail pricing is implemented, except RTP. This dissertation does not focus on price risk mitigation, so the risk hedging cost of the utility only includes the cost of quantity risk.

To summarize, the steps of the day-ahead and real-time operation under CfD are as follows:

Day-ahead

Step 1: The utility provider predicts the day-ahead wholesale price, and announces hourly retail price; Step 2: Each building conducts day-ahead planning optimization (detailed in Chapter 3), and submits demand schedule for the next operating day; Step 3: The utility provider calculates the demand bid by aggregating the demand schedules submitted by all the customers; Step 4: After the day-ahead wholesale market is cleared, the demand schedule that the utility provider submitted becomes a financially binding contract. Meanwhile, the demand schedule submitted by each customer is also binding under CfD;
Operating day (each hour) Step 1: Each building executes its most updated control action sequences; Step 2: Each building updates the weather and occupancy forecasts as well as system responses, and then conducts real-time tracking optimization (detailed in Chapter 3). It then decides the control action sequence for the remaining hours of the day. Collaborative load tracking optimization/negotiation is also performed at this step;
Bill generation

Each building's energy bill is calculated based on the submitted demand schedule, actual energy consumption and hourly retail price.

4.2.3 Community Cost Function

Consider the hourly cost of the community at time t, Y_t. It is formulated as the summation of three elements: the procurement the cost in day-ahead market ($U_{DA,t}$), the procurement cost in real-time market ($U_{RT,t}$), and the risk hedging cost (R), as shown by Eq. 32

$$Y_t = U_{DA,t} + U_{RT,t} + R \qquad \text{Eq. 32}$$

The two procurement cost terms are defined by Eq. 33 and Eq. 34, respectively.

$$U_{DA,t} = \pi_{DA,t} P_t^I \qquad \text{Eq. 33}$$

$$U_{RT,t} = \pi_{RT,t}\left(P_t^{II} - P_t^I\right) \qquad \text{Eq. 34}$$

where,

P^I: the planned demand of the community (P_t^I is the element associated with time step t);

P^{II}: the actual demand of the community (P_t^{II} is the element associated with time step t);

π_{DA}: the day-ahead LMP ($\pi_{DA,t}$ is the element associated with time step t);

π_{RT}: the real-time LMP ($\pi_{RT,t}$ is the element associated with time step t);

This dissertation focuses on mitigating the quantity risk that is caused by demand uncertainty. Therefore, the risk in real-time market is considered. The risk hedging cost is hence formulated as the CVaR of the real-time procurement cost multiplied by a user specific risk parameter, ρ (Eq. 35) [158].

$$R = \rho CVaR_{\alpha}(U_{RT}) \quad \text{Eq. 35}$$

Use $f(u)$ and $F(u)$ to represent the probability distribution function and cumulative distribution function of U_{RT}, respectively. Then $CVaR_{\alpha}(U_{RT})$ can be expressed as:

$$CVaR_{\alpha}(U_{RT}) = \frac{1}{1-\alpha}\int_{\xi}^{\infty} uf(u)du \quad \text{Eq. 36}$$

where, ξ is the VaR of U_{RT}, which can be obtained by solving Eq. 37.

$$F(\xi) = \alpha \quad \text{Eq. 37}$$

4.2.4 Collaborative Load Tracking

In the original design of community microgrid, each LC only exchanges price and demand schedules with MGCC. LCs conduct day-ahead planning and real-time load tracking optimizations independently, based on the forecasts of the weather and their own occupancy.

The optimization objectives are the building's total cost, including energy cost, CfD charges as well as penalties for thermal comfort violation and change of action.

It is possible that certain unexpected events (e.g., occupancy surge) occur in an operating day without any provisions for them in the day-ahead plan. This can cause serious demand deviation and hence significant CfD charges, even with the building owner having the ability of adjusting the occupancy forecast several hours before the event, the real-time load tracking may still be inadequate to lower CfD charges through any proper control actions. Meanwhile, another building may suffer from elevated CfD charges due to demand lower than the planned level. If these two buildings are aware of the problems facing the other, they may be willing to collaborate via what we called "demand transaction" mechanism. The building that is about to experience an occupancy surge (the buyer) may want to "buy" electricity from the other building, instead of buying from the utility provider. This will keep its demand in check, as measured by the utility provider. On the other hand, the building whose demand is lower than planned (the seller) may want to draw more than enough electricity from the utility, and "sell" the excessive amount to the buyer, so that the seller's demand is close to the planned level. In all, the demand transaction lowers the CfD charges of both buildings.

The collaborative load tracking can be implemented in many ways. In this dissertation, the author explores two simplest designs of tracking collaboration mechanisms – the centralized load tracking and the distributed tracking with fixed transaction rates.

4.2.4.1. Centralized Load Tracking

In the previous design of community microgrid, MGCC is not responsible for any planning or tracking optimization. Individual LCs perform day-ahead planning and real-time tracking

controls. A minor modification, which turns MGCC responsible for real-time tracking of all the buildings, can enable collaborative load tracking.

Consider the case of two-building community. The buildings are annotated by A and B. Assume that MGCC has, for each building, the same load prediction model as is used by the LC. Then, MGCC solves, in real-time, an optimization problem with respect to the control actions of all the buildings and the demand transactions for the remaining time of the planning horizon, minimizing a cost function that integrates CfD charges, thermal comfort violation penalty and change of action costs, for all buildings. The optimization problem is formulated as follows:

The <u>Centralized Real-time Tracking</u> optimization: At time step k

Decision variable: $x_t^{A,II}\big|_{t=k}^{H}$, $x_t^{B,II}\big|_{t=k}^{H}$ and $E_t\big|_{t=k}^{H}$

Minimize:
$$G_{t=k}^{II} = \sum_{t=k}^{H} \begin{Bmatrix} q_1\left[\left(P_t^{A,I} - P_t^{A,II} + E_t\right)^2 + \left(P_t^{B,I} - P_t^{B,II} - E_t\right)^2\right] \\ + q_2\left[\left(x_t^{A,I} - x_t^{A,II}\right)^2 + \left(x_t^{B,I} - x_t^{B,II}\right)^2\right] \\ + p_1\left(u_t^{A,II} + u_t^{B,II}\right) + p_2\left(l_t^{A,II} + l_t^{B,II}\right) \end{Bmatrix} \quad \text{Eq. 38}$$

Subject to:
$$\begin{bmatrix} P_t^{A,II} \\ T_t^{A,II} \end{bmatrix}\Bigg|_{t=k}^{H} = F^A\left(x_t^{A,II}\big|_{t=k}^{H}, \hat{\omega}_t^k\big|_{t=k}^{H}\right) \quad \text{Eq. 39}$$

$$\begin{bmatrix} P_t^{B,II} \\ T_t^{B,II} \end{bmatrix}\Bigg|_{t=k}^{H} = F^B\left(x_t^{B,II}\big|_{t=k}^{H}, \hat{\omega}_t^k\big|_{t=k}^{H}\right) \quad \text{Eq. 40}$$

$$T^l - l_t^{A,II} \le T_t^{A,II} \le T^u + u_t^{A,II} \quad \text{Eq. 41}$$

$$T^l - l_t^{B,II} \le T_t^{B,II} \le T^u + u_t^{B,II} \quad \text{Eq. 42}$$

$$E^l \le E_t \le E^u \quad \text{Eq. 43}$$

$$x^l \le x_t^{A,II} \le x^u \quad \text{Eq. 44}$$

$$x^l \le x_t^{B,II} \le x^u \quad \text{Eq. 45}$$

where,

$x_t^{A,II}\big|_{t=k}^{H}$ and $x_t^{B,II}\big|_{t=k}^{H}$: the vectors of thermostat setpoint schedule obtained at time step t for the remainder of the time horizon ($x_t^{A,II}$ and $x_t^{B,II}$ are the elements associated with time step t, for building A and B, respectively);

E: the vectors of electricity A purchases from B (E_t is the element associated with time step t). The negative value means transaction is from B to A;

$P^{A,I}$ and $P^{B,I}$: the vectors of planned consumption for the next day ($P_t^{A,I}$ and $P_t^{B,I}$ are the elements associated with time step t, for building A and B, respectively);

F^A and F^B: the function of the prediction model for building A and B, respectively;

$P^{A,II}$ and $P^{B,II}$: the vectors of actual consumption conditioned on the realization of weather and occupancy, ω ($P^{A,II}$ and $P^{B,II}$ are the elements associated with time step t, for building A and B, respectively);

$T^{A,II}$ and $T^{B,II}$: the vectors of actual average room temperature ($T_t^{A,II}$ and $T_t^{B,II}$ are the elements associated with time step t, for building A and B, respectively);

$x^{A,I}$ and $x^{B,I}$: the vectors of thermostat setpoint planned schedule ($x_t^{A,I}$ and $x_t^{B,I}$ are the elements associated with time step t, for building A and B, respectively);

$u^{A,II}$ and $u^{B,II}$: the vectors of actual violations of upper bound of comfort range ($u_t^{A,II}$ and $u_t^{B,II}$ are the elements associated with time step t, for building A and B, respectively);

$l^{A,II}$ and $l^{B,II}$: the vectors of actual violations of lower bound of comfort range ($l_t^{A,II}$ and $l_t^{B,II}$ are the elements associated with time step t, for building A and B, respectively);

$\hat{\omega}^k$: the vector of forecasted weather and occupancy, updated by time step k ($\hat{\omega}_t^k$ is the element associated with time step t);

T^u and T^l: the upper and lower bound of thermal comfort range, respectively;

E^u and E^l: the upper and lower bound of demand transaction, respectively;

x^u and x^l: the upper and lower bound of setpoint, respectively.

Eq. 38 is the new objective function. It is different than the previous version (Eq. 19) in two ways. First, the new function is the summation of the objectives of real-time tracking optimization for both buildings. Second, in the new objective function, the actual demands used in CfD charge calculation are the actual *grid* demand, which, for the buyer of the demand transaction, equals to actual demand minus demand transaction quantity ($P_t^{A,II} - E_t$), and for the seller, it equals to the actual demand plus demand transaction quantity ($P_t^{B,II} + E_t$). Most of constraints are the same as in previous individual tracking optimization, except that a new boundary constraint is added to demand transaction quantity (Eq. 43).

With centralized load tracking, MGCC performs the above optimization and determines the setpoint sequences for both buildings as well as the demand transaction, if any, between them. At the end, the bill for each building (Z^A and Z^B), is the energy cost based on actual consumption plus CfD charge based on actual *grid* demand, as shown in Eq. 46 and Eq. 47.

$$Z^A = \sum_{t=1}^{H} \left[C_t P_t^{A,II} + q_1 \left(P_t^{A,I} - P_t^{A,II} + E_t \right)^2 \right] \quad \text{Eq. 46}$$

$$Z^B = \sum_{t=1}^{H} \left[C_t P_t^{B,II} + q_1 \left(P_t^{B,I} - P_t^{B,II} - E_t \right)^2 \right] \quad \text{Eq. 47}$$

4.2.4.2. Distributed Tracking Control

In contrast to the centralized tracking conducted by MGCC, distributed tracking is performed by individual LCs. When LCs perform tracking optimization during real-time, the demand transaction is just another decision variable. We assume that each demand transaction has a corresponding financial transaction with a predetermined fixed rate and variable rate. For example, given that, during time step t a demand transaction of quantity E_t is executed, the corresponding cost of this transaction becomes as follows:

$$Y_t = \begin{cases} 0 & if\ E_t = 0 \\ C_f + C_v E_t & f\ E_t > 0 \end{cases} \qquad \text{Eq. 48}$$

where,

C_f : the fixed cost per transaction;

C_v : the variable cost per KWh demand transaction.

During each hour of the operating day (except the first hour – when no tracking is needed), each LC solves a real-time tracking optimization problem to determine the setpoint sequence and how much demand it needs to purchase from the other building for the remaining period of the operating day. The following real-time tracking optimization model determines the LC's proposal on demand transaction.

The <u>Distributed Real-time Tracking</u> optimization: at time step k

Decision variable: $x_t^{II}\big|_{t=k}^{H}$ and $E_t\big|_{t=k}^{H}$

Minimize: $$G_{t=k}^{II} = \sum_{t=k}^{H} \begin{bmatrix} q_1\left(P_t^I - P_t^{II} + E_t\right)^2 + Y_t \\ + q_2\left(x_t^I - x_t^{II}\right)^2 + p_1 u_t^{II} + p_2 l_t^{II} \end{bmatrix}$$ Eq. 49

Subject to: $$\begin{bmatrix} P_t^{II} \\ T_t^{II} \end{bmatrix}\Bigg|_{t=k}^{H} = F\left(x_t^{II}\Big|_{t=k}^{H}, \hat{\omega}_t^k\Big|_{t=k}^{H} \right)$$ Eq. 50

$$T^l - l_t^{II} \le T_t^{II} \le T^u + u_t^{II}$$ Eq. 51

$$E^l \le E_t \le E^u$$ Eq. 52

$$x^l \le x_t^{II} \le x^u$$ Eq. 53

Eq. 48

Having solved this optimization, if the subject LC decides that a demand transaction is needed, it will make a proposal to the other building. The LC of the other building will then perform a real-time tracking optimization, formulated as follows:

The <u>Distributed Real-time Tracking</u> optimization: at time k

Decision variable: $x_t^{II}\Big|_{t=k}^{H}$

Minimize a: $$G_{t=k}^{IIa} = \sum_{t=k}^{H} \begin{bmatrix} q_1\left(P_t^I - P_t^{II}\right)^2 \\ + q_2\left(x_t^I - x_t^{II}\right)^2 + p_1 u_t^{II} + p_2 l_t^{II} \end{bmatrix}$$ Eq. 54

Minimize b: $$G_{t=k}^{IIb} = \sum_{t=k}^{H} \begin{bmatrix} q_1\left(P_t^I - P_t^{II} - E_t\right)^2 - Y_t \\ + q_2\left(x_t^I - x_t^{II}\right)^2 + p_1 u_t^{II} + p_2 l_t^{II} \end{bmatrix}$$ Eq. 55

Subject to: Eq. 48, Eq. 50, Eq. 51 and Eq. 53

In the above real-time tracking optimization, the transaction schedule ($E_t|_{t=k}^{H}$) is given by the proposal and the sale to the first building is included in the objective function as a cost reduction term (Eq. 54). The second building will only accept the transaction proposal if it will not increase its optimal objective value, i.e. $G_{t=k,\min}^{IIa} \geq G_{t=k,\min}^{IIb}$.

The above real-time load tracking formulation has a sliding-window style, so that, for a given sequence of actions determined from the above models, only the actions for the immediate next time step are executed. Then all the forecasts and system responses are updated, load tracking and collaboration restart for the time window that has shifted one time step forward.

4.3 Microgrid Model

4.3.1 The Hotel

We consider a community with an office building and a hotel building. Each of these two buildings is represented by an EnergyPlus simulation model. As has been explained in Section 3.3, this study uses existing and validated simulation models rather than real buildings for data collection and testing, because real buildings are not readily available for our study. Simulation models have some advantages in terms of inexpensive data collection and sufficient data variation. The simulation models are developed and validated by the National Renewable Energy Laboratory for a "Reference Medium Office" building and a "Reference Small Hotel" building

[151]. The basic information about the office model and its geometry have been presented in Table 10 and Figure 13, respectively. The basic information about the small hotel model is summarized in Table 14, and its geometry is illustrated in Figure 29.

Table 14 Summary of the demonstration building (Reference Small Hotel)

Building Location	Chicago, IL
Building Function Type	Hotel
Floor area	4,014 m^2 (43,200 ft^2)
Floor number	4
Number of conditioned zones	67
Window-to-wall ratio	0.109
HVAC system	PTAC for guest rooms, PSZ-AC for common areas, Electrical unit heaters in stairs and storage areas. Economizers on common area systems per 90.1-2004. No economizers on guest room PTACs

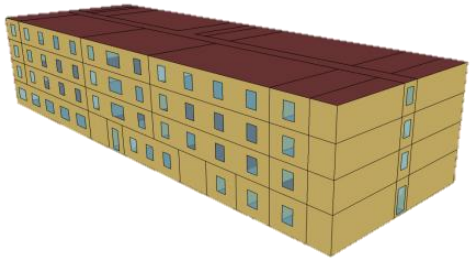

Figure 29 Small hotel model - building geometry

Hotels generally have different occupancy patterns than an office. The assumed average occupancy ratio profile, together with standard deviations, are plotted in Figure 30.

Similar to the study with the office model in Chapter 3, a NARX network model is developed to approximate the simulated hotel system. After the same procedure of data generation and training, the NARX model with 4 nodes on the first hidden layer, 3 nodes on the second hidden

layer and 2-step delay produces the best prediction results. This network is denoted as NARX-H04H03D02. The validation of this NARX network will be detailed later in Section 4.4.1.

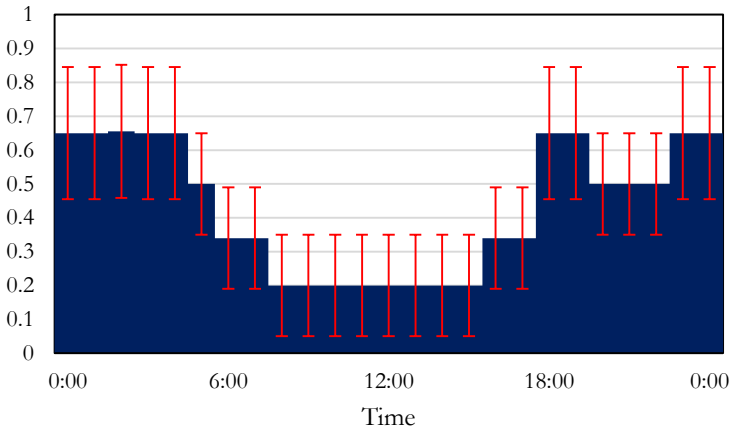

Figure 30 Building occupancy ratio profile (small hotel)

4.3.2 The Event

In testing collaborative load tracking, in order to ensure that load tracking control without demand transaction is inadequate to reduce CfD charges and then that demand transaction is necessary, EV charging is added as an extra load associated with the event. It is assumed that, during the event, the occupancy level reaches to the maximum (i.e., the occupancy ratio equals to 1), and EV charging level is 80% of its capacity (Figure 31). The capacity of the charging facility is assumed to be 40 KW, therefore the EV charging load during the event is 32 KW.

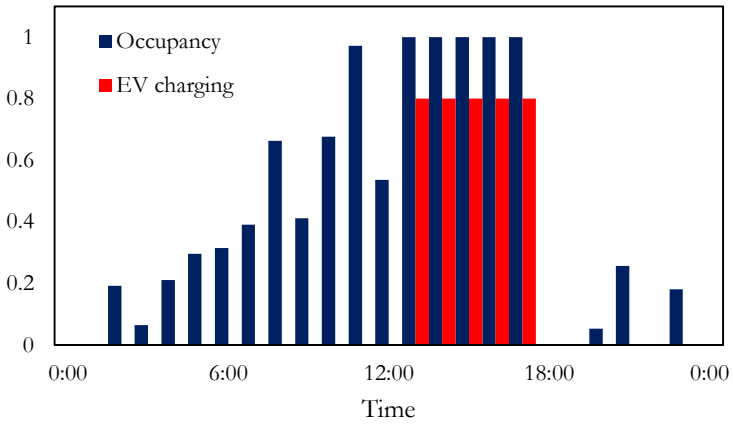

Figure 31 Exemplary occupancy and EV charging profile (office, event 14:00-18:00)

4.4 Validation

4.4.1 The Prediction Model

The same methods as detailed in Section 3.3 are involved to train an ANN model that approximates the Reference Small Hotel EnergyPlus simulation model. A NARX network with 4 nodes in the first hidden layer, 3 nodes in the second hidden layer and 2-step delay produces the best prediction results in both hourly and day-ahead prediction tests. This network is denoted as NARX-H04H03D02. The evaluation matrices of this network are summarized in Table 15 and Table 16.

NARX-H04H03D02 network predicts hotel hourly demand with 5.3 KW error (4.6%), in average. The prediction explains 96% of the variation of the building demand, and the error relative standard deviation is about 6.2%. The day-ahead load prediction has a slightly larger error. Both prediction results are acceptable compared to those studies in literatures [36, 38, 39]. The room temperature predicted by the NARX network model has about 0.9 °C errors (3.1%),

which is greater than the error of temperature prediction of the office NARX model (0.7 °C), and also greater than those in the literatures (0.1~0.6 °C) [152-154]. For the same reasons as have been discussed in Section 3.4.1, this prediction error is considered acceptable. Figure 32 and Figure 33 plot the load and room temperature comparison between model prediction and EnergyPlus simulation.

Table 15 NARX-H04H03D02 network demand prediction evaluation

Test	MAPE	RMSE	CV	R^2
1-Step	0.046	5.3	0.0619	0.9557
24-Step	0.053	6.0	0.0695	0.9387

Table 16 NARX-H04H03D02 network room temperature prediction evaluation

Test	MAPE	RMSE	CV	R^2
1-Step	0.031	0.9	0.0388	0.8710
24-Step	0.031	0.9	0.0378	0.8448

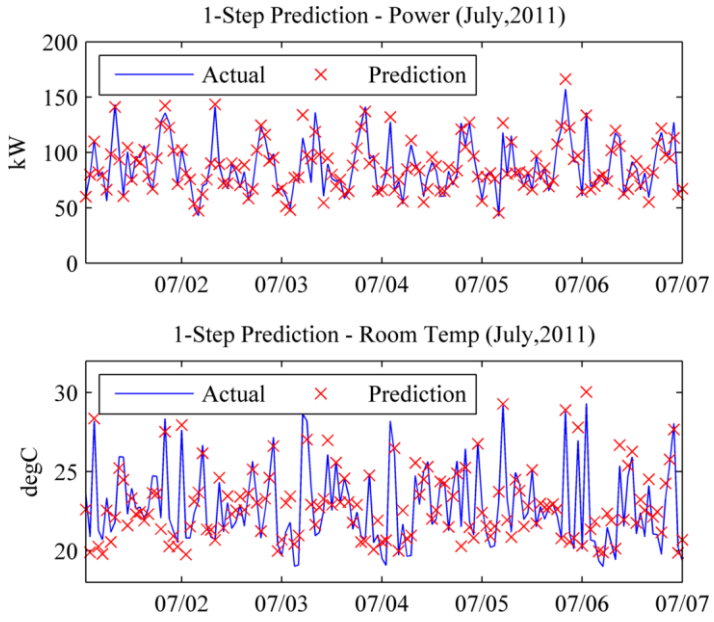

Figure 32 NARX-H04H03D02 network 1-step prediction

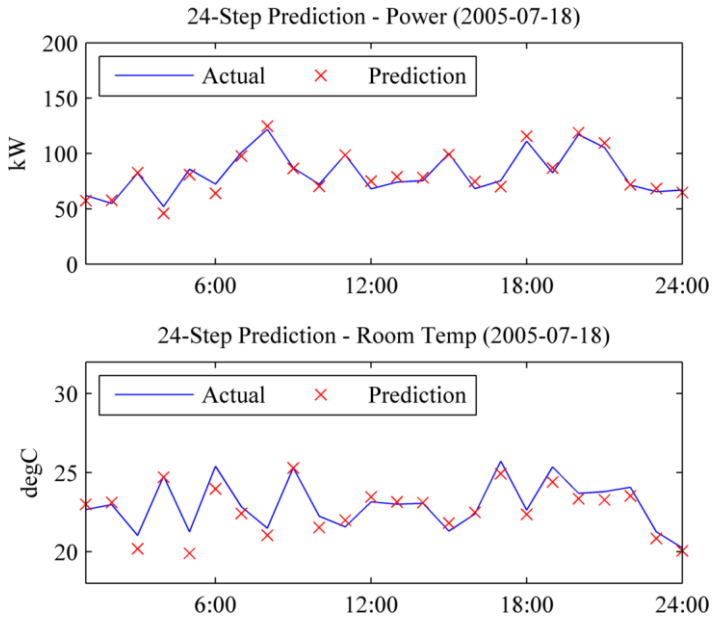

Figure 33 NARX-H04H03D02 network 24-step prediction

4.4.2 Control Optimization of the Community

In Section 3.4.2, the individual building control optimization is validated by testing the building's demand deviation sensitivity to various CfD rates. The result shows building demand deviation declines as CfD rate increases. This validates the control optimization, as the greater CfD rate puts more weight on CfD charges than on penalties of thermal comfort violations and change of actions, in the objective function. It drives the building harder to track the demand schedule.

To validate the control optimization in the context of a community, a similar sensitivity test is conducted. The community risk hedging cost, instead of demand deviation, is compared under various CfD rates ranging from 0.005 to 0.03 $/KW^2. The reason for comparing the risk hedging cost, rather than the overall cost, is that CfD rate mainly affects load tracking, and the impact is reflected by lower demand uncertainty, and hence lower quantity risk. Figure 34 presents the test result with all settings the same as in the base case detailed later in Section 4.5.1.1. According to this result, greater CfD rate drives the risk hedging cost down. This result perfectly agrees with the demand deviation sensitivity test on individual buildings (Figure 17). Therefore, it validates the community control optimization.

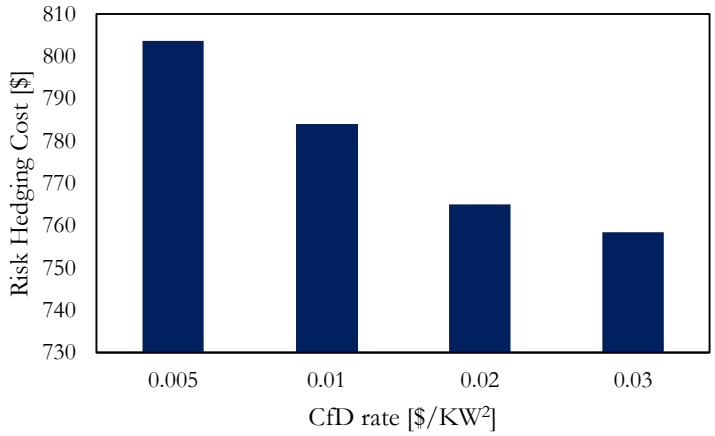

Figure 34 Risk hedging cost under different CfD rates

4.4.2.1. Centralized Tracking

CfD charge is the driving force for individual buildings to conduct real-time tracking control. In the case where collaborative tracking control is necessary, it is expected to be sensitive to the CfD rate. Hypothetically, under greater CfD, the building that is experiencing an unexpected demand surge has more motivation to buy from another building, so more demand transaction must be conducted. The following test is designed to examine the sensitivity of collaborative tracking to various CfD rates. Consider the same scenario as will be detailed in Section 4.5.2.1, where the demand of the office building will rise significantly due to unexpected events, and the MGCC decides demand transaction will be needed to mitigate the resulting spike of CfD charge. Under CfD rates ranging from 0.005 to 0.03 $/KW^2, the demand deviation of the two buildings is illustrated in Figure 35. The corresponding total transactions are plotted in Figure 36.

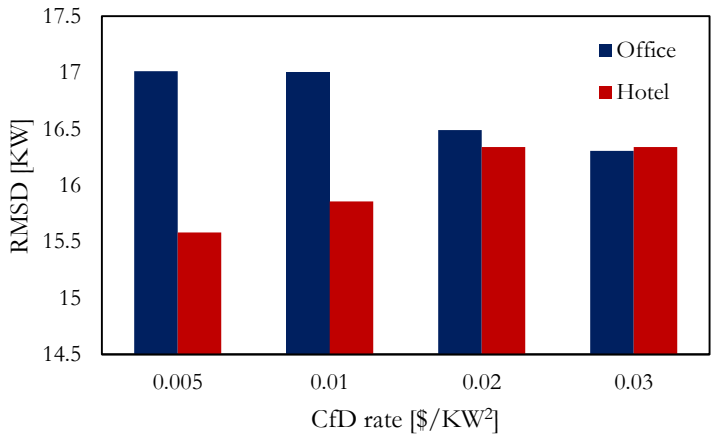

Figure 35 Demand deviation with central tracking control under different CfD rates

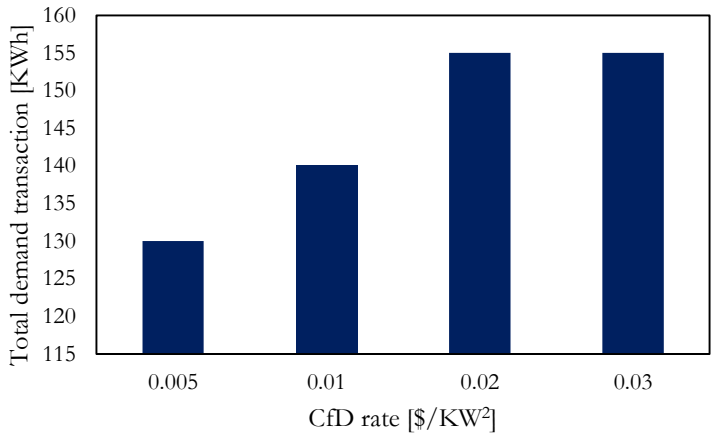

Figure 36 Demand transaction with centralized tracking control under different CfD rates

Apparently, when CfD rate is low (0.005 $/KW^2), the centralized tracking control decides to perform 130 KWh demand transaction. Meanwhile, the office building has demand deviation as high as 17.0 KW, and the hotel demand deviation is as low as 15.6 KW. As CfD rate increases, the centralized tracking control determines that more demand transaction becomes required, and the office demand deviation is declining while the hotel demand deviation is increasing. Until CfD rate reaches 0.02 $/KW^2, the total demand transaction is 150 KWh and the demand deviations of the two buildings are at similar levels (about 16.4 KW). Beyond this point, the greater CfD rate will not change the central controller's decision about tracking control and demand transaction.

This result demonstrates the theory that the centralized tracking control is sensitive to CfD rate, when CfD rate is lower than or equal to 0.02 $/KW^2. Therefore, the proposed centralized tracking control optimization is validated.

4.4.2.2. Distributed Tracking

When load tracking controls and demand transaction are determined by distributed optimizations and communication between the involved buildings, the price sensitivity becomes more complicated. Two types of costs are under consideration – the CfD charge and demand transaction cost (revenue for the seller). When CfD rate is high, the buyer is motivated to buy more electricity from the seller in order to mitigate the demand surge due to unexpected events, as long as the transaction cost is lower than CfD charge; however, high CfD rate also lowers the possibility that the seller will accept the proposed transaction because it will increase the seller's CfD charge too. The rate for demand transaction cost also affects the tracking control. In this study, the demand transaction cost is assumed to have two rates – the rate for fixed cost, i.e. C_f in Eq. 48, and the rate for variable cost, i.e. C_v. With lower transaction rates, the buyer is willing to propose demand transactions with larger quantity, but whether the seller will accept the proposal is determined by the comparison between the increased CfD charge and the revenue from selling demand.

Figure 37 shows the total demand transaction under different combinations of fixed and variable cost rates, where CfD rate is assumed to be 0.01 \$/KW^2. When C_v equals to 0.4 \$/KWh (the red bars), the buyer tends to propose more transaction as C_f decreases from 16 to 4 \$/transaction; then the total transaction rises. When C_f is lower than 1 \$/transaction, the seller starts to reject transaction proposals; then the total transaction reduces as well. When C_v is 0.8 \$/KWh (the dark blue bars), the buyer starts to propose demand transactions when C_f is greater than 8 \$/transaction. When C_v is 0.2 \$/KWh (the green bars), the seller starts to decline demand transaction proposals when C_f is lower than 8 \$/transaction and when C_v is 0.1 \$/KWh (the

yellow bars), the seller starts to decline demand transaction proposals when C_f is lower than 16 $/transaction.

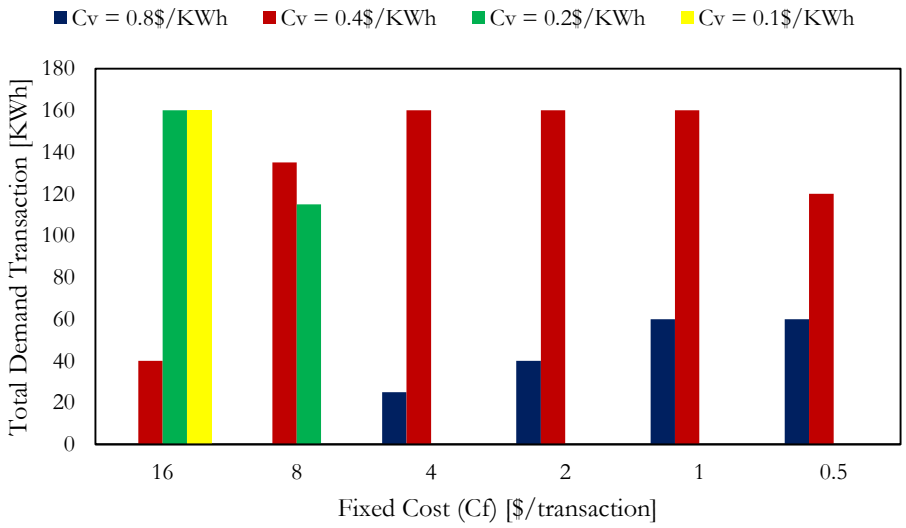

Figure 37 Total demand transaction under different fixed and variable cost rates

Figure 38 shows the sensitivity of the demand transaction to CfD rate under different combinations of fixed and variable transaction rates. Comparing the plots in each row, it is clear that with a lower variable rate (C_v), the demand transaction will be performed under lower CfD rate. Similarly, when comparing the plots in each column, the demand transaction is shifted to lower CfD rate when the fixed transaction rate (C_f) is lower.

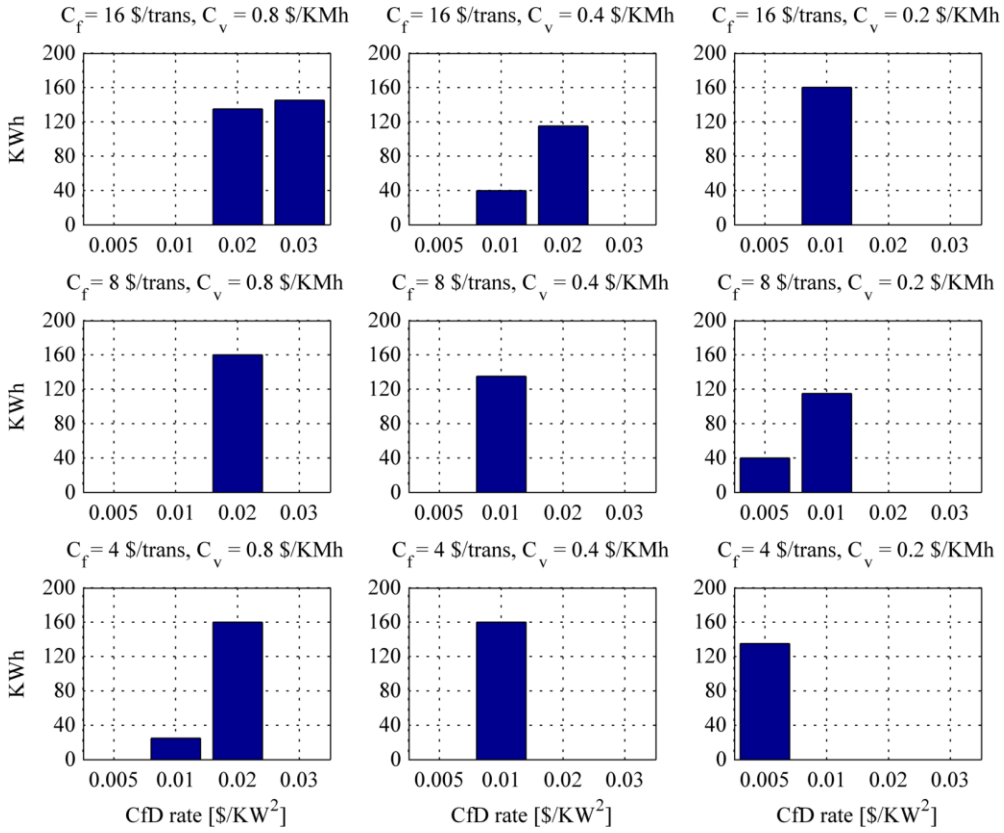

Figure 38 Demand transaction with distributed tracking control
under different CfD rates

The sensitivity test result proves the previous hypothesis. The distributed load tracking control is hence validated. In the following studies, the CfD rate is assumed to be 0.01 $/KW^2, demand transaction fixed cost rate is 8 $/transaction and variable cost rate is 0.4 $/KWh.

4.5 Experiments

CfD pricing is designed to minimize the demand uncertainty of individual customers. This is accomplished by incurring charges on the deviation between planned and actual demand. Experiments in Chapter 3 have shown that, under CfD pricing, individual buildings are encouraged to perform day-ahead planning and real-time load tracking control optimizations. The two-stage control effectively reduces the building's demand deviation. In the case where

some unexpected event may cause significant surge of demand, the load tracking control is able to largely mitigate the demand deviation caused by the event, as long as the forecast is updated in a timely manner. In this chapter, the performance of CfD is studied at the community level. It is subject to test whether demand deviation reduction of individual customers generates saving in the overall cost of the community over a long period of time. If cost saving is achieved, its sensitivities towards wholesale market condition and customers' occupancy forecasts are also evaluated by a series of experiments. Additionally, two collaborative load tracking mechanisms are demonstrated in this section.

4.5.1 Community Cost

4.5.1.1. The Base Case

In the base case, the community microgrid is connected to the NYISO's utility grid. Every day the utility provider submits demand bid for the next day into NYISO day-ahead wholesale market based on the demand predictions that all buildings provide. This day-ahead demand schedule will be charged at day-ahead price. During the next day, the utility provider settles the demand deviation in the real-time wholesale market. The NYISO day-ahead and real-time prices are plotted in Figure 39, for July of 2013.

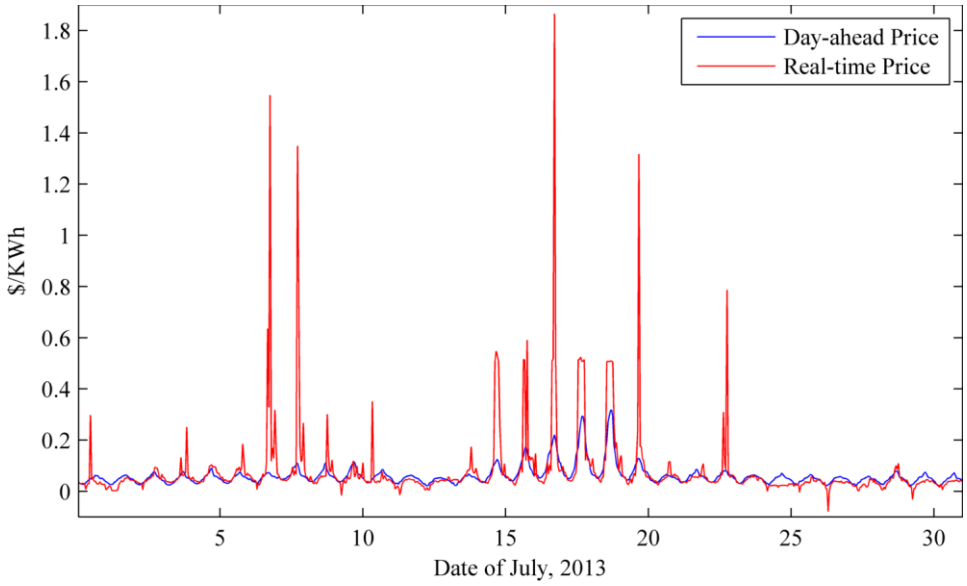

Figure 39 NYISO electricity wholesale price

As shown in Figure 39, NYISO day-ahead price ranges between 0 and $0.3/KWh, having an apparent daily pattern. The real-time price, most of the time, is close to the day-ahead price, but substantial spikes exist. The magnitude of the real-time price spikes can reach as high as $1.9/KWh. Negative real-time price is also observed, which is most likely contributed by the use of renewable generations, because renewable generation sometimes may have negative cost due to tax credit and other incentives. In the end, the real-time price is significantly more volatile than the day-ahead price.

If CfD retail rate structure is implemented, individual buildings will use the day-ahead price to plan for the demand schedule. In fact, the day-ahead retail price that the utility provider announces is assumed to be proportional to the day-ahead wholesale price. Since the difference between day-ahead retail price and wholesale price is small, the planning result (including the demand and control action schedules) will not be significantly altered by this assumption. Figure

40 illustrates the procurement costs of the community under CfD in both wholesale markets (the CfD rate is assumed to be 0.01 $/KW^2).

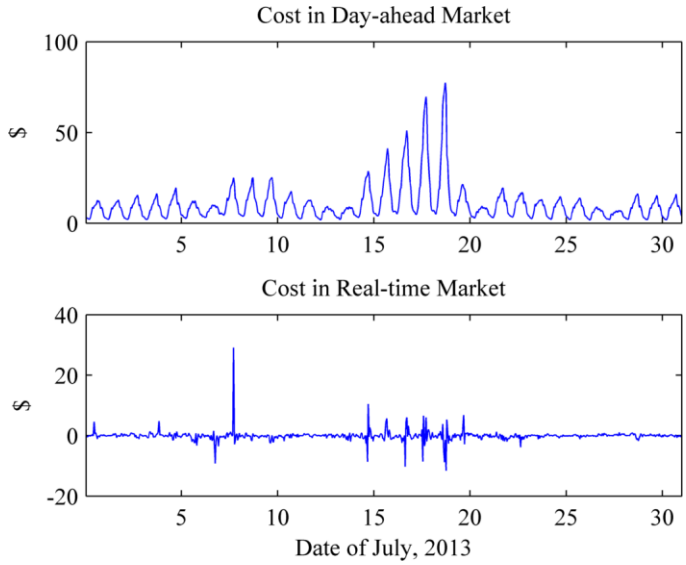

Figure 40 Procurement costs of the community under CfD

The mean and standard deviation of the hourly procurement cost in the real-time market is -$0.09 and $1.75, respectively. The total cost in the day-ahead market is $7,744.39, and the total cost in the real-time market is -$66.01. Assuming normal distribution, the CVaR of hourly procurement cost in the real-time market at confidence level of 0.95, i.e., $CVaR_{0.05}(U_{RT})$, is equal to $3.51. Assuming that the risk parameter (ρ) is 0.3, the risk hedging cost in each hour, R, is then equal to $1.054. Then the risk hedging cost for the month is $784.08. The overall cost of the community is $8,462.47. The calculation is summarized in Table 17.

Table 17 Overall cost calculation sheet

		Flat Rate	DAP	CfD
Hourly Procurement Cost in Real-time Market ($)	**Mean**	0.04	-0.05	-0.09
	Std.	2.73	2.30	1.75
	$CVaR_{0.95}$	5.67	4.69	3.51
Day-ahead Market Procurement Cost ($)		8,585.69	7,744.39	7,744.39

Real-time Market Procurement Cost ($)	26.64	-37.57	-66.01
Risk Hedging Cost ($) $\rho = 0.3$	1,264.81	1,047.88	784.08
Total Cost ($)	9,877.14	8,754.69	8,462.47

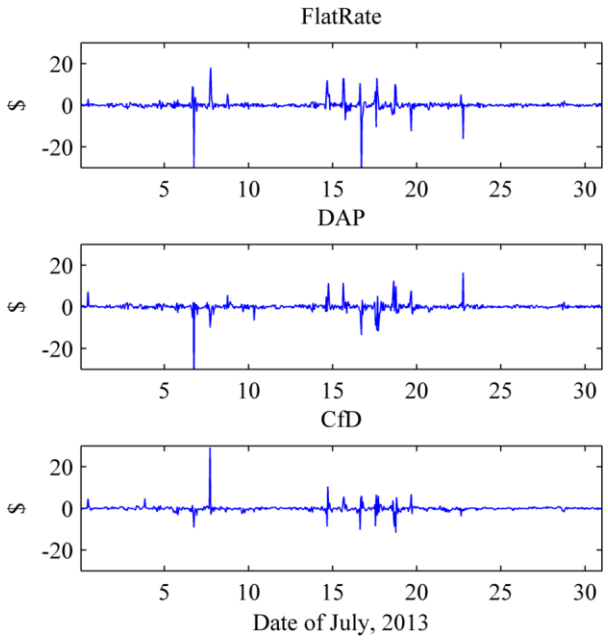

Figure 41 Hourly procurement cost in real-time market under different retail tariffs

If flat rate is implemented in the retail market, individual buildings will not conduct planning optimization. Instead, they will submit their demand schedules predicted using constant control actions (setpoint). If only day-ahead hourly price is implemented without CfD charge, individual buildings will perform planning optimization, with a similar formulation to Eq. 19~Eq. 22, but they will not conduct tracking control. It is hereby denoted as "DAP". Under CfD rate, individual buildings will perform both planning optimization and load tracking controls. Figure 41 plots the hourly procurement cost under these three tariffs. The calculation of overall cost is detailed in Table 17. The result is plotted in Figure 42.

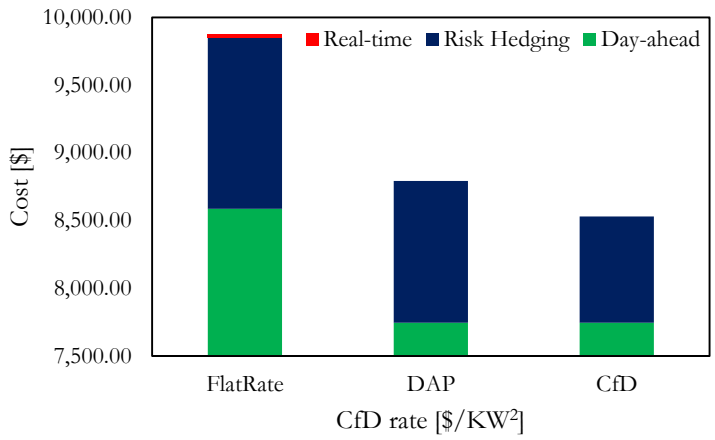

Figure 42 Community overall cost under different retail tariffs

According to the results in Table 17 and Figure 42, the real-time cost is negligible in all scenarios. This is because the deviation of the demand is nearly normally distributed, with mean close to 0. Therefore, the expected cost in the real-time market will be close to 0. The day-ahead cost makes the largest portion of the overall cost, followed by the risk hedging cost. Compared to the flat rate, DAP drives the individual buildings to perform day-ahead planning, and as a result, the day-ahead cost is reduced by $841.31 (about 9.8%). DAP does not enforce tracking control, so the risk hedging cost is similar to that under flat rate. CfD, however, encourages both day-ahead planning and real-time tracking. Therefore, the day-ahead cost is the same as under DAP. But CfD reduces the risk hedging cost by $480.72 (about 38.0%, compared to the flat rate scenario). In all, the total cost is reduced by $1,414.67 (about 14.3%).

4.5.1.2. Impact of Occupancy

In the base case, the buildings are operating in ordinary days, i.e. no unexpected events occur. As has been illustrated in Chapter 3, building occupancy forecast is crucial for the controls under CfD. CfD pricing promotes better occupancy forecasts and forces individual buildings to update occupancy forecast in order to minimize the demand deviation caused by unexpected events. At

community level, the cost is also sensitive to the occupancy forecast error. As shown by the box plots in Figure 43, three levels of occupancy forecast error are tested. When both buildings have high forecast errors, the risk hedging cost is high, resulting in a high overall cost (Figure 44). This is reasonable because occupancy is a major source of uncertainty other than weather. All the planning and load tracking (if applies) are based on such forecasts. Even if occupancy forecasts are updated but the updated forecasts are still inaccurate, load tracking is not able to reduce the demand deviation as expected.

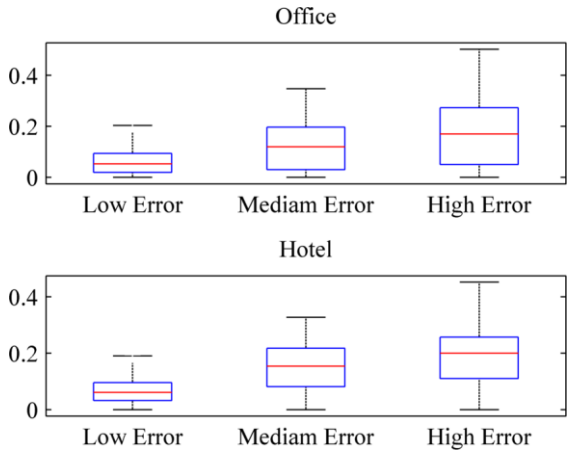

Figure 43 Occupancy forecast error

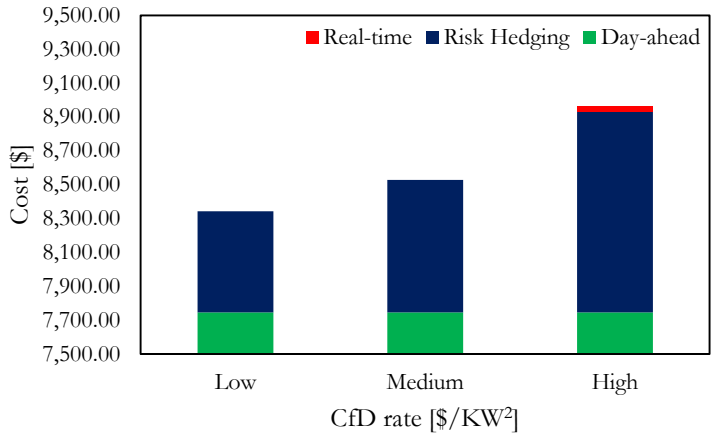

Figure 44 Community overall cost under different occupancy forecast errors

Figure 45 shows the impact of unexpected events and occupancy forecast updates on the cost. If a building experiences 2 unexpected events during the month of July, it is considered as a low event frequency month, denoted as "Low Event Freq." in Figure 45. If 6 unexpected events occurred, it is a high event frequency month, denoted as "High Event Freq.". Likewise, the scenarios where the occupancy forecast is updated accordingly 2 hours before unexpected event are denoted by "w/ Update", and "w/o Update" indicates the scenarios where the occupancy forecast update is not conducted. Apparently, with similar forecast error levels, CfD is capable of reducing the risk hedging cost with forecast update, especially in the high event frequency case.

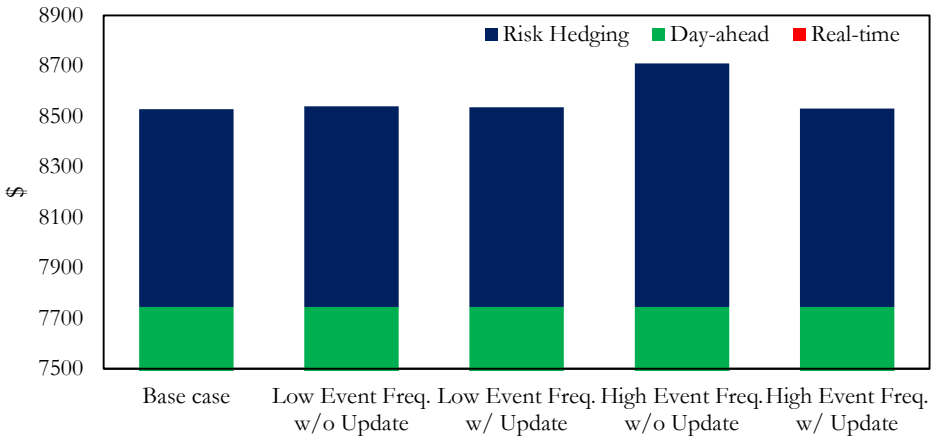

Figure 45 Cost comparison on event and occupancy forecast updates

4.5.1.3. Impact of Wholesale Market

CfD is able to reduce the community cost, because it forces individual buildings to maintain a predictable demand profile so that the individual demand uncertainty is reduced, then the overall demand uncertainty of community can be minimized. As a result, the community is able to rely more on less risky day-ahead market, rather than riskier real-time market. When real-time electricity price is more volatile, CfD offers cost reduction for the community. However, if the real-time price is not volatile, cost reduction by CfD may not be as exciting.

The wholesale prices for the month of July 2013 in three ISOs, including NYISO (which is also shown in Figure 39), PJM and MISO, are plotted in Figure 46. It seems that the real-time price in NYISO is substantially more volatile than those in PJM and MISO. The real-time and day-ahead prices in MISO are very close to each other and are the least volatile. Figure 47 shows the comparison of costs under flat rate and CfD, in the three regional markets.

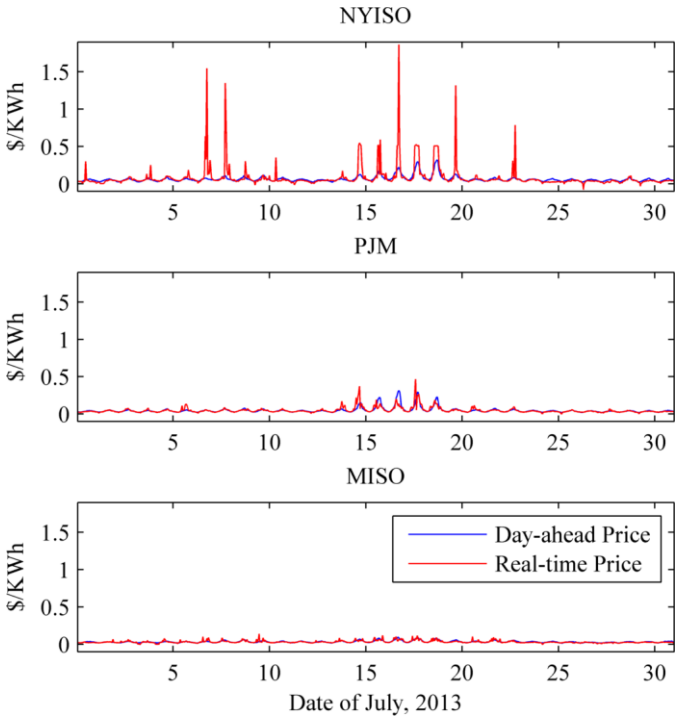

Figure 46 Electricity wholesale prices of different ISOs

According to Figure 47, using the costs under flat rate as references, CfD reduces the monthly cost by $1,414.67 (or 14.3%) in NYISO, while the cost reduction is $ 308.50 (or 4.7%) in PJM and $ 162.31 (or 3.7%) in MISO. In NYISO, 34% cost reduction is contributed by risk hedging cost and 66% by day-ahead cost, while in PJM and MISO, almost all cost reduction is from day-ahead cost reduction. This suggests that the day-ahead planning is able to reduce day-ahead cost, but load tracking control can reduce risk hedging cost only when the real-time price is volatile.

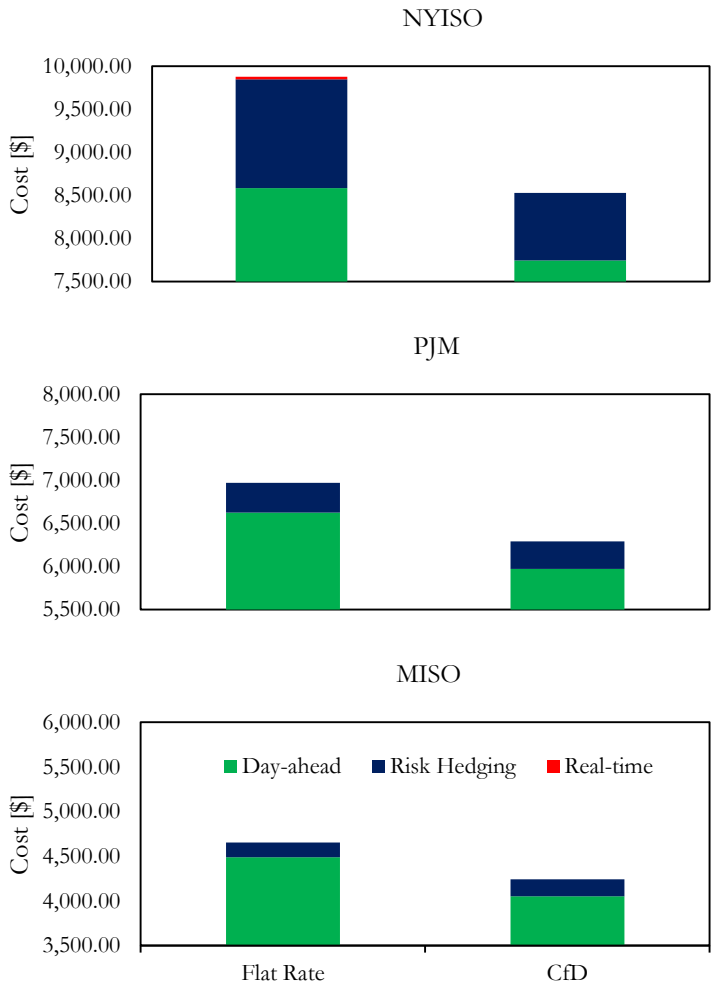

Figure 47 CfD cost reduction in different ISOs

4.5.2 Collaborative Load Tracking

Under CfD pricing, individual buildings are driven to conduct load tracking controls in order to minimize the CfD charges. However, load tracking control may have constraints. In previous sections of this dissertation, only thermostat setpoint is subject to control. When demand increases significantly due to unexpected events, load tracking may push thermostat setpoint to its upper or lower bounds, but still cannot reduce the demand deviation any further. This building operator may want to utilize the "load tracking capacity" of other buildings. We call this "demand transaction". Even though demand transactions may incur additional cost, such action

will be justified as long as the cost for purchasing "load tracking capacity" is smaller than the potential saving in CfD charges. In this dissertation, the author investigates two basic mechanisms of tracking collaboration: the centralized and the distributed load tracking.

4.5.2.1. Centralized Load Tracking

The centralized load tracking assumes that individual buildings outsource their load tracking controls to a central controller (MGCC). MGCC receives the demand schedule planned day-ahead and real-time update from each building. Tracking optimization with respect to the control actions of all the buildings can be performed based on the aggregated information. The optimal demand transactions can be determined at the same time. The objective function of the centralized tracking control is to minimize the CfD charges of all the buildings. Section 4.2.3 has detailed the optimization formulation for a simplified community microgrid with a medium office building and a small hotel building.

In the case study, the office building is assumed to be experiencing an unexpected event, as illustrated in Figure 48. The event is between 14:00 and 18:00. It was not accounted for when making the day-ahead plan, but the occupancy forecast is updated 3 hours before the event (i.e., at 11:00). An EV charging load of 32 KW during the event is also assumed. EV charging is not included in the demand forecast until the occupancy forecast is updated at 11:00. During non-event hours, EV charging is assumed to be zero (Figure 31).

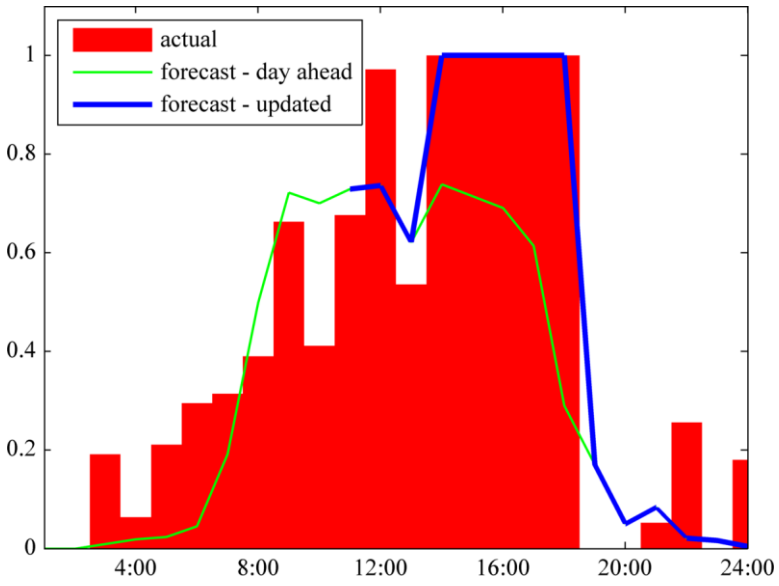

Figure 48 Office occupancy level with an unexpected event and forecast update

Since, the unexpected event together with corresponding EV charging causes significant increase of demand. It is not possible for the building operator to use only thermostat control to mitigate the demand surge and reduce the potential CfD charge. Figure 49 shows the result of centralized load tracking. The red curves show the demand profiles determined from the day-ahead planning. During the operating day, if only non-collaborative load tracking is performed, the office demand will deviate from its planned schedule by as much as 64 KW during the event (the blue curve). By collaborative load tracking, the centralized tracking control is able to lower the demand deviation to about 34 KW (the green curve). The 30 KW difference is covered by demand transaction from the hotel to the office (the bottom panel of Figure 49).

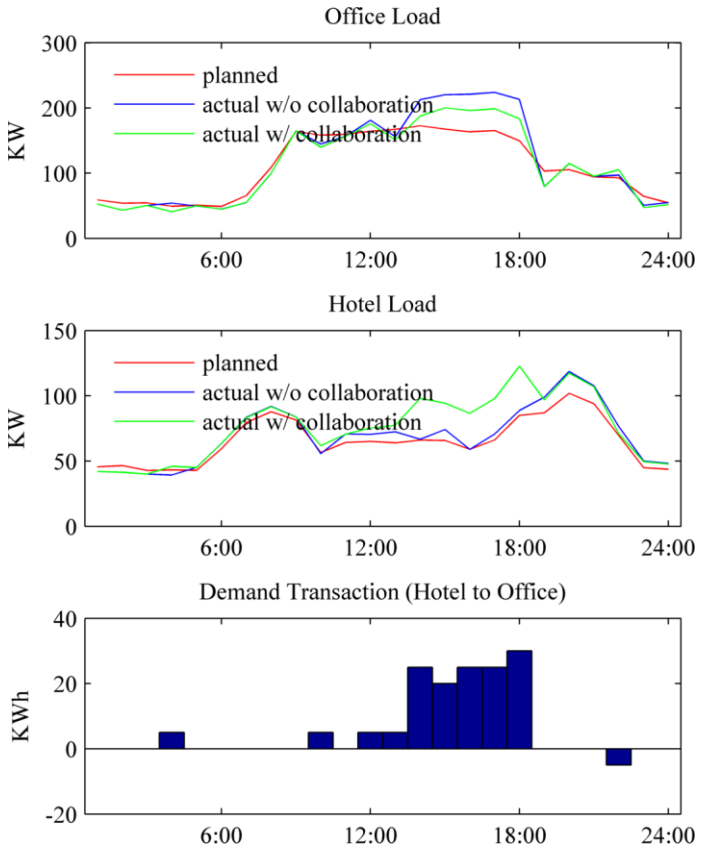

Figure 49 Load profiles with centralized collaborative load tracking (demand transaction)

It is noticed that the centralized load tracking does not necessarily create demand transaction in one direction only, as the negative transaction is observed at 22:00. In other words, transferring electricity from the office to the hotel during those periods results in minimal overall CfD charges, as determined by the MGCC.

With centralized load tracking, the cost reduction effect is significant. As shown in Figure 50, the total billed cost of the community is reduced by $50 (about 5.6%). Although, the office building is able to reduce its own CfD charge by $101 (about 59%) and reduce billed cost by $132 (about 21%), the hotel's cost is increased, due to greater CfD charge. This is not a fair result, because the office's failure to plan on the event is the cause of high CfD charge. The hotel

shares the consequence by paying more CfD charge while receiving no benefit. This is certainly not a sustainable solution. A financial transaction should associate with any demand transaction. It is possible for the office to pay the hotel a share from the saving in CfD charge. But under the centralized load tracking mechanism, bilateral financial transactions will not influence the tracking result.

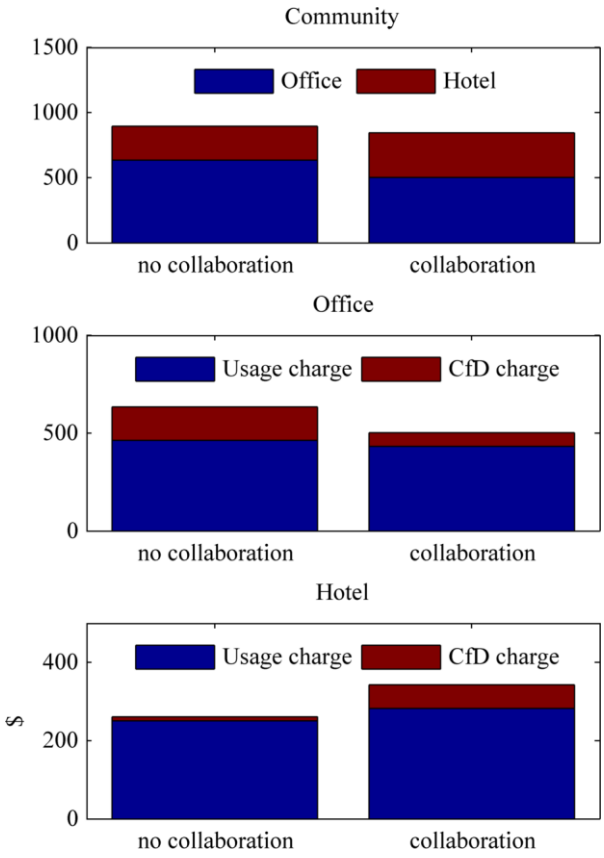

Figure 50 Billed cost under centralized load tracking

4.5.2.2. Distributed Load Tracking

As has been discussed in Section 4.5.2.1, centralized load tracking may result in an unfair cost increase in the building that does not cause the high CfD charge. To avoid such unfairness, it is necessary to associate any demand transaction with the proper financial transaction, so that the participant that is not the source of major risk, can benefit from the tracking collaboration, or at

least, will not bear any extra cost. A distributed load tracking mechanism is designed to accomplish that. With distributed load tracking, individual LCs perform their own tracking optimization independently. When one LC (the buyer, e.g. the office) finds it necessary to buy electricity from another building (the seller, e.g. the hotel), rather than from the utility provider in order to avoid the high CfD charge, the buyer's LC will make a transaction proposal to the seller's LC. This proposal includes the time and quantity of electricity that the buyer is willing to buy. Then the seller's LC decides whether to accept this proposal by comparing the optimal objective value if the proposed demand transaction is carried out with the one without demand transaction. If the proposed transaction generates an even better optimal objective value, then the proposal is accepted, otherwise, it will be rejected and no demand transaction will be carried out in this time step. The tracking control optimizations are formulated as detailed in Section 4.2.3.2. It is assumed that there are fixed cost and variable cost associated with demand transactions (Eq. 48), and the rates of these two costs are given.

In the case study, the fixed cost of demand transaction is assumed to be \$8/transaction, and the variable cost rate is assumed to be \$0.4/KWh, the occupancy and weather conditions are the same as have been studied in Section 4.5.2.1. The distributed load tracking result is presented in Figure 51. Four demand transactions are performed between the two buildings, all of which occur during the event. A total of (35+30+30+40=) 135 KWh electricity is purchased from the hotel to the office. Those demand transactions help the office reduce the demand to the grid (from blue curve to green curve), but raise the demand of the hotel. In terms of cost, on one hand, the demand transactions substantially reduce the office's CfD charge, but incur some transaction cost. The overall cost of the office is reduced by the tracking collaboration. On the other hand, the hotel's CfD charge is increased, but the increased cost is compensated by the

revenue from demand transaction (Figure 52). The total billed cost of the community is reduced by $9 (about 1%).

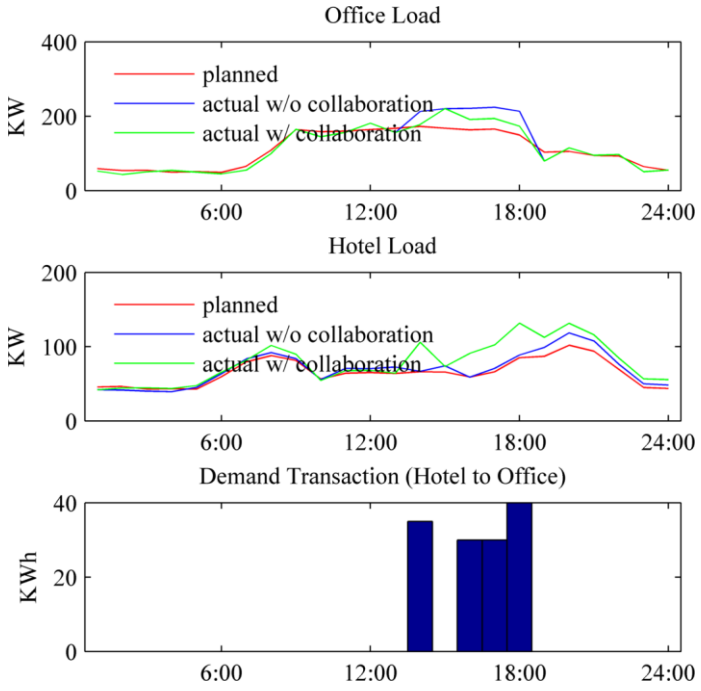

Figure 51 Load profiles with distributed collaborative load tracking (demand transaction)

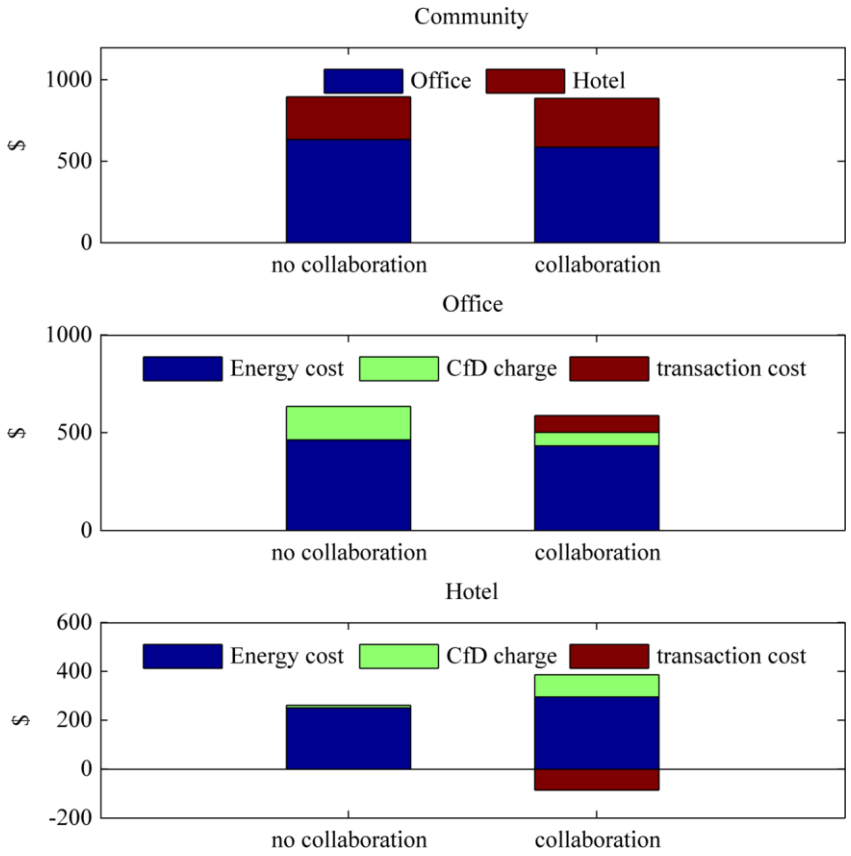

Figure 52 Billed cost under distributed load tracking

4.6 Discussion

Electricity wholesale markets usually have day-ahead and real-time elements. The electricity price in day-ahead market is less volatile, therefore day-ahead market is less risky. As a contrast, the real-time price can be very volatile and poses significant risk to utility providers who act as buyers in the electricity wholesale markets and as sellers in electricity retailing. With conventional flat rate or TOU rate, the customers in retail markets are not adequately exposed to the wholesale market dynamics. Many believe that such disconnection between the wholesale and the retail is the primary cause of unusual price spikes. The CfD rate structure proposed in this dissertation is a retail pricing mechanism that promotes fair share of wholesale market risks among customers and utility providers. The reasoning is that individual customers are more capable than any others

of understanding and predicting their demand as well as tracking such demand schedule during real-time. If there is a tariff that can ensure all customers maintain predictable consumption behavior, the aggregated demand of a community would be predictable as well. Then the community may rely more on a less risky day-ahead market to purchase electricity, and less on the riskier real-time market. The community's overall cost will ultimately be reduced.

In Chapter 3, it has been demonstrated how individual building LCs are able to perform day-ahead planning and real-time load tracking, under CfD pricing. Such two-stage control, together with proper forecast updating, is able to reduce the demand deviation, especially when there is an unexpected event. In this chapter, CfD pricing is studied at community level. A simplified, two-building community is adopted as a subject model. The two buildings, an office and a hotel, are assumed to be equipped with the LCs that have planning, tracking and necessary communication functionalities. The experiments using real market data prove that CfD pricing is able to reduce the community cost in the wholesale market. This is especially true if the real-time electricity price is volatile.

Another effect that CfD pricing may have on the community is that it promotes collaborative demand management among individual buildings. Since failure to predict demand may result in substantial CfD charge, individual customers will try to prevent this from happening. When an unexpected event does occur, the building LC may want to receive electricity from peers, rather than from the utility provider, in order to lower the potential CfD charges. This is accomplished via collaborative load tracking. This dissertation demonstrates two basic designs: the centralized and the distributed load tracking. The centralized load tracking is performed by a central controller who is also an information collector. The load tracking optimization is conducted based on the aggregated information on the operation of all the buildings. The objective to the

centralized tracking is to minimize the total CfD charges of all the buildings. The experiment shows that the centralized load tracking is able to achieve lower total CfD charge, and thus lower total cost to the community. But, this overall cost reduction is considered unfair to one of the collaboration participants, who is not the cause of unexpected event but faces increased CfD charges. To avoid such unfair result, a distributed load tracking mechanism is proposed. It associates proper financial transaction with demand transaction. The demand transaction is determined by bilateral communication between these two buildings. In the case study, a linear transaction cost is assumed. It shows that demand transaction can help the building that experiences unexpected event reduce CfD charge, while, at least, compensating the increased CfD charge of the other transaction participant with the revenue from demand transaction. Although the overall cost reduction is not as significant as the centralized load tracking may achieve, the distributed load tracking will not result in an unfair cost increase to any collaboration participant.

Chapter 5 Conclusion and Future Work

Price risk and quantity risk are the two major risks that utilities face in electricity wholesale markets. The price risk is caused by the uncertain condition between supply and demand, as well as congestion, on the grid. The utilities are usually considered as price takers, therefore, their operations focus on maximizing the efficiency (maximum profit or minimum cost) given the estimate of price uncertainty. The quantity risk, however, is caused by the deviation between the predicted and the actual demand of all the customers served by the utility. Similar to the price uncertainty, the demand uncertainty is usually considered as a risk factor subject to estimation and works as constraint in the operation and management of the utilities. In a few studies that apply portfolio optimization concept in microgrid operation, asset management and market strategies, the demand uncertainty together with other uncertain factors appear in the objective function in the form of risk hedging cost or certainty equivalent [157, 158, 170]. Few studies, if any, consider managing the demand uncertainty at its source – the individual customers. There are several reasons: first, weather is the number one cause of uncertain demand, and error of weather forecast is inevitable. Second, human behavior is recognized as another major risk source, and human behavior is extremely difficult to characterize and predict. And last, but more importantly, there exists neither economic nor social measure that could promote a predictable consumption manner in the customer population.

However, the author of this dissertation argues that it is possible to get individual customers involved in quantity risk mitigation because they are more capable of understanding their own activities than any others. The success of DR programs proves that individual customers are responsive toward economic measures. As long as a rate structure is properly designed so as to

convey the signal that uncertain consumption is more costly than others, it is able to influence the customers' consumption decisions and promote a desired behavior.

A CfD retail pricing is proposed in this dissertation. This new rate structure requires an hourly price schedule to be announced day ahead so that all customers are able to make optimal plans. Then it incurs CfD charge in the next day if the actual demand is different from the day-ahead plan. CfD has DAP element, which is a popular time-varying price scheme. DAP together with the day-ahead planning optimization are effective in reducing system peak demand, which has been discussed by many researchers. The notion of charging on the demand deviation is new. CfD charge forces individual customers to track their demand schedule in real-time in order to keep the demand deviation low. In other words, CfD promotes a low uncertainty consumption behavior.

In this dissertation, simulation-based and black-box model-based predictive controls are studied. Both can be used in the control optimizations under time-varying price or under CfD. However, simulation-based approach may need special techniques to overcome the obstacle posed by intense computation requirement. A new two-stage approach called Optimal Strategy Pool (OSP) is designed to move time consuming simulation runs to off-line stage as much as possible, so it will take a much shorter time when making planning decisions on-line. The experiments, as well as scale-up tests, all demonstrate that OSP is efficient and robust. But simulation-based approach is still not the best choice for fast response or real-time control optimization. An ANN model is then used for the day-ahead planning and real-time tracking controls under CfD. The formulations of the planning and tracking control problems are presented in this dissertation. Simulation experiments show that the planning and tracking controls are able to reduce the building demand uncertainty as measured by demand deviation (RMSD). It is also shown that

accurate weather and occupancy forecasts are helpful in the demand deviation reduction. If certain demand surge is not expected while planning day-ahead, timely update will help mitigate the spike of demand deviation. This again proves that individual customers are encouraged to maintain full awareness of their own consumption activities in order to reduce the demand uncertainty.

The author studies the effectiveness of CfD in reducing the overall cost of the community in the wholesale market. Simulation experiments using real price record from US regional markets demonstrate that the DAP element of CfD reduces the community cost in the day-ahead market, and the CfD charge element reduces the cost for hedging real-time market risk. The risk/cost reduction is substantial, especially when the real-time market price is volatile. This result justifies CfD pricing, because even with additional CfD charges on the utility bill, the total billed cost of the customers is expected to be lower under CfD.

CfD also created an opportunity for collaborative demand management among individual customers. Under some circumstances, one customer may want to purchase electricity from another customer, rather from the utility provider, in order to maintain a low demand deviation. A centralized approach and a distributed approach are presented in this dissertation to coordinate such demand transaction. The centralized approach is similar to other collaborative management approaches in microgrid regime, where a higher level central coordinator gathers all the information, solves a comprehensive optimization problem and allocates the resources accordingly. Simulation experiments demonstrate that the centralized load tracking reduces the CfD charge of the buyer, but at the cost of increasing CfD charge of the seller. This consequence is considered unfair, even though it achieves minimal total billed cost of the two parties. A distributed approach solves this problem by asking the buyer to initiate a negotiation and make

a transaction proposal. The demand transaction is associated with financial transaction, so the seller may compensate the increased CfD charge by the transaction revenue. The seller, based on its own optimization results, accepts or rejects the transaction proposal, so the unfair cost increase can be completely avoided.

Such collaborative demand management has the opportunity to evolve further into demand transaction market among individual customers. If that becomes true, those customers who have better awareness and control of their own properties, and those who invested in intelligent energy management systems, are able to benefit from selling the demand transaction capacity. In the end, the demand uncertainty reduction is accomplished not only with individual customers but also with the entire community.

To sum up, CfD tariff is designed to expose the individual customers to the wholesale quantity risk. It adds the notion of uncertainty reduction into the demand management of individual customers. Extensive experiments have demonstrated that CfD is effective in reducing the community cost, and in the end reducing individual customers' billed cost. More studies on the modeling, control optimization formulation and solution technique, refining the rate structure and strategy in collaborative demand management will be expected in the future.

REFERENCE

1. Rahimi, F.A. and A. Ipakchi, *Transactive Energy Techniques: Closing the Gap between Wholesale and Retail Markets*. The Electricity Journal, 2012. **25**(8): p. 29-35.
2. IEA, *Key World Energy Statistics 2012*. 2012: OECD/IEA.
3. EIA, U., *Annual energy review*. Energy Information Administration, US Department of Energy: Washington, DC www. eia. doe. gov/emeu/aer, 2012.
4. EIA, U., *Annual energy outlook 2013*. 2013.
5. USDOE, *Building Energy Data Book*. 2011.
6. Laboratory, U.o.W.-.-M.S.E. and S.A. Klein, *TRNSYS, a transient system simulation program*. 1979: Solar Energy Laborataory, University of Wisconsin--Madison.
7. Crawley, D.B., et al., *EnergyPlus: creating a new-generation building energy simulation program*. Energy and Buildings, 2001. **33**(4): p. 319-331.
8. Morris, F.B., J.E. Braun, and S.J. Treado, *Experimental and simulated performance of optimal control of building thermal storage*. ASHRAE Transactions, 1994. **100**: p. 402-4114.
9. Elliott, A.S. *A Highly Efficient, General-Purpose Approach for Co-Simulation with ADAMS*. in *15th European ADAMS User's Conference*. 2000. Rome, Italy.
10. Mathews, E.H. and C.P. Botha, *Improved thermal building management with the aid of integrated dynamic HVAC simulation*. Building and Environment, 2003. **38**(12): p. 1423-1429.
11. Brandwein, P.F., *The selection and training of future scientists*. Sci Mon, 1947. **64**(3): p. 247-52.
12. Xu, P. and L. Zagreus, *Demand Shifting With Thermal Mass in Light and Heavy mass Commercial Buildings*. 2006.
13. Xu, P. and R. Yin, *Demand Shifting with Thermal Mass in Large Commercial Buildings in a California Hot Climate Zone*. 2009.
14. Yin, R., et al., *Scenario Analysis of Peak Demand Savings for Commercial Buildings with Thermal Mass in California*. 2010.
15. Trčka, M. and J. Hensen. *Case studies of co-simulation for building performance prediction*. in *The 38th International Congress on Heating, Ventilation and Air-Conditioning*. 2007. Belgrade.
16. Wetter, M. and P. Haves, *A modular building controls virtual test bed for the integration of heterogeneous systems*, in *SimBuild 2008*. 2008: Berkeley, California.
17. Trčka, M., J.L.M. Hensen, and M. Wetter, *Co-simulation of innovative integrated HVAC systems in buildings*. Journal of Building Performance Simulation, 2009. **2**(3): p. 209-230.
18. Wetter, M., *Co-simulation of building energy and control systems with the Building Controls Virtual Test Bed*. Journal of Building Performance Simulation, 2011. **4**(3): p. 185-203.
19. Trčka, M., J.L.M. Hensen, and M. Wetter, *Co-simulation for performance prediction of integrated building and HVAC systems – An analysis of solution characteristics using a two-body system*. Simulation Modelling Practice and Theory, 2010. **18**(7): p. 957-970.
20. Sagerschnig, C., et al., *Co-simulation for building controller development: The case study of a modern office building.*, in *CISBAT*. 2011: Lausanne, Switzerland.
21. Nghiem, T.X. *MLE+: a Matlab-EnergyPlus Co-simulation Interface*. Available from: http://www.seas.upenn.edu/~nghiem/mleplus.html.
22. Zhu, J., et al., *A Two-Stage Simulation-Based On-line Optimization Scheme for HVAC Demand Response*, in *SimBuild 2012*. 2012: Madison, Wisconsin.
23. Zhu, J., et al. *HVAC Degradation and Asset Management - A Novel Application of Whole Building Simulation*. in *Building Simulation Conference*. 2014. Atlanta, GA.

24. Pang, X., et al., *A framework for simulation-based real-time whole building performance assessment.* Building and Environment, 2012. **54**(0): p. 100-108.
25. Eisenhower, B., et al., *A methodology for meta-model based optimization in building energy models.* Energy and Buildings, 2012. **47**(0): p. 292-301.
26. MacArthur, J., A. Mathur, and J. Zhao, *On-line recursive estimation for load profile prediction.* ASHRAE Transactions, 1989. **95**: p. 621-628.
27. Dhar, A., T. Reddy, and D. Claridge, *A Fourier series model to predict hourly heating and cooling energy use in commercial buildings with outdoor temperature as the only weather variable.* Journal of solar energy engineering, 1999. **121**(1): p. 47-53.
28. Forrester, J. and W. Wepfer, *Formulation of a load prediction algorithm for a large commercial building.* ASHRAE Transactions, 1984. **90**(2): p. 536-551.
29. Åkesson, B.M. and H.T. Toivonen, *A neural network model predictive controller.* Journal of Process Control, 2006. **16**(9): p. 937-946.
30. Azadeh, A., et al., *Integration of artificial neural networks and genetic algorithm to predict electrical energy consumption.* Applied Mathematics and Computation, 2007. **186**(2): p. 1731-1741.
31. Chow, T.T., et al., *Global optimization of absorption chiller system by genetic algorithm and neural network.* Energy and Buildings, 2002. **34**(1): p. 103-109.
32. Ferreira, P.M., et al., *Neural networks based predictive control for thermal comfort and energy savings in public buildings.* Energy and Buildings, 2012. **55**: p. 238-251.
33. Kajl, S., et al. *Evaluation of building energy consumption based on fuzzy logic and neural networks applications*. in *Proceedings of CLIMA 2000 Conference on CDROM*. 2000.
34. Kalogirou, S.A., *Applications of artificial neural-networks for energy systems.* Applied Energy, 2000. **67**(1-2): p. 17-35.
35. Kalogirou, S., *Artificial neural networks for the prediction of the energy consumption of a passive solar building.* Energy, 2000. **25**(5): p. 479-491.
36. Khalil, E.E., et al., *Neural Networks Approach for Energy Consumption in Air-Conditioned Administrative Building.* ASHRAE Transactions, 2012. **118**(1): p. 257-264.
37. Kreider, J.F., et al., *Expert systems, neural networks and artificial intelligence applications in commercial building HVAC operations.* Automation in Construction, 1992. **1**(3): p. 225-238.
38. Li, K., H. Su, and J. Chu, *Forecasting building energy consumption using neural networks and hybrid neuro-fuzzy system: A comparative study.* Energy and Buildings, 2011. **43**(10): p. 2893-2899.
39. Neto, A.H. and F.A.S. Fiorelli, *Comparison between detailed model simulation and artificial neural network for forecasting building energy consumption.* Energy and Buildings, 2008. **40**(12): p. 2169-2176.
40. Pedersen, M.W., *Optimization of Recurrent Neural Networks for Time Series Modeling*, in *Department of Mathematical Modeling*. 1997, Technical University of Denmark.
41. Yang, J., H. Rivard, and R. Zmeureanu, *On-line building energy prediction using adaptive artificial neural networks.* Energy and Buildings, 2005. **37**(12): p. 1250-1259.
42. Dong, B., C. Cao, and S.E. Lee, *Applying support vector machines to predict building energy consumption in tropical region.* Energy and Buildings, 2005. **37**(5): p. 545-553.
43. Li, Q., et al., *Applying support vector machine to predict hourly cooling load in the building.* Applied Energy, 2009. **86**(10): p. 2249-2256.
44. Alcalá, R., et al., *A genetic rule weighting and selection process for fuzzy control of heating, ventilating and air conditioning systems.* Engineering Applications of Artificial Intelligence, 2005. **18**(3): p. 279-296.
45. Gouda, M.M., S. Danaher, and C.P. Underwood, *Thermal comfort based fuzzy logic controller.* Building Service Engineering Research and Technology, 2001. **22**(4): p. 237-253.

46. Sarimveis, H. and G. Bafas, *Fuzzy model predictive control of non-linear processes using genetic algorithms.* Fuzzy sets and systems, 2003. **139**(1): p. 59-80.
47. Solomon, D., et al., *Forecasting energy demand in large commercial buildings using support vector machine regression.* Department of Computer Science, Columbia University, Tech. Rep. CUCS-040-11, 2011.
48. Yalcintas, M. and S. Akkurt, *Artificial neural networks applications in building energy predictions and a case study for tropical climates.* International Journal of Energy Research, 2005. **29**(10): p. 891-901.
49. Zhou, Q., et al., *A grey-box model of next-day building thermal load prediction for energy-efficient control.* 2008. p. 1418.
50. Wetter, M., *Simulation-Based Building Energy Optimization.* 2004, University of California, Berkeley.
51. Wetter, M. and J. Wright, *A comparison of deterministic and probabilistic optimization algorithms for nonsmooth simulation-based optimization.* Building and Environment, 2004. **39**(8): p. 989-999.
52. Wang, S. and Z. Ma, *Supervisory and Optimal Control of Building HVAC Systems: A Review.* HVAC&R Research, 2008. **14**(1): p. 3-32.
53. Olafsson, S. and N. Gopinath. *Optimal selection probability in the two-stage nested partitions method for simulation-based optimization.* in *Simulation Conference, 2000. Proceedings. Winter.* 2000.
54. Fong, K.F., V.I. Hanby, and T.T. Chow, *HVAC system optimization for energy management by evolutionary programming.* Energy and Buildings, 2006. **38**(3): p. 220-231.
55. Huh, J.-H. and M.J. Brandemuehl, *Optimization of air-conditioning system operating strategies for hot and humid climates.* Energy and Buildings, 2008. **40**(7): p. 1202-1213.
56. Yao, Y. and J. Chen, *Global optimization of a central air-conditioning system using decomposition–coordination method.* Energy and Buildings, 2010. **42**(5): p. 570-583.
57. Matthewman, P.D. and H. Nicholson, *Techniques for load prediction in the electricity-supply industry.* Proceedings of the Institution of Electrical Engineers, 1968. **115**(10): p. 1451.
58. Abu-El-Magd, M.A. and N.K. Sinha, *Short-Term Load Demand Modeling and Forecasting: A Review.* IEEE Transactions on Systems, Man, and Cybernetics, 1982. **12**(3): p. 370-382.
59. Gross, G. and F.D. Galiana, *Short-term load forecasting.* Proceedings of the IEEE, 1987. **75**(12): p. 1558-1573.
60. Moghram, I. and S. Rahman, *Analysis and Evaluation of Five Short-Term Load Forecasting Techniques.* IEEE Power Engineering Review, 1989. **9**(11): p. 42-43.
61. Alfares, H.K. and M. Nazeeruddin, *Electric load forecasting: Literature survey and classification of methods.* International Journal of Systems Science, 2002. **33**(1): p. 23-34.
62. Samadi, P., et al., *Tackling the Load Uncertainty Challenges for Energy Consumption Scheduling in Smart Grid.* Smart Grid, IEEE Transactions on, 2013. **4**(2): p. 1007-1016.
63. Samadi, P., R. Schober, and V.W.S. Wong. *Optimal energy consumption scheduling using mechanism design for the future smart grid.* in *Smart Grid Communications (SmartGridComm), 2011 IEEE International Conference on.* 2011.
64. Conejo, A.J., J.M. Morales, and L. Baringo, *Real-Time Demand Response Model.* IEEE Transactions on Smart Grid, 2010. **1**(3): p. 236-242.
65. Li, N., L. Chen, and S.H. Low. *Optimal demand response based on utility maximization in power networks.* in *Power and Energy Society General Meeting, 2011 IEEE.* 2011.
66. Kim, T.T. and H.V. Poor, *Scheduling Power Consumption With Price Uncertainty.* Smart Grid, IEEE Transactions on, 2011. **2**(3): p. 519-527.

67. Ferrero, R.W. and S.M. Shahidehpour, *Short-term power purchases considering uncertain prices.* Generation, Transmission and Distribution, IEE Proceedings-, 1997. **144**(5): p. 423-428.
68. Wang, L., et al., *Oligopoly models for market price of electricity under demand uncertainty and unit reliability.* European Journal of Operational Research, 2007. **181**(3): p. 1309-1321.
69. Wu, L., M. Shahidehpour, and T. Li, *Stochastic Security-Constrained Unit Commitment.* Power Systems, IEEE Transactions on, 2007. **22**(2): p. 800-811.
70. Feng, Y., et al. *A new approximation method for generating day-ahead load scenarios*. in *Power and Energy Society General Meeting (PES), 2013 IEEE*. 2013. IEEE.
71. Kazarlis, S.A., A.G. Bakirtzis, and V. Petridis, *A genetic algorithm solution to the unit commitment problem.* IEEE Transactions on Power Systems, 1996. **11**(1): p. 83-92.
72. Ruiz, P.A., C.R. Philbrick, and P.W. Sauer. *Wind power day-ahead uncertainty management through stochastic unit commitment policies*. in *Power Systems Conference and Exposition, 2009. PSCE '09. IEEE/PES*. 2009.
73. Padhy, N.P., *Unit Commitment—A Bibliographical Survey.* IEEE Transactions on Power Systems, 2004. **19**(2): p. 1196-1205.
74. Richter, C.W. and G.B. Sheble, *A profit-based unit commitment GA for the competitive environment.* IEEE Transactions on Power Systems, 2000. **15**(2): p. 715-721.
75. Valenzuela, J. and M. Mazumdar. *Making unit commitment decisions when electricity is traded at spot market prices*. in *Power Engineering Society Winter Meeting, 2001. IEEE*. 2001.
76. Chattopadhyay, D. and J. Momoh, *A multiobjective operations planning model with unit commitment and transmission constraints.* IEEE Transactions on Power Systems, 1999. **14**(3): p. 1078-1084.
77. Xie, L. and M.D. Ilic. *Model predictive economic/environmental dispatch of power systems with intermittent resources*. in *Power & Energy Society General Meeting, 2009. PES'09. IEEE*. 2009. IEEE.
78. Xuebin, L., *RETRACTED: Study of multi-objective optimization and multi-attribute decision-making for economic and environmental power dispatch.* Electric Power Systems Research, 2009. **79**(5): p. 789-795.
79. YUAN, T.-j., et al., *An Environmental/Economic Dispatch Model for Power Grid Containing Wind Power Generation Units and Its Simulation in Electricity Market Environment [J].* Power system technology, 2009. **6**: p. 019.
80. Ott, A.L., *Experience with PJM market operation, system design, and implementation.* IEEE Transactions on Power Systems, 2003. **18**(2): p. 528-534.
81. Joskow, P.L., *Why do we need electricity retailers? or can you get it cheaper wholesale?* 2000.
82. Littlechild, S.C., *Why we need electricity retailers: A reply to Joskow on wholesale spot price pass-through.* 2000: Judge Institute of Management Studies.
83. Defeuilley, C., *Retail competition in electricity markets.* Energy Policy, 2009. **37**(2): p. 377-386.
84. EIA. *State electric retail choice programs are popular with commercial and industrial customers*. 2012; Available from: http://www.eia.gov/todayinenergy/detail.cfm?id=6250#.
85. FERC, *Report to Congress on Competition in Wholesale and Retail Markets for Electric Energy*. 2005.
86. Caves, D., K. Eakin, and A. Faruqui, *Mitigating Price Spikes in Wholesale Markets through Market-Based Pricing in Retail Markets.* The Electricity Journal, 2000. **13**(3): p. 13-23.
87. Perez-Arriaga, I.J., *Electricity retail.* MIT course: ESD.934, 6.974 Session 18 Module G.
88. Balijepalli, V.S.K.M., et al. *Review of demand response under smart grid paradigm*. in *Innovative Smart Grid Technologies - India (ISGT India), 2011 IEEE PES*. 2011.
89. Albadi, M.H. and E.F. El-Saadany. *Demand Response in Electricity Markets: An Overview*. in *Power Engineering Society General Meeting, 2007. IEEE*. 2007.

90. USDOE, *Benefits of demand response in electricity markets and recommendations for achieving them*. 2006.
91. Faruqui, A. and S. George, *Quantifying Customer Response to Dynamic Pricing*. The Electricity Journal, 2005. **18**(4): p. 53-63.
92. Boisvert, R.N., P.A. Cappers, and B. Neenan, *The Benefits of Customer Participation in Wholesale Electricity Markets*. The Electricity Journal, 2002. **15**(3): p. 41-51.
93. Kirschen, D.S., *Demand-side view of electricity markets*. IEEE Transactions on Power Systems, 2003. **18**(2): p. 520-527.
94. Borenstein, S., *The Long-Run Efficiency of Real-Time Electricity Pricing*. Energy Journal, 2005. **26**(3).
95. Allcott, H., *Real Time Pricing and Electricity Markets*. 2009.
96. Al-Faris, A.R.F., *The demand for electricity in the GCC countries*. Energy Policy, 2002. **30**(2): p. 117-124.
97. Urga, G. and C. Walters, *Dynamic translog and linear logit models: a factor demand analysis of interfuel substitution in US industrial energy demand*. Energy Economics, 2003. **25**(1): p. 1-21.
98. Zachariadis, T. and N. Pashourtidou, *An empirical analysis of electricity consumption in Cyprus*. Energy Economics, 2007. **29**(2): p. 183-198.
99. Holtedahl, P. and F.L. Joutz, *Residential electricity demand in Taiwan*. Energy Economics, 2004. **26**(2): p. 201-224.
100. Beenstock, M., E. Goldin, and D. Nabot, *The demand for electricity in Israel*. Energy Economics, 1999. **21**(2): p. 168-183.
101. Boonekamp, P.G.M., *Price elasticities, policy measures and actual developments in household energy consumption – A bottom up analysis for the Netherlands*. Energy Economics, 2007. **29**(2): p. 133-157.
102. Lijesen, M.G., *The real-time price elasticity of electricity*. Energy economics, 2007. **29**(2): p. 249-258.
103. Brännlund, R., T. Ghalwash, and J. Nordström, *Increased energy efficiency and the rebound effect: Effects on consumption and emissions*. Energy Economics, 2007. **29**(1): p. 1-17.
104. Filippini, M. and S. Pachauri, *Elasticities of electricity demand in urban Indian households*. Energy Policy, 2004. **32**(3): p. 429-436.
105. Mohsenian-Rad, A.-H. and A. Leon-Garcia, *Optimal Residential Load Control With Price Prediction in Real-Time Electricity Pricing Environments*. IEEE Transactions on Smart Grid, 2010. **1**(2): p. 120-133.
106. Goldman, C., et al., *Customer strategies for responding to day-ahead market hourly electricity pricing*. Lawrence Berkeley National Laboratory, 2005.
107. Lasseter, R.H. and P. Paigi. *Microgrid: a conceptual solution*. in *Power Electronics Specialists Conference, 2004. PESC 04. 2004 IEEE 35th Annual*. 2004.
108. Lasseter, R.H. *MicroGrids*. in *Power Engineering Society Winter Meeting, 2002. IEEE*. 2002.
109. LaMonica, M., *Microgrids Keep Power Flowing Through Sandy Outages*. 2012, MIT Technology Review.
110. Dimeas, A.L. and N.D. Hatziargyriou, *Operation of a multiagent system for Microgrid control*. IEEE Transactions on Power Systems, 2005. **20**(3): p. 1447-1455.
111. Misra, A. and H. Schulzrinne. *Policy-driven distributed and collaborative demand response in multi-domain commercial buildings*. in *Proceedings of the e-Energy 2010 - 1st Int'l Conf. on Energy-Efficient Computing and Networking*. 2010.
112. Duong Tung, N. and L. Long Bao. *Optimal energy management for cooperative microgrids with renewable energy resources*. in *Smart Grid Communications (SmartGridComm), 2013 IEEE International Conference on*. 2013.

113. Zhou, H., et al., *Composite Energy Storage System Involving Battery and Ultracapacitor With Dynamic Energy Management in Microgrid Applications*. Power Electronics, IEEE Transactions on, 2011. **26**(3): p. 923-930.
114. Heydt, G., *The Impact of Electric Vehicle Deployment on Load Management Straregies*. IEEE Transactions on Power Apparatus and Systems, 1983. **PAS-102**(5): p. 1253-1259.
115. Katiraei, F., A.R. Iravani, and P.W. Lehn, *Micro-grid autonomous operation during and subsequent to islanding process*. IEEE Transactions on Power Delivery, 2005. **20**(1): p. 248-257.
116. Katiraei, F. and M.R. Iravani, *Power management strategies for a microgrid with multiple distributed generation units*. IEEE Transactions on Power Systems, 2006. **21**(4): p. 1821-1831.
117. Guttromson, R.T. *Residential Energy Resource Models for Distribution Feeder Simulation*. in *Power Engineering Society General Meeting*. 2003.
118. Chassin, D.P., K. Schneider, and C. Gerkensmeyer. *GridLAB-D: An open-source power systems modeling and simulation environment*. in *Transmission and Distribution Conference and Exposition, 2008. T&D. IEEE/PES*. 2008.
119. Chassin, D.P. and S.E. Widergren. *Simulating demand participation in market operations*. in *Power & Energy Society General Meeting, 2009. PES '09. IEEE*. 2009.
120. Schneider, K.P., et al. *A Taxonomy of North American radial distribution feeders*. in *Power & Energy Society General Meeting, 2009. PES '09. IEEE*. 2009.
121. Schneider, K.P., et al. *Distribution power flow for smart grid technologies*. in *Power Systems Conference and Exposition, 2009. PSCE '09. IEEE/PES*. 2009.
122. Galus, M.D. and G. Andersson. *Demand Management of Grid Connected Plug-In Hybrid Electric Vehicles (PHEV)*. in *Energy 2030 Conference, 2008. ENERGY 2008. IEEE*. 2008.
123. Shi, S.S., et al. *Modeling and simulation of the microgrid prototype in China*. in *Advances in Power System Control, Operation and Management (APSCOM 2009), 8th International Conference on*. 2009.
124. Amigoni, F., et al., *Agent-based coordination techniques for matching supply and demand in energy networks*. Integrated Computer-Aided Engineering, 2010. **17**(4): p. 373-382.
125. Huang, T. and D. Liu, *A self-learning scheme for residential energy system control and management*. Neural Computing and Applications, 2011. **22**(2): p. 259-269.
126. Tanaka, K. and K. Maeda. *Simulation-based design of microgrid system for a resort community*. in *Clean Electrical Power (ICCEP), 2011 International Conference on*. 2011.
127. Vuppala, S.K., et al. *Incorporating fairness within Demand response programs in smart grid*. in *Innovative Smart Grid Technologies (ISGT), 2011 IEEE PES*. 2011.
128. Zhu, J., M. Jafari, and Y. Lu. *Optimal energy management in community micro-grids*. in *Innovative Smart Grid Technologies - Asia (ISGT Asia), 2012 IEEE*. 2012.
129. Widergren, S., et al. *Residential transactive control demonstration*. in *Innovative Smart Grid Technologies Conference (ISGT), 2014 IEEE PES*. 2014.
130. Fanger, P.O., ed. *Thermal Comfort*. 1970, Danish Technical Press: Copenhagen.
131. Yin, R., S. Kiliccote, and M.A. Piette, *CITRIS Building Energy Simulation Model Development and Application*. 2012, LBNL: http://i4energy.org/.
132. Rabl, A. and L.K. Norford, *Peak load reduction by preconditioning buildings at night*. International Journal of Energy Research, 1991. **15**: p. 781-798.
133. Keeney, K.R. and J.E. Braun, *Application of building precooling to reduce peak cooling requirements*. ASHRAE Transactions, 1997. **103**: p. 463-469.
134. Yin, R., et al., *Study on Auto-DR and pre-cooling of commercial buildings with thermal mass in California*. Energy and Buildings, 2010. **42**: p. 967-975.

135. Liao, R., et al., *Weather-clustering based strategy design for dynamic demand response building HVAC control*, in *Proceedings of the Fourth ACM Workshop on Embedded Sensing Systems for Energy-Efficiency in Buildings*. 2012, ACM: Toronto, Ontario, Canada. p. 33-35.
136. Barricelli, N.A., *Symbiogenetic evolution processes realized by artificial methods*. Methodos, 1957. **9**(35-36): p. 143-182.
137. Fraser, A.S., *Simulation of genetic systems by automatic digital computers vi. epistasis*. Australian Journal of Biological Sciences, 1960. **13**(2): p. 150-162.
138. Bremermann, H.J., *Optimization through evolution and recombination*. Self-organizing systems, 1962: p. 93-106.
139. Bledsoe, W. *The use of biological concepts in the analytical study of systems*. in *Proceedings of the ORSA-TIMS National Meeting*. 1961.
140. Nassif, N., S. Moujaes, and M. Zaheeruddin, *Self-tuning dynamic models of HVAC system components*. Energy and Buildings, 2008. **40**(9): p. 1709-1720.
141. Xu, X. and S. Wang, *Optimal simplified thermal models of building envelope based on frequency domain regression using genetic algorithm*. Energy and Buildings, 2007. **39**(5): p. 525-536.
142. Huang, W. and H.N. Lam, *Using genetic algorithms to optimize controller parameters for HVAC systems*. Energy and Buildings, 1997. **26**(3): p. 277-282.
143. Xu, P., *Evaluation of Demand Shifting with Thermal Mass in Two Large Commercial Buildings*. 2006.
144. Bjorgan, R., L. Chen-Ching, and J. Lawarree, *Financial risk management in a competitive electricity market*. IEEE Transactions on Power Systems, 1999. **14**(4): p. 1285-1291.
145. Deng, S. and S. Oren, *Electricity derivatives and risk management*. Energy, 2006. **31**(6-7): p. 940-953.
146. Kathan, D., et al., *Assessment of Demand Response and Advanced Metering*. 2012, Federal Energy Regulatory Commission.
147. Rumelhart, D.E., G.E. Hintont, and R.J. Williams, *Learning representations by back-propagating errors*. Nature, 1986. **323**(6088): p. 533-536.
148. Cybenko, G., *Approximation by superpositions of a sigmoidal function*. Mathematics of control, signals and systems, 1989. **2**(4): p. 303-314.
149. Marquardt, D.W., *An algorithm for least-squares estimation of nonlinear parameters*. Journal of the Society for Industrial & Applied Mathematics, 1963. **11**(2): p. 431-441.
150. Demuth, H., M. Beale, and M. Hagan, *Neural Network Toolbox™ 6*. User Guide, COPYRIGHT, 1992. **2008**.
151. Deru, M., et al., *US Department of Energy commercial reference building models of the national building stock*. 2011.
152. Thomas, B. and M. Soleimani-Mohseni, *Artificial neural network models for indoor temperature prediction: investigations in two buildings*. Neural Computing & Applications, 2007. **16**(1): p. 81-89.
153. Tao, L. and M. Viljanen, *Prediction of indoor temperature and relative humidity using neural network models: model comparison*. Neural Computing & Applications, 2009. **18**(4): p. 345-357.
154. Mustafaraj, G., G. Lowry, and J. Chen, *Prediction of room temperature and relative humidity by autoregressive linear and nonlinear neural network models for an open office*. Energy and Buildings, 2011. **43**(6): p. 1452-1460.
155. Rubinstein, F., et al., *Analyzing occupancy profiles from a lighting controls field study*. 2003. Medium: ED; Size: 4 pages.
156. Bertsekas, D.P., et al., *Dynamic programming and optimal control*. Vol. 1. 1995: Athena Scientific Belmont, MA.

157. Carrio, et al., *Forward Contracting and Selling Price Determination for a Retailer*. Power Systems, IEEE Transactions on, 2007. **22**(4): p. 2105-2114.
158. Hatami, A.R., H. Seifi, and M.K. Sheikh-El-Eslami, *Optimal selling price and energy procurement strategies for a retailer in an electricity market*. Electric Power Systems Research, 2009. **79**(1): p. 246-254.
159. Schultz, R. and S. Tiedemann, *Conditional Value-at-Risk in Stochastic Programs with Mixed-Integer Recourse*. Mathematical Programming, 2006. **105**(2/3): p. 365-386.
160. Ahmed, S., *Convexity and decomposition of mean-risk stochastic programs*. Mathematical Programming, 2006. **106**(3): p. 433-446.
161. Ahmed, S. and S. Takriti, *On robust optimization of two-stage systems*. Mathematical Programming, 2004. **99**(1): p. 109-126.
162. Rockafellar, R.T. and S. Uryasev, *Optimization of conditional value-at-risk*. Journal of risk, 2000. **2**: p. 21-42.
163. Rockafellar, R.T. and S. Uryasev, *Conditional value-at-risk for general loss distributions*. Journal of Banking & Finance, 2002. **26**(7): p. 1443-1471.
164. Artzner, P., et al., *Coherent measures of risk*. Mathematical finance, 1999. **9**(3): p. 203-228.
165. Alam, M.R., M.B.I. Reaz, and M.A.M. Ali, *A Review of Smart Homes—Past, Present, and Future*. IEEE Transactions on Systems, Man, and Cybernetics, Part C (Applications and Reviews), 2012. **42**(6): p. 1190-1203.
166. Conejo, A.J., et al., *Day-ahead electricity price forecasting using the wavelet transform and ARIMA models*. Power Systems, IEEE Transactions on, 2005. **20**(2): p. 1035-1042.
167. Conejo, A.J., et al., *Forecasting electricity prices for a day-ahead pool-based electric energy market*. International Journal of Forecasting, 2005. **21**(3): p. 435-462.
168. Garcia, R.C., et al., *A GARCH forecasting model to predict day-ahead electricity prices*. Power Systems, IEEE Transactions on, 2005. **20**(2): p. 867-874.
169. Amjady, N., *Day-ahead price forecasting of electricity markets by a new fuzzy neural network*. Power Systems, IEEE Transactions on, 2006. **21**(2): p. 887-896.
170. Farzan, F., *Towards uncertainty in micro-grids: planning, control and investment*. 2013, Rutgers University-Graduate School-New Brunswick.